November 2019

Rice Response to Nitrogen Fertilization and Comparison of Unmanned Aerial Systems and Active Crop Canopy Sensors Vegetative Index to Estimate Rice Yield Potential

Anna Coker
Louisiana State University and Agricultural and Mechanical College

RICE RESPONSE TO NITROGEN FERTILIZATION AND COMPARISON OF UNMANNED AERIAL SYSTEMS AND ACTIVE CROP CANOPY SENSORS VEGETATIVE INDEX TO ESTIMATE RICE YIELD POTENTIAL

A Thesis

Submitted to the Graduate Faculty of the
Louisiana State University and
Agricultural Mechanical College
is partial fulfillment of the
requirements for the degree of
Master of Science

in

The School of Plant, Environmental & Soil Sciences

by
Anna E. Coker
B.S. University of Arkansas, 2017
December 2019

Acknowledgements

I would like to express my utmost appreciation to my major advisor, Dr. Dustin Harrell providing me with this opportunity and giving me his time and dedication. I am also especially appreciative of my committee members: Dr. Brenda Tubana, Dr. Thanos Gentimis, and Dr. Luciana Shiratsuchi. These 4 excellent people were great leaders on my committee giving me valuable feedback and guidance during the development of my research and thesis.

I am grateful to have been given this opportunity by my major professor, Dr. Harrell and the School of Plant, Soil, and Environmental Sciences to work and study at Louisiana State University. My research project and time here at Louisiana State University wouldn't have been made possible without the financial support from Louisiana State University AgCenter. I am extremely appreciative of the financial support.

I would also like to thank Dr. Harrell's team of people Dr. Manoch Kongchum, Dr. Nutifafa Adotey, James Leonard, Jacob Fluitt, and Jason Hartman. Each of them contributed greatly to this project and it wouldn't have been possible without their help.

Table of Contents

List of Tables

List of Figures

Abstract

Nitrogen (N) fertilization is a key component in producing profitable, maximized rice grain yields because yield is directly affected by N fertilizer applications. Economical optimum N rate (EONR) is used to estimate where the N fertilization rate impacts rice grain yield but is still economically efficient. Three common response models, linear-plateau, quadratic-plateau, and quadratic models were used to determine the response of rice to N fertilizer to determine the optimum N fertilization rate. The objective of the first part of this study was to evaluate the models by assessing the coefficients of determination (R^2), maximum rice grain yields each model produced, and the estimated EONRs of fertilization. Coefficients of determination (R^2) of the linear-plateau, quadratic-plateau, and quadratic were found to be similar (0.77, 0.79, 0.78). Other factors beyond just R^2 alone need to be taken into consideration when choosing which response model best fits a data set and should be used to estimate the EONR of fertilization for an individual variety.

Normalized difference vegetation index (NDVI) is a known indication of yield potential, one component needed to determine mid-season N requirements. The GreenSeeker has been the pre-dominant tool used to collect NDVI measurements. Unmanned aerial systems (UAS) have shown potential to collect NDVI measurements also. The objectives of the second part of this study were to: 1) evaluate the relationship between GreenSeeker (an active sensor) derived NDVI and UAS (a passive sensor) derived NDVI, and 2) evaluate the ability of GreenSeeker and UAS derived NDVI to estimate rice yield potential. This research was done in 2017 and 2018 at 5 locations in Louisiana. Remote sensor data was taken between panicle initiation and panicle differentiation using a GreenSeeker and UAS mounted remote sensor. All 5 locations showed a highly significant correlation between GreenSeeker and UAS derived NDVI. The linear

relationship between GreenSeeker and UAS derived NDVI to rice grain yield were not similar. The different relationships could have been caused by the differences between ground and air-borne based sensors. More research will need to be conducted before UAS mounted sensors can be used to accurately predict mid-season N needs in rice.

Chapter 1. Introduction

Rice (*Oryza sativa*) is one of the most important cereal grains in the world today. Rice is grown in many countries around the world producing roughly 162 million hectares of rice (USDA, 2019). The United States grows approximately 1 million hectares of rice in the states of California, Arkansas, Louisiana, Texas, Missouri, and Mississippi (USDA, 2019). Louisiana is the third leading state in the United States for rice production, producing approximately 176,000 hectares of rice harvested in 2018 (USDA, 2019). Rice is a highly valuable, edible starchy grain that is grown using management techniques that enhance growth and development and maximize rice grain yields.

The average growth and development of rice from germination to maturity ranges between 105 to 145 days depending on the variety and climatic conditions. The Louisiana State University (LSU) AgCenter researchers conduct several date-of-planting studies that are used to determine and adjust the optimum planting date recommendations of new and popular varieties (Saichuk and Harrell, 2014). In Southwest Louisiana rice is recommended to be planted between March 10th and April 15th and in North Louisiana between April 1st and May 5th (Saichuk and Harrell, 2014). The planting date ranges give farmers flexibility on when to plant depending on the field and environmental conditions. Planting rice during the recommended planting date window will typically produce the highest rice grain yield potential and the rice will be easier to manage throughout the growing season (Saichuk and Harrell, 2014). Once the rice seeds are planted, rice has two distinct growth phases: 1) vegetative and 2) reproductive. The vegetative growth phase is the growth stages between germination and panicle initiation. The reproductive growth phase is the growth stages between panicle initiation and heading. Once rice has reached

maturity, the whole grain is hard, and rice has reached a moisture of approximately 20 to 22%, then rice will be ready for harvest (Arkansas Rice Production Handbook, 2013).

Rice growth and development is influenced by nutrient availability in the soil. A rice nutrient management program should identify available nutrients and address any nutrient deficiencies. The nutrient availability and nutrient needs of rice should be monitored with the proper fundamental management strategy. Rice should obtain an adequate amount of nutrients for rice to produce maximum grain yields, higher profitability, enhanced nutrient efficiency, and reduced inputs (Fageria, 2001; Singh and Singh, 2017). There are three macronutrients that are highly valuable to rice: nitrogen (N), phosphorus (P), and potassium (K). Nitrogen is typically often the most limiting nutrient in rice and has a heavy impact on rice grain yields (Yoshida, 1981). Nitrogen stimulates the growth and development of the vegetative parts of rice (Leghari, 2016). The amount of N supplied to rice can either positively or negatively affect the development of rice. Inadequately supplying N to rice can lead to N deficiency across the whole rice field. The symptoms of N deficiency are recognized as chlorosis of the older leaves, reduced tillering, and shorter plant heights. Abundantly applying N to rice also have a negative impact on the growth of rice. The symptoms of over-application of N are presented in the field as excessive vegetative growth, increased disease pressure, lodging, and ultimately decrease in grain yield. The proper management of N fertilization is accomplished by determining the right N source, right N rate, right N application, and right placement of N to diminish the possibility of N having a detrimental effect on rice. The key outcome of rice fertilization is to produce high rice grain yields while minimizing N losses and costs associated with N fertilization (Singh and Singh, 2017).

Nitrogen has a very dynamic behavior in the soil and plant, it is important to have a basic understanding of the N-cycle processes and N losses that can occur when N is applied to rice. Obtaining an understanding of the N-cycle processes will help when making decisions about rice to N fertilization requirements so that maximum grain yields are profitably produced with minimal N losses. The main N source that makes up 78% of the Earth's atmosphere is N gas (N_2) (Havlin et al., 2014). Rice can only uptake N when N_2 is converted into a plant available N form. Organic and inorganic-N are two classes of N found in the soil and available to the plant. The inorganic-N forms are most abundantly found and used in a plant (Fageria, 2001). There are two inorganic forms of N taken up by the rice; nitrate (NO_3^-) and ammonium (NH_4^+).
Nitrate-N exists at great quantities in the soil as extractable N (Bronson, 2008). Nitrate has become a concern to our environment because of the increase in NO_3^- levels in the surface and ground water coming from the crop production systems (Bronson, 2008). Rice is grown in flooded, anaerobic field conditions, which causes NO_3^- to be unstable and lost quickly through N-loss pathways. Leaching is one of the major loss pathways for NO_3^- due to its solubility and mobility characteristics (Havlin et al., 2014). Ammonium-N fertilizer sources are recommended over NO_3^- fertilizer sources because NH_4^+ fertilizers are found to have greater stability under flooded, anaerobic conditions (Snyder and Slaton, 2002). Ammonium-N will remain available and not lost during the flood establishment on rice. Nitrification is a potential risk and loss pathway for NH_4^+ fertilizers if the flood is not maintained throughout the growing season. The N-loss pathways are highly influenced by environmental conditions, management practices, N application rates, N application method, and irrigation techniques

Nitrogen can be supplied to rice by fertilizer applications. Nitrogen is the most expensive fertilizer input to rice. Determining the right N fertilizer requirement is important to rice growers

to decrease excessive N applications and increase the economic return of investment of rice. Current N recommendations are based on fertilizer response trials conducted each year on an individual cultivar basis, by state experiment scientists, across multiple locations (Neeteson and Wadman, 1987). The N fertilizer response trials result in optimum N rates, or N rate ranges, that should be further refined by growers by considering their soils and past crop performance. The nitrogen use efficiency (NUE) of rice can be affected by the field conditions at the time of N application (wet, dry, or flood soils). The soil type, environmental conditions, and type of N application should also be taken into consideration by an individual grower when modifying the recommended N rate for that grower's rice field and N application conditions.

Nitrogen is an expensive fertilizer input of rice but is of high demand and required for proper growth and development of rice. Despite the range of N rates provided to the rice growers, there is only one economic optimum N rate (EONR). The rice grain yield response to N fertilization trials conducted to determine the N rate recommendations for individual cultivars can be done to determine the economic optimum N rate (EONR). The optimum N fertilization rate is determined by fitting certain statistical response models to rice grain yield data (Cerrato and Blackmer, 1990). Three popular response models include: 1) linear-plateau, 2) quadratic-plateau, and 3) quadratic. These response models evaluate the response curve determined by fitting the response model to data for various trials. Increasing N fertilizer rates may greatly increase rice grain yield, but the producer might not be able to cover the additional expenses of added fertilizer applications (Harrell et al., 2011). The response curve evaluates the value of additional grain yield as additional N fertilizer is applied until an economic increase associated with grain yield and N fertilizer application is no longer observed. Predicting the EONR for

individual variety-site-year is fundamental for maximizing rice grain yield, grain quality, profitability, and decreasing environmental risks (Belanger et al., 2000).

The three popular response models that the data is evaluated through can project three different EONR's. The three response models have the potential to estimate different EONR and grain yield outcome which, in turn, can highlight how different the three response models fit different data sets for individual variety-site-years. It is not always known why one statistical model is chosen over another when fitting a response model to a data set. The choice of which response model to use will have a strong impact on the predicted optimum N fertilizer rate. Choosing the less accurate response model could result in an inaccuracy of determining the optimal N recommendations and reduce the profitability of producers (Tumusiime et al., 2011). The response model choice can be validated by testing multiple statistical models for a valid description of yield response to N fertilization to justify why one model should be selected over another (Cerrato and Blackmer, 1990).

Nitrogen fertilizer application methods in rice can impact the spatial distribution of N and, in turn, impact the nitrogen use efficiency (NUE) of the N fertilizer rate applied. The application method of N fertilizer to rice is an important to help lessen N-losses and optimize rice grain yield and quality. The conventional method of applying N fertilizer to rice is to uniformly apply the N fertilizer to the whole field, at one time, on a certain date. The conventional N fertilizer application results in an imbalance between the N supplied and N demanded because it does not consider variability and the potential of N-losses during rice growth and development (Xue & Yang, 2008). In the mid-southern United States, the preferred N fertilizer application method is referred to as the two-way split application. The advantage of the two-way split method is the methods practicality in areas where the flood establishment and

maintenance of the flood can be difficult (Snyder and Slaton, 2002). The two-way split N application can lower the potential of N-losses and gives growers the possibility to adjust the second N application to accommodate for the N needs of rice.

Fertilizer N is applied at 2 different application times when using the split-application method. The first N fertilizer application is applied just before flooding, when rice is at the 4- to 5-leaf growth stage. The pre-flood N fertilizer recommendation rate in Louisiana is determined by N response trials conducted by research scientists, at the Louisiana State University AgCenter, evaluating multiple rice varieties. The recommended pre-flood N fertilizer rate is two-thirds of the recommended rate provided by LSU AgCenter on a variety basis (Harrell et al., 2018). The LSU AgCenter provides a N rate range for every currently available variety grown. The range of recommended N fertilizer rates gives individual growers leverage to adjust the N fertilizer rates based off the soil texture, rice variety, and environmental factors that could affect the N uptake by rice. The pre-flood N fertilizer is incorporated into the dry soil bed by establishing a flood onto the field within 1- 3-days after the N fertilizer application. The flood establishment decreases the possibilities of N losses through nitrification and denitrification when the N fertilizer is incorporated down into the root zone in a timely manner (Snyder & Slaton, 2002).

The second N fertilizer application time is completed at mid-season. Mid-season is the beginning of reproductive growth between panicle initiation (green ring or beginning internode elongation [BIE]) and panicle differentiation (1/2-inch IE) growth stages. The timing for the second N fertilizer application can be applied during the window between these two growth stages because of the short developmental period between panicle initiation and panicle differentiation (Harrell et al., 2011). However, N fertilizer applications applied closer to panicle

initiation will have a greater effect on rice grain yield than N fertilizer applied at the later growth stage, panicle differentiation when N is limiting (Harrell et al., 2011). The mid-season N fertilizer recommendations are determined by visual observation done by the grower or consultant. The determination of mid-season N fertilizer rates can be inaccurately estimated because not all in-season characteristics of rice can be determined solely by the eye of a grower or consultant. Mid-season N fertilizer applications are highly valuable to the outcome of rice grain yield and quality (Nguyen and Lee, 2006). Therefore, accurate strategies and methods for prescribing in-season N fertilizer rates at mid-season are crucial to rice producers.

Precision agriculture tools have become increasingly important in determining a crops health status since the management system emerged in the mid-1980's. Agricultural producers must make strategical, tactical, and operational management decisions based on the future of the farm, potential yields, profitability, environmental quality, crop varieties, fertilization requirements, when to fertilize, and so on (Bouma, 1997). In today's agriculture, where farm size exceeds 800 hectares it would be difficult for producers to manually switch between certain established production practices without an advancement in technology to evaluate the spatial variability across fields (Stafford, 2000). Site-specific recommendations derived from precision agriculture techniques which evaluate the spatial and temporal variability of a field may provide more accurate recommendations than traditional mid-season N recommendations (Geebers & Adamchuk, 2010). Spatial variability is the variability across the field due to difference in soil structure, soil fertility, irrigation applications, pests and diseases, and plant genetics. Temporal variability describes how these factors vary over time.

Precision agriculture includes an abundance of data which can be used to optimize nutrient recommendations to reduce input fertilizer cost and improve environmental quality

(Stafford, 2000). Nutrient recommendations can now be based on a variable-rate fertilizer application with the use of precision agricultural tools. These tools will play a part in limiting N losses and allowing for varying N applications that fit specific areas of a field (Bronson, 2008). Site-specific management systems are a source used to increase crop productivity allowing for greater economical returns and maximizing crop yield.

Before the advancement of the use of precision farming tools to estimate crop health and N status of a crop, N fertilization requirements have been a challenge to accurately determine. A crop yield goal has been used to help predict N fertilization requirements. A yield goal should be based on crop yield history, soil characteristics, management practices, and the crop variety being planted to manage the unpredictability of the factors affecting yield. Nitrogen requirements based off a yield goal can be adjusted to establish N rates that result in an efficient crop production system (Stanford, 1973). Crop yield potential is influenced by soil-related, anthropogenic, topographic, biological, and meteorological spatial variability factors (Corwin, USDA). Along with spatial variation, temporal variation must be taken into consideration also when adjusting a crop yield goal because yield varies from year-to-year due to an influence from environmental conditions (Yao et al., 2012; Schlegel, 2005; Shanahan et al., 2008). Spatial and temporal variation characteristics encompass many uncertainties and fluctuations. Therefore, it is very difficult to determine accurate N requirements based solely on a crop yield goal without having another tool to assess spatial and temporal variability.

Remote sensing technology has shown to be promising in predicting practical on-site management applications evaluating spatial and temporal variability. Variables of a crop's growth and development can be obtained in a fast, reliable, non-destructive method by using remote sensing technology (Nguyen et al., 2006). Fertilizer recommendations, irrigation

strategies, and variable crop seeding rate can all be determined via remote sensing technology. Crop field assessments have progressed with the use of remote sensing technologies delivering quantitative data of the crop's spatial variability properties (Elarab, 2016).

Active crop canopy sensors, a remote sensing tool, can be used to estimate crop health and N status of a crop (Xue et al., 2004; Lee et al., 2008). Active crop canopy sensors may potentially be effective in a flooded production system when mid-season N fertilizer needs are difficult to determine and often inaccurately assessed by visual physical characteristics only. An imbalance between N demand and supply can result in an under or over application of N fertilizer. Active remote sensing technology has the potential to decrease the uncertainty in determining N needs at mid-season. According to Foster et al. (2017), mid-season N requirements based from remote sensing decision making showed the potential to lower the total N application rate by 18 to 108 kg ha^{-1}. In return, this will optimize yield and NUE. Active crop canopy sensors can develop a more sustainable agricultural approach by determining correct application rates at critical fertilization timings to diminish N losses.

The predominant remote sensing tool used to aid in predicting a rice crop's health during major growth and developmental phases is the GreenSeeker handheld sensor. Growers have become more sustainable farmers and made more suitable in-season fertilizer applications using GreenSeeker based technology (Yao et al., 2012, AR yearly fertilization guide or handbook). The GreenSeeker tool is unaffected by environmental conditions because it is equipped with a pre-calibrated, active, optical light sensor. Specific regions in the red (670 ± 10 nm) and near-infrared (780 ± 10 nm) wavelength bands of the electromagnetic spectrum are used to measure the canopy reflectance derived with the GreenSeeker remote sensing tool. Canopy reflectance measurements can determine the chlorophyll level of the rice crop to conclude the amount of N

present. GreenSeeker evaluates the reflectance value of the crop canopy by calculating the normalized difference vegetation index (NDVI) using the red and near-infrared wavelengths in the following equation:

$$NDVI = \frac{(NIR + R)}{(NIR - R)} \quad [1.1]$$

where:

NIR = Reflectance at the near-infrared region of the electromagnetic spectrum

R = Reflectance at the red region of the electromagnetic spectrum

Absorption and reflectance of the rice crop canopy is measured with the calculation of NDVI. The visible region (red) tends to absorb light, but the vegetation reflects light in the NIR regions. Normalized difference vegetation index (NDVI) has been shown to be effective in determining disease damage, leaf area index, and fertilization requirements. The assessment of GreenSeeker NDVI measurements evaluates the variations of a rice fields crop response to N fertilizer applied at pre-flood and the different rates of N needed at future critical growth stages (Xue & Yang, 2008). The GreenSeeker NDVI has shown to be a more reliable source to predict a crop's overall health status because the tool collects an average of readings over an entire area unlike past techniques of leaf color charts and chlorophyll meters (Girma et al., 2006; Lee et al., 2008).

GreenSeeker derived NDVI can currently be used in an on-site sensor-based N rate calculator to determine mid-season N requirements. Three factors must be known for mid-season N rates to be determined by the on-site sensor-based N rate calculator: 1) response index, 2) rice grain yield potential, and 3) rice response to N fertilization (Harrell et al., 2011). The collection of NDVI by the GreenSeeker must be done at critical timings for it to be used in this calculator to determine in-season plant needs. The calculated algorithm has potential to be an economical

and environmental benefit to farmers predicting the N fertilization requirement needs for adequate rice growth and development.

The response index portion of the algorithm is the crops quantitative response to N fertilizer within a field. A controlled, strip with no N fertilizer applied must be stationed in an area that most represents the characteristics of the field in order to calculate the response index. The check plot is used to exhibit the supply of soil N without any fertilization additions. The rice response to N fertilization is calculated by dividing the average NDVI from the non-N-limiting strip by the average NDVI from a highly representative strip across the field in an area where N was applied by the farmers practice (Raun et al., 2001). The response index was the first part in developing the algorithm because it can be multiplied by the predicted yield potential to determine the potential yield with additions of N fertilizer. Raun et al. (2002), demonstrated a positive correlation with the response index of applied N using the sensor-based approach to the grain yield response.

The second and third parts of the algorithm are calculating the yield potential with no N fertilizer additions (YP_0) and the yield potential with N fertilizer additions (YP_N). Nitrogen fertilizer rates are strongly influenced by crop yield potential and N responsiveness (Ruan et al., 2010). The GreenSeeker NDVI has been shown to be an accountable measurement of crop yield potential and final grain yield (Girma et al., 2006; Teal et al., 2006; Tubana et al., 2008; Harrell et al., 2011). Therefore, NDVI and rice grain yield can exist as components to predict rice grain yield potential in the computed algorithm for the sensor-based N requirement decision tool (Raun et al., 2002; Harrell et al., 2011). Raun et al. (2001), found a strong, correlated relationship between actual grain yield and estimated grain yield enabling the alteration of N fertilization rates by estimated yield potential during the crops growing season. The yield potential with N

fertilizer additions has been shown to be accurately estimated as the product of response index and YP_0 (Raun et al., 2005).

The computed algorithm has already shown to be successful with the ground-based remote sensor, GreenSeeker, derived NDVI. The algorithm has not been extensively adopted by growers or consultants because the GreenSeeker handheld sensor does not justify for variation across a whole field and the slow timing of collecting NDVI readings manually through a field. Air-borne remote sensors have progressed with the advancements in technology and are now being evaluated for their potential in collecting data for a crop's overall health status. Unmanned aerial systems (UAS) have produced a related ability to other remote sensing tools in evaluating different crop responses (Rasmussen et al., 2016).

The GreenSeeker collects NDVI measurements on a point-to-point basis over a small site-specific portion of a rice field. The UAS collects readings accounting for variation on a whole field basis increasing the field scale average. Both tools have the ability to lower N fertilizer inputs, equalize N demand and supply, and increase NUE. A larger data collection, flexible transport, and rapid data collection are advantages of the UAS technology system. UAS remote sensors generate data easier than handheld sensors and can be navigated with pre-programmed flight plans (Huang et al., 2013). The UAS mounted remote sensor collects readings at a high spatial resolution compared to the ground-sensor NDVI readings, but there is still a high correlation between air-borne and ground-sensor based NDVI measurements (Primicero et al., 2012). The maneuvering in a flooded rice field can be difficult however UAS mounted remote sensors can be transported in the field much easier. The UAS can limit the time producers spend on field assessments and crop decision making producing a more time-efficient management system to estimate a rice crops health status (Zhu et al., 2009).

All UAS mounted remote sensors are considered passive light sensors. Passive light sensors use the sunlight as a light source which can introduce variability in collective data. In the process of collecting data with an UAS mounted sensor, variability results from: 1) intensity of the light, 2) bidirectional reflectance, and 3) environmental conditions. There are accommodations to overcome the variability of the UAS mounted sensors data collection. Variability in remote sensing collective data can be reduced by flying in low cloud cover, flying mid-day between 10 a.m. and 2 p.m. (reducing the variability in the angle of sunlight incidence), equipping the UAS with a sunshine normalizing sensor, and by using advanced multispectral image software. Variability can also be decreased by including georeferencing points to help stabilize geographical and geometrical data (Lelong et al., 2008). Despite the concern of variation in remote sensing data, the technology still shows potential for successful data collection in crop production systems and a significant relationship with ground-level sensors. For example, remote sensors have been shown to accurately predict the chlorophyll measurements in corn and were shown to have a strong relationship with ground-level chlorophyll meters (Quemada et al., 2014).

Time-management for large producers is a difficult skill to master. Remote sensing can help make crop management decisions and can minimize the time producers spend on field sampling and field assessments (Zhu et al., 2009). Many studies have been conducted using the UAS remote sensing technology to evaluate chlorophyll and nitrogen content in cereals (Li et al., 2015; Zheng et al., 2016), weed mapping (Stroppiana et al., 2018), and disease damage (Yang et al., 2017). The UAS remote sensors show similarities to the GreenSeeker technology in relation to collecting NDVI readings at critical growth stages to evaluate grain yield. Swain et al. (2010) showed a high correlation with yield and NDVI measurements taken at panicle initiation with the

UAS mounted remote sensor. This relationship between GreenSeeker and UAS derived NDVI to evaluate rice grain yield can mean there is a possibility of only using a UAS sensor to determine mid-season N fertilization rates with a computed algorithm similar to the GreenSeeker based algorithm. Mid-season fertilization rate decisions made in-season could be determined faster and more accurately with the use of a UAS remote sensor.

The on-site sensor-based N fertilization rate decision tool using GreenSeeker derived NDVI has been shown to be an effective decision tool. An on-site sensor-based N rate fertilization tool has not been derived for UAS remote sensors. Vegetative indices derived from a UAS remote sensor has the potential to improve rice grain yield, reduce fertilizer inputs, and economically benefit producers due to UAS's ability to collect information about the nutrient status of rice at critical growth stages on a whole field basis. The objectives of this study were to: 1) determine the economical optimum N rates for multiple rice varieties and hybrids using three common response models, 2) evaluate the relationship between GreenSeeker and UAS remote sensor derived NDVI, and 3) evaluate the GreenSeeker and UAS remote sensor derived NDVI relationships to rice grain yield.

Chapter 2. Determination of Rice Grain Yield Response to Nitrogen Fertilization

2.1. Introduction

Rice (*Oryza sativa)* is one of the major nutritional sources for the world's population. The worldwide production of rice is approximately 162 million hectares (USDA, 2019). The growth and development of rice depends heavily on the nutrients supplied to the crop throughout the growing season. Nitrogen (N) is the most essential nutrient to rice due to the heavy impact this nutrient has on rice grain yield. Nitrogen is the most abundantly applied fertilizer of all fertilizer nutrients and makes up the bulk of the fertilizer budget in a rice crop. Nitrogen sti1mulates the growth and development of rice and gives rice its dark-green pigmentation (Leghari, 2016). Rice will not develop efficiently if the demand of N is not adequately met. Nitrogen deficiency symptoms in rice include chlorosis of the older leaves, reduced tillering, shorter plant heights, and ultimately a decrease in rice grain yield. Over application of N to rice will result in excessive vegetative growth, increased disease pressure, lodging, and reduced yield potential.

Nitrogen fertilizer application methods in rice can impact the spatial distribution of N and, in turn, impact nitrogen use efficiency (NUE). In the mid-southern U.S., N is typically applied using two split applications in rice. The two-way split application method is most practical in areas where N losses are prone due to the difficulty of the flood establishment and maintenance of the flood (Snyder and Slaton, 2002). The first N fertilizer application is done just before flooding when the rice is at the 4- to 5 -leaf growth stage. In Louisiana, the recommended N rate applied at this growth stage is two-thirds of the recommended rate on a variety basis provided by the LSU AgCenter (Harrell et al., 2018). The LSU AgCenter recommends a N rate range for every currently available variety grown. The recommended N range is determined from

N response trials conducted by research scientists at different sites, evaluating multiple varieties over multiple years. Refinements of the recommended pre-flood N rate should be made by a farmer based on the soil texture, environmental factors at the time of fertilizer application, and past performance. A flood should be established between one to three days after the N application to incorporate the N fertilizer into the soil, decreasing the chances of N losses through nitrification and denitrification (Snyder and Slaton, 2002). The pre-flood N fertilizer application is the most important N application because it directly impacts the yield potential of rice (Saichuk and Harrell, 2014). The second N fertilizer application time is completed at mid-season, the end of vegetative growth and the beginning of reproductive growth, between the panicle initiation (green ring or beginning internode elongation [BIE]) and panicle differentiation (1/2-inch IE) growth stages.

Current N recommendations are based on N fertilizer response trials conducted each year by state experiment scientists across multiple locations (Neeteson and Wadman, 1987). These studies result in optimum N rates, or N rate ranges, on an individual cultivar basis which are recommended to rice growers. These recommendations are further refined by the individual growers by considering their soils and past crop performance. Field conditions at the time of application (wet, dry, or flooded soils) can greatly affect the efficiency of the pre-flood N application and should also be considered by growers. A rice producer should also consider the soil type, environmental conditions, and type of application when modifying the recommended N rate. Over application of N fertilizer can lead to excessive N losses, which can greatly affect the economic value of rice and have a negative impact on the environment. Chen et al. (2010) found that N loss will exceed N uptake when the N fertilizer applications exceed the optimum N rate.

The main objectives of N fertilization are to produce high rice grain yields while minimizing N losses and costs associated with N fertilization (Singh and Singh, 2017).

Predicting the optimum N fertilization rate is fundamental for maximizing rice grain yield, grain quality, profitability, and decreasing environmental risks (Belanger et al., 2000). Increasing N rates may greatly increase rice grain yield, but the producer might not be able to cover the additional expenses of added fertilizer applications (Harrell et al., 2011). The economical optimum N rate (EONR) is used to estimate where the N fertilization rate impacts rice grain yield but is still economically efficient. The optimum N fertilization rate is determined by fitting certain statistical models to rice grain yield data (Cerrato and Blackmer, 1990). There are several different statistical models that can be used to determine the EONR. Three popular models include: 1) linear-plateau, 2) quadratic-plateau, and 3) quadratic. These models evaluate the value of additional grain yield as additional fertilizer is applied until an economic increase associated with yield and fertilizer application is no longer observed. The response curve determined by fitting the model to the data for various trials can define the relationship between the rice grain yield response to numerous N fertilizer applications (Neeteson and Wadman, 1987).

The estimated EONR can vary between each of the statistical models even when using the same data set. It is not well known why one model is chosen over the others, but a valid reason should be given as to why a certain statistical model was chosen over another (Cerrato and Blackmer, 1990). The reasoning for this is because the models may produce the same coefficient of determination (R^2) but might determine different optimum N fertilizer rates. Only considering the highest R^2 for the 3 statistical models is not always reliable when selecting the best model for determining the EONR. Cerrato and Blackmer (1990) concluded the R^2 values

and maximum yields were relatively similar from the five models evaluated in their study but found the quadratic-plateau model the best to describe the yield responses. Harrell et al. (2011) found the linear-plateau model to estimate the best economic return estimates because the model estimated lower maximum grain yields and EONRs. Other studies showed the quadratic-plateau model to be preferred over the linear-plateau model. Alivelu et al. (2003) found that the quadratic-plateau model produced the same maximum rice grain yield as the linear-plateau model, but with a lower EONR. Tumusiime et al. (2011) also found that both the plateau statistical models were found to fit the data sets better than the quadratic model. Cerrato and Blackmer (1990) found that the quadratic model estimated optimum N rates which were too high to give a valid explanation of yield responses to N fertilization. Harrell et al. (2011) however, when basing the data on economical estimates, found the quadratic model estimated much higher EONRs in rice and was superior to the quadratic-plateau model. Belanger et al. (2000) discovered a decrease in the potential of economic losses when estimating optimum N rates when using the quadratic model (Belanger et al., 2000). The results from these studies show how different each model can fit different data sets and how each model has a different outcome EONR and grain yield. The model of choice will have a strong effect on the estimated optimum N fertilizer rate.

Economical optimum N rates vary significantly between varieties and locations (Belanger et al., 2000). Determining a different optimum N rate is necessary for different soils, environmental conditions, and varieties. Optimum N rates that produce maximum rice grain yield, profitability, and decrease N losses to the environment need to be determined for new varieties coming into the market.

It is not always known why one statistical model is chosen over another when fitting a model to a data set. Inaccuracy of determining optimal N recommendations can occur between the different statistical models and reduce the profitability of producers (Tumusiime et al., 2011). Multiple statistical models should be evaluated for a valid description of yield response to N fertilization to justify why one model should be selected over another (Cerrato and Blackmer, 1990). The objectives of this study were to: 1) evaluate rice grain yield response to N fertilization using three regression models (linear-plateau, quadratic-plateau, and quadratic models) and 2) determine the EONR for each model. This study evaluated the models by assessing the coefficients of determination (R^2), maximum rice grain yields each model produced, and the estimated EONRs of fertilization.

2.2. Materials and Methods

2.2.1. Site Description, Planting Method, Treatment Structure, and Trial Establishment

Field trials were conducted in Louisiana at two locations in 2017 and four locations in 2018. A total of seventeen difference rice cultivars were evaluated for their response to N fertilization. Cultivars evaluated included: 'Aura 115', 'CLJ01', 'CLXL745', 'CL153', 'CL172', 'CL272', 'CLX6 1030', 'CLX6 1111', 'CLX6 1133', 'Diamond', 'FullPage RT7321', 'FullPage RT 7323', 'PVL01', 'Titan', 'XL760', 'XP113', and 'XP760'. Not all seventeen varieties were included at each location for each year. Data were collected from each individual variety-site-year trial for use in the fertilizer response analyses. The locations of each site, year, and soil information for the trials are shown in Table 2.1.

Table 2.1. The soil series, taxonomy, and taxonomic classification for each individual location-year.

Location	GPS Location	Year	Series	Taxonomy	Taxonomic Classification
Crowley, LA	30°14’50.8”N 92°20’56.8”W	2017-2018	Crowley	Silt loam	Fine, smectitic, thermic Typic Albaqualf
Palmetto, LA	30°47’41.9”N 91°53’29.9”W	2017-2018	Dundee	Silty clay loam	Fine-silty, mixed, active, thermic, Typic Endoalqualf
Monroe, LA	32°23’23.8”N 91°58’47.2”W	2018	Herbert	Silty clay	Fine-silty, mixed, active, thermic, Aeric Eqiaqualf
Saint Joseph, LA	31°56’41.3”N 91°13’54.0”W	2018	Commerce	Silt loam	Fine-silty, mixed, superactive, nonacid, thermic Fluvaquentic Endoaquepts

A drill-seeded delayed flood production system was used to grow rice in all trials. The seed treatment for the rice varieties consisted mancozeb (Dithane - fungicide), gibberellic acid (Release), Zinc Plus (10% Zn & 4.9% combined S), and anthraquinone (AV-1011 - bird repellent), and chlorantraniliprole (Dermacor – insecticide). Hybrid seed was treated with Clothianidin (Nipsit Inside), Fludioxonil (Spirato 480FS), Fludioxonil (Maxim 4FS), gibberellic acid, zinc, and anthraquinone (AV-1011 -bird repellent). The rice cultivars were planted to a depth of 1.27 cm at 366 seeds per m^2 for varieties and 111 seeds per m^2 for hybrids using a small plot grain drill (Almaco, Iowa). Plot length was 4.88 m consisting of 7 rows with 20 cm spacing. The variety N rates included 0, 34, 67, 101, 135, 168, 202, and 235 kg ha^{-1}. The hybrid N rates included 0, 67, 101, 135, 168, and 202 kg ha^{-1}. The N pre-flood rates were surface broadcast applied on rice at the 4- to 5- leaf physiological growth stage. A flood was established between one to three days after the pre-flood N fertilizer applications. The planting, pre-flood N fertilizer applications, and flood establishments dates are presented in Table 2.2. The rice was managed according to state recommendations during the growing season (Rice Management Tips, 2018). A small plot combine equipped with a HarvestMaster H2 high capacity graingage (Logan, Utah) was used to determine the weight and moisture of the harvested rice plots.

Table 2.2. Important agronomic dates including planting date, pre-flood N application timing, flood establishment, and sensor reading dates for each location-year.

Location	Year	Planting Date	Pre-Flood N Application	Flood Establishment
Crowley, LA	2017	13-Mar	2-May	3-May
Palmetto, LA	2017	21-Mar	11-May	12-May
Crowley, LA	2018	14-Mar	1-May	3-May

(Table 2.2 Cont'd.)

Location	Year	Planting Date	Pre-Flood N Application	Flood Establishment
Palmetto, LA	2018	27-Mar	17-May	18-May
Monroe, LA	2018	1-May	23-May	25-May
Saint Joseph, LA	2018	3-May	22-May	23-May

2.2.2. Statistical Data Analysis

Statistical analysis was performed on all data collected for each variety-site-year using R-Studio 1.1.456 (RStudio, Inc., 2009-2018). The linear-plateau, quadratic-plateau, and quadratic models were fit to the fertilizer response data from each variety-site-year trial using R-Studio. Linear-plateau model is defined by

$$\begin{aligned} Y &= a + bN, \quad N < C \\ Y &= P, \quad N \geq C \end{aligned} \qquad [2.1]$$

where Y is rice grain yield (kg ha^{-1}) and N is the rate of pre-flood N fertilizer application (kg ha^{-1}), a is the yield when no N is applied (intercept), b is the linear coefficient, C is the critical rate of fertilization that occurs at the intersection of the linear and plateau response lines and P corresponds to the plateau yield. The parameters of a, b, P, and C are defined by fitting the linear-plateau model to the data.

The quadratic-plateau model for a given variety-site-year is defined by

$$\begin{aligned} Y &= a + bN + cN^2, \quad N < C \\ Y &= P, \quad N \geq C \end{aligned} \qquad [2.2]$$

where Y is rice grain yield (kg ha^{-1}) and N is the rate of N application (kg ha^{-1}), a is the yield when no N is applied (intercept), b is the linear coefficient, c is the quadratic coefficient, C is the critical rate of fertilization that occurs at the intersection of the quadratic and plateau response

lines and *P* is the plateau yield. The parameters for *a*, *b*, *c*, *P*, and *C* are defined by fitting the quadratic-plateau model to the data.

The quadratic model is defined by

$$Y = a + bN + cN^2 \quad [2.3]$$

where *Y* is rice grain yield (kg ha^{-1}) and *N* is the rate of N application (kg ha^{-1}), *a* is the yield when no N is applied (intercept), *b* is the linear coefficient, *c* is the quadratic coefficient. The parameters explaining *a*, *b*, and *c* are determined by fitting the quadratic model to the data.

Non-linear (linear-plateau and quadratic-plateau) and linear (quadratic) regression analyses were performed to determine the coefficients of determination (R^2) values for all variety-site-year trials. The economical optimal nitrogen rate (EONR) of fertilization was determined for the linear-plateau, quadratic-plateau, and quadratic models. The linear-plateau models EONR were shown as the intersection line of the linear and plateau lines from the linear-plateau regression model (Cerrato and Blackmer, 1990; Harrell et al., 2011). The quadratic-plateau and quadratic models EONR of fertilization were determined by calculating the first derivative of the quadratic-plateau and quadratic equations to a fertilizer-to-rice price ratio and solving for N (Nelson et al., 1985; Harrell et al., 2011).

2.3. Results and Discussion

The rice grain yield response to N fertilization for each variety-site-year trial was derived from the R^2 determined from the results of the linear-plateau, quadratic-plateau, and quadratic non-linear regression analyses are presented in Table 2.3. An example of the data fit to the linear-plateau, quadratic-plateau, and quadratic fertilizer response models for one variety-site-year is presented in Figure 2.1.

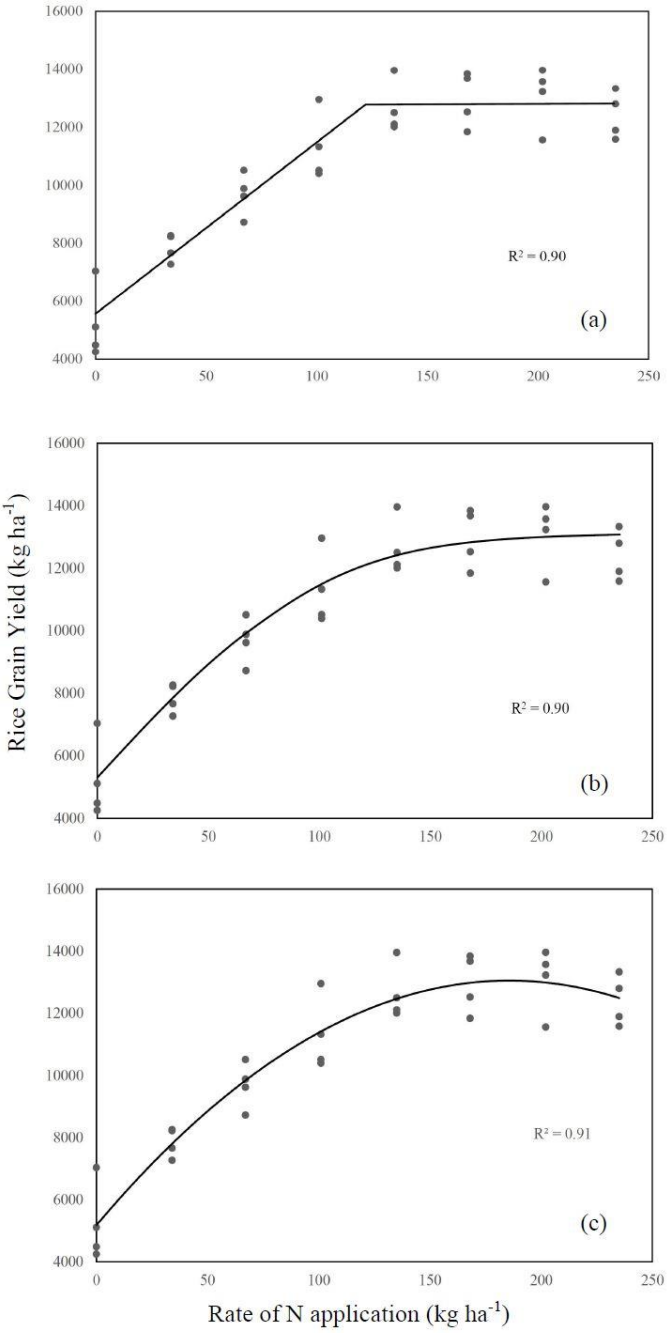

Figure 2.1. Example of (a) linear-plateau, (b) quadratic-plateau, and (c) quadratic fertilizer response models for one variety-site-year (CLX6-1030-Crowley, LA-2018).

The mean R^2 value for the linear-plateau, quadratic-plateau, and quadratic models were: 0.80, 0.82, and 0.81, respectively, indicating how similar the three models are to each other when determining the rice grain yield response to N fertilization applications in this data set. Alivelu et

al. (2003) also found the R^2 values to be relatively similar between non-linear regression models when evaluating the rice grain yield response to N fertilization. Similarities were also observed between the ranges of the R^2 values derived from each of the three non-linear regression models (linear-plateau: 0.46-0.92; quadratic-plateau: 0.46-0.94; quadratic: 0.48-0.94). Deciding which of the three models is the most appropriate fit for estimating the optimum N fertilizer rate, is difficult when basing the decision solely off the R^2. This data set presents highly related R^2 values therefore, deciding which of the three models best estimates the optimum N fertilizer rate would be difficult to estimate based solely off the R^2 However the three different models may estimate different optimum N fertilizer rates despite the similar coefficients of determination used to evaluate the rice grain yield response to N fertilizer (Belanger et al., 2000; Cerrato and Blackmer, 1990). Estimated economical optimum N fertilization rates may vary between models however, there can only be one true EONR for a certain variety-site-year (Cerrato and Blackmer, 1990; Belanger et al., 2000; Harrell et al., 2011). Therefore, the R^2 should not be the only factor taken into consideration when choosing one model over another to estimate the optimum N fertilizer rate for a given variety-site-year.

Table 2.3. Coefficients of determination (R^2) results for the linear-plateau, quadratic-plateau, and quadratic regression models describing the relationship between N fertilizer application rate and rice grain yields.

			Linear-Plateau	Quadratic-Plateau	Quadratic
Variety	Location	Year	R^2	R^2	R^2
Aura 115	CM	2017	0.85	0.91	0.91
Aura 115	SLP	2017	0.77	0.80	0.80
CL153	CM	2017	0.92	0.92	0.92
CL153	SLP	2017	0.80	0.82	0.82
CL153	CM	2018	0.75	0.82	0.82
CL172	CM	2017	0.81	0.81	0.81
CL172	SLP	2017	0.60	0.69	0.68

(Table 2.3 Cont'd.)

			Linear-Plateau	Quadratic-Plateau	Quadratic
Variety	Location	Year	R^2	R^2	R^2
CL172	CM	2018	0.68	0.76	0.76
CL272	CM	2017	0.90	0.92	0.92
CL272	SLP	2017	0.69	0.71	0.66
CLJ01	CM	2018	0.91	0.94	0.94
CLJ01	SLP	2018	0.82	0.84	0.83
CLX6-1030	SJ	2018	0.88	0.89	0.84
CLX6-1030	CM	2018	0.90	0.90	0.91
CLX6-1111	CM	2018	0.89	0.91	0.89
CLX6-1111	RP	2018	0.76	0.77	0.76
CLX6-1111	SJ	2018	0.88	0.89	0.89
CLX6-1111	SLP	2018	0.84	0.88	0.82
CLX6-1133	CM	2018	0.88	0.88	0.88
CLXL745	CM	2018	0.85	0.85	0.82
Diamond	CM	2017	0.85	0.83	0.81
Diamond	SLP	2017	0.61	0.60	0.58
Diamond	CM	2018	0.86	0.89	0.89
Diamond	SJ	2018	0.74	0.76	0.74
FullPage RT 7321	CM	2018	0.89	0.90	0.89
FullPage RT 7321	RP	2018	0.89	0.91	0.91
FullPage RT 7321	SLP	2018	0.75	0.85	0.84
FullPage RT 7323	RP	2018	0.71	0.74	0.75
FullPage RT 7323	SLP	2018	0.64	0.74	0.72
PVL01	CM	2018	0.91	0.91	0.88
PVL01	SJ	2018	0.83	0.83	0.83
PVL01	SLP	2018	0.86	0.88	0.84
Titan	SLP	2017	0.64	0.75	0.74
Titan	CM	2018	0.82	0.81	0.82
XL760	CM	2017	0.85	0.84	0.84
XP113	CM	2018	0.87	0.83	0.83
XP760	CM	2018	0.88	0.90	0.90
XP760	SLP	2018	0.75	0.82	0.82

The estimated maximum rice grain yield (kg ha^{-1}) determined by the linear-plateau, quadratic-plateau, and quadratic models are presented in Table 2.4. Mean maximum grain yields for the linear-plateau, quadratic-plateau, and quadratic models were all relatively similar and

were 11,513, 11,483, and 11,723 kg ha^{-1}, respectively. The range of estimated maximum grain yield values was similar amongst the three models also (linear plateau: 8,298 – 14,048 kg ha^{-1}; quadratic-plateau: 8,378 – 14,164 kg ha^{-1}; quadratic: 8,618 – 14,503 kg ha^{-1}). Harrell et al. (2011) found the quadratic model to estimate higher maximum grain yields 78% of the time, which is similar to the findings in this study where the quadratic model estimated higher maximum grain yields 79% of the time. The linear-plateau model estimated higher grain yields 18% of the time. The quadratic-plateau model estimated the highest grain yields 5% of the time. While the quadratic model was shown to be the most suitable model to describe rice grain yield responses to N fertilization in previous studies (Cerrato and Blackmer, 1990; Chen et al., 2011), the variability in the estimated maximum rice grain yield between the models in the current study indicates why the determination of the optimum N fertilization rate should not be the only factor in determining the appropriate prediction model.

Table 2.4. Maximum rice grain yields (kg ha^{-1}) estimated by the linear-plateau, quadratic-plateau, and quadratic response models.

Variety	Location	Year	Linear-Plateau Max yield (kg ha^{-1})	Quadratic-Plateau Max yield (kg ha^{-1})	Quadratic Max yield (kg ha^{-1})
Aura 115	CM	2017	12391	12835	12835
Aura 115	SLP	2017	11848	11913	12062
CL153	CM	2017	10960	11179	11246
CL153	SLP	2017	8925	8957	8989
CL153	CM	2018	10539	10069	10151
CL172	CM	2017	9482	9678	9718
CL172	SLP	2017	11421	10778	11043
CL172	CM	2018	10392	9751	9925
CL272	CM	2017	10377	10413	10432
CL272	SLP	2017	10039	10021	10318
CLJ01	CM	2018	12313	12307	12440
CLJ01	SLP	2018	9216	9257	9426
CLX6-1030	SJ	2018	10118	10225	10773
CLX6-1030	CM	2018	12779	12857	13054

(Table 2.4 Cont'd.)

Variety	Location	Year	Linear-Plateau Max yield (kg ha^{-1})	Quadratic-Plateau Max yield (kg ha^{-1})	Quadratic Max yield (kg ha^{-1})
CLX6-1111	CM	2018	12261	12283	12619
CLX6-1111	RP	2018	10875	10907	11024
CLX6-1111	SJ	2018	12818	13021	13146
CLX6-1111	SLP	2018	10711	10679	11114
CLX6-1133	CM	2018	11107	11124	11687
CLXL745	CM	2018	12401	12401	12870
Diamond	CM	2017	9060	9161	9555
Diamond	SLP	2017	11240	11219	11480
Diamond	CM	2018	13276	13346	13407
Diamond	SJ	2018	11171	11135	11743
FullPage RT 7321	CM	2018	13944	14164	14503
FullPage RT 7321	RP	2018	12756	12932	12992
FullPage RT 7321	SLP	2018	13895	13315	13527
FullPage RT 7323	RP	2018	12101	12072	12318
FullPage RT 7323	SLP	2018	13690	13162	13582
PVL01	CM	2018	10833	10879	11294
PVL01	SJ	2018	8298	8378	8618
PVL01	SLP	2018	8627	8657	8935
Titan	SLP	2017	11685	11164	11373
Titan	CM	2018	11453	11538	12056
XL760	CM	2017	12391	12552	12551
XP113	CM	2018	12865	12935	13081
XP760	CM	2018	14048	14104	14404
XP760	SLP	2018	13768	13522	13705

The economical optimum N rate of fertilization estimated by the linear-plateau, quadratic-plateau, and quadratic response models for each variety-site-year trial is presented in Table 2.5. The economical N rate of fertilization ranges for the linear-plateau, quadratic-plateau, and quadratic models were 54-219, 81-229, and 149-229 kg ha^{-1}, respectively. The linear-plateau model estimated a wider range of EONR of fertilization across the variety-site-year trials while the quadratic model estimated the narrowest range of EONR of fertilization. The average EONR of fertilization for the linear-plateau, quadratic-plateau, and quadratic models were 123, 155, and 181 kg ha^{-1}, respectively. The EONR of fertilization values presented in Table 2.5 highlight how

the EONR of fertilization varies between the response models, and the rice varieties, sites, years. A study by Belanger et al. (2000) demonstrated how varieties, sites, and annual environmental variations from year-to-year cause the EONR of fertilization to fluctuate between the response models. The EONR of fertilization differences between the three response models in the current study further supports why R^2 values should not be the only factor considered when determining which response model to choose for estimating the optimum N fertilization rate (Cerrato and Blackmer, 1990; Belanger et al., 2000; Alivelu et al., 2003; Harrell et al., 2011). The quadratic model resulted in a greater EONR of fertilization 87% of the time. Harrell et al. (2011) concluded that the quadratic model estimated a higher EONR of fertilization 61% of the time. In this study, the linear-plateau model estimated the highest EONR of fertilization 8% of the time while the quadratic-plateau model estimated the highest EONR of fertilization only 3% of the time. Choosing one model over another can effect N fertilization recommendations (Harrell et al., 2011). The differences observed between the EONR of fertilization values estimated by the response models highlight why a range of the N fertilizer recommendations are often recommended to growers. Recommending an optimum N rate range gives farmers leverage to adjust the N recommendations based on their soil and environmental conditions.

Table 2.5. Economical optimum nitrogen rates (EONR) of fertilization estimated by the linear-plateau, quadratic-plateau, and quadratic regression models for each variety-site-year trial.

Variety	Location	Year	Linear-Plateau EONR	Quadratic-Plateau EONR	Quadratic EONR
Aura 115	CM	2017	121	229	229
Aura 115	SLP	2017	113	162	176
CL153	CM	2017	134	201	206
CL153	SLP	2017	142	186	193
CL153	CM	2018	205	209	217
CL172	CM	2017	129	197	197
CL172	SLP	2017	219	141	200
CL172	CM	2018	218	179	209

(Table 2.5 Cont'd.)

Variety	Location	Year	Linear-Plateau EONR	Quadratic-Plateau EONR	Quadratic EONR
CL272	CM	2017	155	209	210
CL272	SLP	2017	79	101	172
CLJ01	CM	2018	140	184	192
CLJ01	SLP	2018	109	153	183
CLX6-1030	SJ	2018	54	96	158
CLX6-1030	CM	2018	122	175	181
CLX6-1111	CM	2018	116	160	188
CLX6-1111	RP	2018	121	167	183
CLX6-1111	SJ	2018	124	188	195
CLX6-1111	SLP	2018	70	81	153
CLX6-1133	CM	2018	87	124	156
CLXL745	CM	2018	106	126	179
Diamond	CM	2017	94	144	180
Diamond	SLP	2017	98	125	165
Diamond	CM	2018	149	205	208
Diamond	SJ	2018	81	103	158
FullPage RT 7321	CM	2018	88	140	157
FullPage RT 7321	RP	2018	119	180	185
FullPage RT 7321	SLP	2018	174	157	183
FullPage RT 7323	RP	2018	103	128	149
FullPage RT 7323	SLP	2018	146	91	166
PVL01	CM	2018	92	133	171
PVL01	SJ	2018	96	144	170
PVL01	SLP	2018	75	110	167
Titan	SLP	2017	203	156	192
Titan	CM	2018	97	142	162
XL760	CM	2017	131	190	189
XP113	CM	2018	110	158	163
XP760	CM	2018	105	145	161
XP760	SLP	2018	147	163	183

In Louisiana, the recommended N fertilizer application range for most rice varieties is between 135 – 180 kg ha^{-1} (Louisiana Rice Management Tips, 2018). The optimum N fertilization rates given in the Louisiana Rice Management Tips publication differentiates between the rice varieties and soil textures of the different locations in Louisiana. Clay soils typically have higher N rate recommendations compared to silt loam soils (Saichuk et al., 2008;

Harrell et al., 2011). However, the EONR of fertilization values calculated from our data show that the silt loam soil textures at Crowley, LA and Saint Joseph, LA resulted in the highest optimum N fertilizer recommendations. The models in the current study estimated some EONRs of fertilization to be outside of the recommended range for currently grown varieties. (Table 2.5.). The linear-plateau EONR of fertilization fell below the lowest recommended N range for Louisiana 69% of the time, while the quadratic-plateau EONR of fertilization fell below the lowest N fertilizer recommendation 28% of the time and 1% of the time the quadratic model fell below the lowest N fertilizer recommendation. Harrell et al. (2011) also found the linear-plateau model to estimate the lower optimum N fertilizer recommendations more than the quadratic-plateau and quadratic model. The quadratic EONR values fell into the Louisiana N recommendation range 46% of the time, compared to the 58% for the quadratic-plateau model and 18% for the linear-plateau model. The different EONR of fertilization estimated from each of the linear-plateau, quadratic-plateau, and quadratic models are not logical because only one EONR of fertilization can be determined for a given variety-site-year (Cerrato and Blackmer, 1990; Belanger et al., 2000; Harrell et al., 2011).

The estimated rice grain yield at the EONR of fertilization for the linear-plateau, quadratic-plateau, and quadratic models are present in Table 2.6. When the EONR of fertilization was averaged across all variety-site-years for each of the models, the results were very similar (11,513, 11,475, and 11,621 kg ha^{-}). The quadratic model estimated the greatest range of yields at the EONR of fertilization (6554 – 14,497 kg ha^{-1}). The linear-plateau model estimated the second greatest range of yields at the EONR of fertilization (8298 – 14,048 kg ha^{-1}). The quadratic-plateau model estimated the smallest range of yield at the EONR of fertilization (8363 – 14152 kg ha^{-1}). The highest estimated EONR of fertilization across variety-site-years didn't

estimate the highest yield as compare to the other variety-site-years. The linear-plateau model tended to produce reasonable and similar grain yields and produced low EONRs of fertilization as compared to the quadratic-plateau and quadratic models. Rice grain yield can be significantly affected by the amount of N fertilizer inputs during the growth and development of rice. Inaccurate N fertilizer rate applications can negatively impact rice grain yield and reduced profitability of rice production. The EONR of fertilization are highly dependent on current N fertilizer and rice prices (Harrell et a., 2011). The one economical optimum N fertilization rate that can exist for a given variety-site-location, will be affected by any change in input (N fertilizer) or output (rice grain yield) prices. The optimum N rate estimation models evaluated in this study had similar R^2 values and grain yields, however the estimated range of EONR of fertilization were quite different. Justification for choosing one model over the others could not be made.

Table 2.6. Yield (kg ha^{-1}) at the economical optimal nitrogen rate (EONR) of fertilization for linear-plateau, quadratic-plateau, and quadratic models for each individual trial.

			Linear-Plateau	Quadratic-Plateau	Quadratic
Variety	Location	Year	EONR Yield (kg ha^{-1})	EONR Yield (kg ha^{-1})	EONR Yield (kg ha^{-1})
Aura 115	CM	2017	12391	12799	12799
Aura 115	SLP	2017	11848	11917	12055
CL153	CM	2017	10960	11169	11223
CL153	SLP	2017	8925	8930	8969
CL153	CM	2018	10539	10092	6554
CL172	CM	2017	9482	9682	9690
CL172	SLP	2017	11421	10768	11005
CL172	CM	2018	10392	9719	9931
CL272	CM	2017	10377	10409	10417
CL272	SLP	2017	10039	10014	10321
CLJ01	CM	2018	12313	12292	12449
CLJ01	SLP	2018	9216	9256	9424
CLX6-1030	SJ	2018	10118	10222	10758
CLX6-1030	CM	2018	12779	12862	13037

(Table 2.6 Cont'd.)

Variety	Location	Year	Linear-Plateau EONR Yield (kg ha^{-1})	Quadratic-Plateau EONR Yield (kg ha^{-1})	Quadratic EONR Yield (kg ha^{-1})
CLX6-1111	CM	2018	12261	12271	12631
CLX6-1111	RP	2018	10875	10820	11010
CLX6-1111	SJ	2018	12818	13026	13110
CLX6-1111	SLP	2018	10711	10678	11096
CLX6-1133	CM	2018	11107	11123	11683
CLXL745	CM	2018	12401	12392	12854
Diamond	CM	2017	9060	9162	9541
Diamond	SLP	2017	11240	11222	11476
Diamond	CM	2018	13276	13346	13409
Diamond	SJ	2018	11171	11127	11763
FullPage RT 7321	CM	2018	13944	14152	14497
FullPage RT 7321	RP	2018	12756	12940	12987
FullPage RT 7321	SLP	2018	13895	13308	13530
FullPage RT 7323	RP	2018	12101	12070	12322
FullPage RT 7323	SLP	2018	13690	13163	13559
PVL01	CM	2018	10833	10881	11297
PVL01	SJ	2018	8298	8363	8597
PVL01	SLP	2018	8627	8658	8926
Titan	SLP	2017	11685	11165	11343
Titan	CM	2018	11453	11539	12044
XL760	CM	2017	12391	12544	12545
XP113	CM	2018	12865	12926	13075
XP760	CM	2018	14048	14112	14392
XP760	SLP	2018	13768	13502	13699

The quadratic model estimated the greatest EONR of fertilization and rice grain yield at EONR of fertilization more times than the linear-plateau and the quadratic-plateau response models did in this study. However, since one true EONR of fertilization can exist for each variety-site-year, these three models are purely empirical (Harrel et al., 2011). The EONR of fertilization will vary between the different rice varieties, different locations of where the crop is being grown, and different economical estimates from year to year. Determining the actual economic estimates of the response models will portray a more logical outlook of the response models in determining which model is the most economically efficient. Rice grain yield at the

EONR of fertilization, economic estimates of net returns and net return margins of choosing one models EONR of fertilization over another for each variety-site-year trial are presented in Table 2.7. The net returns and net return margins were calculated to determine which response model was the most economically efficient. Net returns are calculated by determining the difference of the price of rice for the check plot (no N fertilizer additions) and the price of rice at the EONR of fertilization for each of the three response models. In this study, the price of rice that was used in the calculation was $0.245per kg rough rice and the cost of N was $0.538 per kg N. The net return margins are calculated by determining the difference between the selected response model and the response model with the highest net return for each variety-site-year trial. The response model with the highest net returns is shown by the response model that estimates a zero for a certain variety-site-year trial. The quadratic response model was estimated to have a higher net return margin 71% of the time compared to the linear-plateau and quadratic-plateau response models. The linear-plateau response model estimated to have a higher net return margin only 26% of the time. Harrell et al. (2011) found the opposite with the linear-plateau response model estimating the highest net return margin 70% of the time compared to the quadratic and quadratic-plateau response models. This signifies how the response model providing the greatest net returns can change throughout the years, locations, and rice varieties. The trend of this data in this study indicates the net returns derived from the response models were in the following order: quadratic > linear-plateau > quadratic-plateau. However, the trend of the R^2 data derived from the response models in Table 2.3 were in the following order: quadratic-plateau > quadratic > linear-plateau. The data from this study shows how net return estimations can be shifted between the three response models. The differences in these two trends indicates why

other factors besides the R^2 data should be evaluated when choosing which response model should be used to predict the EONR of fertilization.

Table 2.7. Rice grain yields, net returns, and net return margins for linear-plateau, quadratic-plateau, and quadratic response models for each variety-site-year.

			Yield †			Net Returns			Net Return Margins‡		
Variety	Location	Year	LP	QP	Q	LP	QP	Q	LP	QP	Q
			----------kg ha^{-1}----------			----------$ ha^{-1}----------					
Aura 115	CM	2017	12391	12799	12799	1510	1552	1552	-42	0	0
Aura 115	SLP	2017	11848	11917	12055	959	950	976	-17	-26	0
CL153	CM	2017	10960	11169	11223	1555	1570	1581	-26	-11	0
CL153	SLP	2017	8925	8930	8969	569	547	553	0	-22	-17
CL153	CM	2018	10539	10092	6554	1421	1309	438	0	-112	-983
CL172	CM	2017	9482	9682	9690	1340	1352	1354	-14	-2	0
CL172	SLP	2017	11421	10768	11005	876	758	784	0	-118	-92
CL172	CM	2018	10392	9719	9931	1022	878	914	0	-144	-108
CL272	CM	2017	10377	10409	10417	1396	1374	1376	0	-21	-20
CL272	SLP	2017	10039	10014	10321	777	759	796	-19	-37	0
CLJ01	CM	2018	12313	12292	12449	1763	1734	1768	-5	-34	0
CLJ01	SLP	2018	9216	9256	9424	793	779	804	-11	-25	0
CLX6-1030	SJ	2018	10118	10222	10758	1199	1202	1299	-101	-98	0
CLX6-1030	CM	2018	12779	12862	13037	1785	1777	1817	-31	-40	0
CLX6-1111	CM	2018	12261	12271	12631	1828	1806	1879	-52	-73	0
CLX6-1111	RP	2018	10875	10820	11010	814	775	813	0	-38	0
CLX6-1111	SJ	2018	12818	13026	13110	1782	1799	1816	-33	-17	0
CLX6-1111	SLP	2018	10711	10678	11096	844	830	893	-50	-64	0
CLX6-1133	CM	2018	11107	11123	11683	1441	1425	1545	-104	-120	0
CLXL745	CM	2018	12401	12392	12854	1802	1789	1874	-72	-85	0
Diamond	CM	2017	9060	9162	9541	1482	1480	1553	-72	-73	0

(Table 2.7. Cont'd.)

			Yield †			Net Returns			Net Return Margins‡		
Variety	Location	Year	LP	QP	Q	LP	QP	Q	LP	QP	Q
			----------kg ha^{-1}----------			----------$ ha^{-1}----------					
Diamond	SLP	2017	11240	11222	11476	810	791	832	-22	-41	0
Diamond	CM	2018	13276	13346	13409	2291	2278	2292	-1	-14	0
Diamond	SJ	2018	11171	11127	11763	1457	1434	1561	-104	-126	0
FullPage RT 7321	CM	2018	13944	14152	14497	1940	1963	2038	-98	-75	0
FullPage RT 7321	RP	2018	12756	12940	12987	1264	1276	1285	-21	-9	0
FullPage RT 7321	SLP	2018	13895	13308	13530	1291	1156	1197	0	-135	-94
FullPage RT 7323	RP	2018	12101	12070	12322	1053	1032	1082	-29	-50	0
FullPage RT 7323	SLP	2018	13690	13163	13559	1046	947	1004	0	-100	-43
PVL01	CM	2018	10833	10881	11297	1442	1432	1513	-71	-81	0
PVL01	SJ	2018	8298	8363	8597	966	956	1000	-33	-43	0
PVL01	SLP	2018	8627	8658	8926	747	736	771	-24	-35	0
Titan	SLP	2017	11685	11165	11343	1046	944	968	0	-102	-78
Titan	CM	2018	11453	11539	12044	1673	1670	1783	-110	-113	0
XL760	CM	2017	12391	12544	12545	1541	1547	1547	-7	-1	0
XP113	CM	2018	12865	12926	13075	1782	1771	1805	-23	-34	0
XP760	CM	2018	14048	14112	14392	1909	1903	1963	-54	-60	0
XP760	SLP	2018	13768	13502	13699	1418	1345	1382	0	-74	-36

2.4. Conclusions

The economic optimum N rate of fertilization determined for currently used and newly developed rice cultivars will allow rice producers to make N fertilizer decisions that are most profitable and more prone to produce high rice grain yields. Developing a profitable N fertilizer recommendation that still produces high rice grain yields is an important goal of rice producers. The input (N fertilizer) and output (rice grain yield) prices are used to determine the recommended optimum N fertilizer rate. The EONR will be affected if any change exists in input or output prices. Rice grain yield is affected by N fertilizer applications directly. Inaccurate determination of N fertilization rate can result in a negative impact on rice grain yield and potential economic losses. Therefore, determining an accurate, useful, and reliable EONR of fertilization, for current and new rice varieties, is important to rice producers and rice agronomists.

The EONR of fertilization for individual rice varieties in our study was estimated by fitting the linear-plateau, quadratic-plateau, and quadratic response models to the response of rice grain yields to N fertilizer applications. The R^2 averages for the linear-plateau, quadratic-plateau, and quadratic fertilizer response models were all found to be similar (linear-plateau: 0.80; quadratic-plateau: 0.82; quadratic: 0.81). The high R^2 values were an indication that each of the response models fit the data equally well and that each should be able to estimate useful EONR of fertilization for the individual variety-site-years. However, the estimated EONR of fertilization for a given variety-site-year in this data set was drastically different between the linear-plateau, quadratic-plateau, and quadratic models despite the similar R^2 values. Careful consideration should be used when choosing an estimation model to determine the EONR of fertilization. Selecting an estimation model based solely from the R^2 criteria may result in

unrealistic EONR of fertilization. Choosing the EONR of fertilization from the less accurate response model can lead to an insufficient or over application of N fertilizer and produce a negative impact on rice growth and development. There can only be one true EONR of fertilization for a given variety. Therefore, other factors beyond just R^2 alone need to be taken into consideration when choosing which response model best fits a data set and should be used to estimate the EONR of fertilization for an individual variety.

The linear-plateau model estimated lower rice grain yields and EONRs of fertilization compared to the quadratic-plateau and quadratic response models. The quadratic model produced the highest EONRs of fertilization and rice grain yields. The differences between the two fertilizer response models EONR of fertilization and rice grain yield further explains why justification should be given when choosing which response model should be used to fit the data of the rice grain yield response to N fertilization. In our study, the linear-plateau models estimated EONR of fertilization was more likely to fall below the Louisiana N fertilizer recommendation range (130 to 180 kg ha^{-1}) compared to the other two response models. The quadratic response model estimated EONR's of fertilization within the Louisiana N fertilizer recommendation range 46% of the time. Determining which response model would be the most reliable to estimate accurate EONRs of fertilization for currently used and newly released varieties is important to rice growers and agronomists. The selection of the model producing the most appropriate EONR of fertilization will ultimately increase the profitability and economical return estimates of growing rice. Conducting more research evaluating the different N fertilization response models will help determine which response model most accurately estimates EONRs of fertilization for currently used and newly released cultivars.

Chapter 3. Evaluation of the Linear Relationship Between GreenSeeker and UAS Derived Normalized Difference Vegetation Index (NDVI)

3.1. Introduction

Rice is a major cereal crop belonging to the grass family and providing an abundance of mineral nutrition to the world's population (*Oryza sativa*). Rice is grown in several countries around the world producing approximately 162 million hectares of rice (USDA, 2019). The United States produces about one million hectares of rice in the states of California, Arkansas, Mississippi, Texas, and Missouri (USDA, 2019). In 2018, Louisiana was ranked as the third leading state for rice production in the United States. The semi-aquatic plant can be grown in a diverse set of environments, but greatly thrives in wet and warm conditions.

The average days to maturity rice ranges between 105 to 145 days depending on the rice variety and climate conditions. For rice to be managed easier throughout the growing season, rice should be planted within the appropriate planting date ranges. Louisiana State University (LSU) AgCenter researchers conduct several date-of-planting studies used to determine and adjust optimum planting date recommendations of new and popular rice varieties (Saichuk and Harrell, 2014). The recommended planting date range for Southwest Louisiana is between March 10 and April 15. The recommended planting date range for North Louisiana is between April 1 and May 5. The growth of rice will be easier managed, and rice will have greater potential of producing maximum grain yield if rice is planted during the planting date range recommended by the LSU AgCenter (Saichuk and Harrell, 2014). The developmental stages of rice are designated between two categories: 1) vegetative growth phases and 2) reproductive growth phases. The vegetative phase includes 4 stages: 1) emergence, 2) seedling development, 3) tillering, and 4) internode elongation (Dunand and Saichuk, 2014). Active tillering, plant height increase, and leaf emergence begin to take place during the vegetative growth phases. The reproductive phase

consists of five stages: 1) pre-booting, 2) booting, 3) heading, 4) grain-filling, and 5) maturity (Dunand and Saichuk, 2014). The characteristics of the reproductive growth phase is increased plant height, tiller number decrease, emergence of the flag leaf, heading, and flowering.

Monitoring the mineral nutrition of rice is important for the growth and development of rice. There are three main macronutrients supplied to rice to provide adequate mineral nutrition: nitrogen (N), phosphorus (P), and potassium (K). Maximum rice grain yields, increased profitability, enhanced nutrient efficiency, and reduced inputs will be accomplished if a balance supply of these nutrients is provided to the rice crop (Fageria, 2001). Nitrogen is the most abundantly applied fertilizer input stimulating the growth of rice and giving rice its dark-green pigmentation (Leghari, 2016). An inadequate supply of N will cause a N deficiency to occur within a rice field. Symptoms of N deficiency are present in the field as chlorosis of the older leaves, reduced tillering, and shorter plant heights. The extent of these deficiencies will depend upon soil type, agronomic management practices, and crop history (Saichuk and Harrell, 2014). Excessive application of N can have a negative impact on rice. An over-application of N result in excessive vegetative growth, increased disease pressure, lodging, and ultimately economic losses. A proper management strategy of rice should be developed to diminish the possibility of N deficiency in rice or an over-application of N.

Nitrogen can be supplied to rice by different synthetic fertilizers. The behavior of N within the soil and plant is dynamic. Nitrogen exist in both the organic and inorganic forms. Inorganic-N is more abundantly found and used in plants (Fageria, 2001). Nitrate (NO_3^-) and ammonium (NH_4^+) are the two inorganic-N forms available for uptake by rice. These two inorganic N forms have potential to be quickly lost through the major loss pathways in the N-cycle. Ammonium-N fertilizer sources are recommended to be used over NO_3^- fertilizer sources

because rice is grown in a flooded, anaerobic environment (Snyder and Slaton, 2002). Ammonium-N remains stable under the anaerobic field conditions of rice, whereas NO_3^- is unstable and lost quickly in an anaerobic environment from denitrification. Another major loss pathway for NO_3^- due to its solubility and mobility characteristics is leaching (Havlin et al., 2014). The leaching of NO_3^- has a negative impact on crop production systems and surrounding environments when NO_3^- is leached from the agricultural soils. The fertilizer sources for rice are incorporated into the soil by the flood establishment to help eliminate the occurrence of N-fertilizer losses. If the flood establishment is not established in a timely manner or maintained throughout the growing season, NH_4^+ can be converted to NO_3^- by nitrification. The N-loss pathways of N fertilizers are highly influenced by environmental conditions, management practices, N application rates, and irrigation techniques.

The application method of N fertilizer can help eliminate N losses and enhance the growth and development of rice. The preferred application method of N fertilizer in rice is by using a two-way split application. The two-way split application method is most practical in areas where N losses are prone to occur due to a delayed flood establishment and maintenance of the flood (Snyder and Slaton, 2002). There are two N fertilizer application times for this method. The first fertilizer application is done at pre-flood, at the 4- to 5- leaf growth stage (or just before tillering). In Louisiana, the recommended N rate applied at this growth stage is two-thirds of the seasonal recommended rate provided by the LSU AgCenter on a variety basis. Adjustments of the recommended pre-flood N rate should be made depending upon soil texture, rice variety, and environmental conditions at the time of fertilizer application. After the pre-flood N fertilizer is applied to a dry-soil bed, a flood should be established within one to three days. The flood establishment will incorporate the N fertilizer into the soil decreasing the chances of N losses

through nitrification and denitrification (Snyder and Slaton, 2002). The flood establishment is important to eliminate moisture deficiencies, increase availability of essential plant nutrients, minimize weed competition, and provide an appropriate climate for the growth and development of rice (Harrell and Saichuk, 2014).

The second N fertilizer application time is completed at mid-season, at the beginning of reproductive growth between panicle initiation [green ring or beginning internode elongation (IE)] and panicle differentiation (1/2-inch IE) growth stages. Mid-season N application rates are determined by the rice grower or consultant based on their observations of the characteristics of the crop. Fertilizer N rates recommended at mid-season can be inaccurately determined because some in-season characteristics cannot be seen by the human eye. Mid-season N fertilizer applications are vital to the growth and development of rice in the latter growth stages. Mid-season N fertilizer applications are important in times when the pre-flood N fertilizer applications do not supply all the seasonal N needs of the crop or when N was inadequately taken up by the rice plant. Nitrogen fertilizer applications applied at mid-season during the panicle initiation growth stage, have a profound effect on rice grain yield and quality (Nguyen & Lee, 2006). Therefore, it is crucial to have a method or tool to accurately determine mid-season N fertilizer rates for rice.

Precision agricultural tools emerged in the mid-1980's to improve the determination of mid-season N rates and increase the efficiency of N applications. Rice producers must make strategical, tactical, and operational management decisions based on the future of the farm, potential yields, profitability, environmental quality, crop varieties, and fertilization requirements (Bouma, 1997). Rice producers today are growing rice across larger acres and larger production systems, making it difficult to monitor the growth of rice and accurately determine the N

requirements. Before the advancement of precision farming tools, the N status of rice and determination of mid-season N fertilizer requirements have been a challenge to accurately determine. In the past, a crop yield goal was used to help estimate N fertilization requirements. The crop yield goal should be based on crop yield history, soil characteristics, management practices, and the crop variety being planted. A disadvantage of using the crop yield goal in rice to determine N fertilizer needs is that crop yield goal is greatly affected by spatial and temporal variation. Precision agricultural tools can determine N fertilizer rates based on site-specific regions creating variable N rates in a rice field. Data collected by precision agricultural tools can be used to optimize N fertilizer recommendations which in turn will improve the profitability, decrease N losses, and improve environmental quality.

Remote sensing technology is a popular precision agricultural tool in estimating practical on-site N fertilizer rates and eliminating uncertainties of a producer's N fertilizer rates determinations. Remote sensing technology is a site-specific management system accounting for the spatial and temporal variation throughout a rice field. Variables of a crops growth and development can be obtained in a fast, reliable, non-destructive method with remote sensing technology (Nguyen et al., 2006). Crop field assessments have progressed with the usage of remote sensing technologies delivering quantitative data of the crop's spatial variability properties (Elarab, 2016).

Active crop canopy sensors are a type of remote sensing tool used to evaluate the health and N status of crops (Xue et al., 2004; Lee et al., 2008). Active crop canopy sensors could be extremely effective in a flooded production system, such as rice, when mid-season N fertilizer requirements are difficult or inaccurately determined. Active crop canopy sensors have shown the potential in lowering the amount of N applied to a rice field which, in turn, will optimize

grain yield and N use efficiency (NUE) (Foster et al., 2017). The predominant remote sensing and active crop canopy sensor used to aid in estimating the health status of rice and N fertilizer requirements of rice during major growth stages is the GreenSeeker handheld sensor. The GreenSeeker handheld sensor is equipped with an active, pre-calibrated optical light sensor. The active light sensor of the GreenSeeker measures the canopy reflectance of rice using two specific wavelength regions on the electromagnetic spectrum: red (670 ± 10 nm) and near-infrared (780 ± 10 nm). The active crop canopy reflectance measurement of rice is calculated using the normalized difference vegetation index (NDVI) computed from the red and near-infrared values collected by the GreenSeeker in the following NDVI equation:

$$NDVI = \frac{(NIR + R)}{(NIR - R)} \quad [3.1]$$

where:

NIR = Reflectance at the near-infrared region of the electromagnetic spectrum

R = Reflectance at the red region of the electromagnetic spectrum

The GreenSeeker derived NDVI values can be used to evaluate the pre-flood N fertilizer response in rice which can be used to predict mid-season N fertilization needs. (Xue and Yang, 2008). GreenSeeker derived NDVI has increased farmers ability to make crucial management decisions, estimate more suitable in-season N fertilization requirements, and create a more sustainable production approach (Yao et al., 2012). Many studies have been done to show GreenSeeker derived NDVI to be a more reliable source in estimating a crops overall health status unlike past techniques of leaf color charts and chlorophyll meters (Girma et al., 2006; Lee et al., 2008).

Advancements in remote sensing technology have developed an air-borne, remote sensing tool that has potential to collect NDVI measurements of a rice field. Unmanned aerial

systems (UAS) equipped with remote sensors can provide information on a crop's growth and development from a remote location from outside of the field. Spectral cameras attached onto the UAS collect data on the crop from a remote location. The UAS mounted spectral cameras have been shown to produce a similar ability to evaluate crop responses compared to other remote sensing tools (Rasmussen et al., 2015). One advantage of UAS mounted sensors is that NDVI readings are collected from a higher spatial resolution, unlike the GreenSeeker which collects NDVI readings at a lower spatial resolution. Despite the differences of spatial resolution between the two types of remote sensors research has shown a correlation between air-borne and ground-sensor based NDVI measurements (Primicero et al., 2012).

The GreenSeeker collects NDVI readings on a point-to-point basis accounting for information only in site-specific portions of a rice field. UAS mounted sensors collects NDVI readings on a whole field basis increasing the field scale average of the data collection and accounts for variation across the entire field. Data is generated in a faster, more rapid method through the autonomous flight navigation of the UAS through pre-programmed flight plans (Huang et al., 2013). The ability to maneuver within the rice field and from field to field is more difficult with the handheld GreenSeeker. UAS mounted sensors are easily to use to collect data within and between rice fields because they can be flown autonomously. The faster data collection and ease of use of the UAS mounted sensors allows farmers to spend less time on field assessments and make timelier, more efficient crop decisions (Zhu et al., 2009).

The GreenSeeker has an active light sensor that is used to collect NDVI measurements, while the UAS has a passive light sensor. A passive light sensor relies on the sunlight for the tools light source and can have a negative impact on the data collected from the UAS remote sensor. Variability of the NDVI data can occur when using a tool with a passive light sensor.

Intensity of the sunlight, bidirectional reflectance, and environmental conditions are three of the main factors that cause variability to exist in the UAS's remote sensor data collection. Variability can be overcome with the appropriate precautions and setup before the flight takes place. Flying the UAS in the appropriate flight conditions will help eliminate the influence of the light from the sun on the multispectral images collected. A pre-flight tactic to help decrease variability among vegetative indices is to include georeferencing points to help stabilize the geographical and geometric data (Lelong et al., 2008). Advanced technological software applications have been developed for UAS's to stitch the multispectral images together accounting for variation in the images and decreasing the chances of the UAS remote sensors producing invaluable information.

Many studies have been conducted using the UAS technology evaluating chlorophyll and N content in cereals (Li et al., 2015; Zheng et al., 2016), weed mapping (Stropiana et al., 2018), and disease damage (Yang et al., 2017). UAS mounted remote sensor have shown a similar, high correlation between yield and NDVI measurements taken at panicle initiation like the GreenSeeker has shown in the past (Swain et al., 2010). The GreenSeeker and UAS mounted remote sensors, used together or separately, provide producers with valuable information to determine different crop needs. GreenSeeker and UAS mounted sensors have the ability to lower N fertilizer inputs, create a balance between N demand and N supply, determine disease infestations, and increase the economic value of rice.

In-season determination of the health status of rice has been done with the GreenSeeker derived vegetative indices. If a strong relationship exists between GreenSeeker and UAS mounted remote sensor derived data, then there is a possibility that the UAS remote sensor could also be a possible source in determining mid-season N needs of rice. However, variability of

collected NDVI data is still a concern due to the passive light sensor used on UAS's. If the variability of the UAS remote sensor derived NDVI data can be accounted for, then the UAS remote sensor will provide more timely and faster NDVI data as compared with the handheld sensors. The objective of this study was to evaluate the linear relationship between GreenSeeker and UAS remote sensor derived NDVI in rice.

3.2. Materials and Methods

3.2.1. Site Description, Planting Method, Treatment Structure, and Trial Establishment

Table 3.1. presents the soil series, taxonomy, and taxonomic classification for each location in 2017 and 2018. Site one was established in 2017 and 2018 at the Rice Research Station in Crowley, LA on a Crowley silt loam (Fine, smectitic, thermic Typic Albaqualfs) soil. In 2017, ten rice cultivars were evaluated, while fifteen rice cultivars were evaluated in 2018.

The second site was located in St. Landry Parish in Palmetto, LA in 2017 and 2018 on a Dundee silty clay loam (Fine-silty, mixed, active, thermic Typic Endoaqualfs). The data were collected from ten rice cultivars in 2017 and eleven rice cultivars in 2018.

The third site was located in Calcasieu Parish in Iowa, LA on a Crowley-vidrine complex (Fine, smectitic, thermic Typic Albaqualfs and Aquic Glossudalfs) in 2018. There were twelve rice cultivars evaluated at this site.

The fourth site was located in Saint Joseph, LA in Tensas Parish in 2018 on a on a Commerce silt loam (Fine-silty, mixed, superactive, nonacid, thermic Fluvaquentic Endoaquepts) and sharkey clay (Very-fine, smectitic, thermic Chromic Epiaquerts). There were seven rice cultivars evaluated at this site.

The fifth site was located in Richland Parish near Monroe, LA in 2018 on a Herbert silty clay (Fine-silty, mixed, active, thermic Aeric Epiaqualfs) There were seven rice cultivars evaluated at this site.

Table 3.1. The soil series, taxonomy, and taxonomic classification for each individual location-year.

Location	GPS Location	Year	Series	Taxonomy	Taxonomic Classification
Crowley, LA	30°14’50.8”N 92°20’56.8”W	2017-2018	Crowley	Silt loam	Fine, smectitic, thermic Typic Albaqualf
Palmetto, LA	30°47’41.9”N 91°53’29.9”W	2017-2018	Dundee	Silty clay loam	Fine-silty, mixed, active, thermic, Typic Endoalqualf
Iowa, LA	30°13’08,9”N 93°03’52.7”W	2018	Crowley	Vidrine-complex	Fine, smectitic, thermic Typic Albaqualf & Aquic Glossudalf
Monroe, LA	32°23’23.8”N 91°58’47.2”W	2018	Herbert	Silty clay	Fine-silty, mixed, active, thermic, Aeric Eqiaqualf
Saint Joseph, LA	31°56’41.3”N 91°13’54.0”W	2018	Commerce	Silt loam	Fine-silty, mixed, superactive, nonacid, thermic Fluvaquentic Endoaquepts

Important agronomic dates including planting date, pre-flood N application timing, flood establishment, and sensor reading dates for each location-year are presented in Table 3.2. The seed treatment for the rice varieties consisted of mancozeb (Dithane - fungicide), gibberellic acid (Release), zinc plus (10% Zn & 4.9% combined S), anthraquinone (AV-1011 - bird repellent), and chlorantraniliprole (Dermacor – insecticide). The hybrid seed was treated with clothianidin (Nipsit Inside), fludioxonil (Spirato 480FS), fludioxonil (Maxim 4FS), gibberellic acid, zinc, and anthraquinone (AV-1011 - bird repellent). A small-plot grain drill (Almaco, Iowa) was used to plant the rice seeds to a depth of 1.27 cm at a seeding rate of 366 seeds per m^2 for varieties and 111 seeds per m^2 for the hybrid rice varieties. Each plot was a length of 4.88 m consisting of 7 rows with 20 cm spacing. Eight pre-flood N rate treatments were used for the conventional rice varieties (0, 34, 67, 101, 135, 168, 202, and 235 kg ha^{-1}). Six pre-flood N rate treatments were used for the hybrid rice varieties (0, 67, 101, 135, 168, and 202 kg ha). The pre-flood N rate treatments were broadcast applied at the 4- to 5- leaf rice growth stage. A flood was established one to three days after the pre-flood N fertilizer application to incorporate the N fertilizer into the soil and root zone. A small plot combine equipped with a HarvestMaster H2 high capacity graingage (Logan, Utah) was used to determine the weight and moisture of the harvested rice plots.

Table 3.2. Important agronomic dates including planting date, pre-flood N application timing, flood establishment, and sensor reading dates for each location-year.

Location	Year	Planting Date	Pre-Flood N Application	Flood Establishment	Sensor Readings	Growth Stage at Sensor Readings
Crowley, LA	2017	13-Mar	2-May	3-May	26-May	PD
Palmetto, LA	2017	21-Mar	11-May	12-May	8-Jun	PD

(Table 3.2 Cont'd.)

Location	Year	Planting Date	Pre-Flood N Application	Flood Establishment	Sensor Readings	Growth Stage at Sensor Readings
Crowley, LA	2018	14-Mar	1-May	3-May	28-May	PD
Palmetto, LA	2018	27-Mar	17-May	18-May	7-Jun	PD
Iowa, LA	2018	20-Mar	2-May	3-May	25-May	PI
Monroe, LA	2018	1-May	23-May	25-May	20-Jun	PD
Saint Joseph, LA	2018	3-May	22-May	23-May	19-Jun	PI

3.2.2. Remote Sensing Data Collection

Sensor data was collected between the panicle initiation and panicle differentiation growth stages of rice. A GreenSeeker handheld optical active sensor was used to collect data from each variety-site-year trial. The Red (670 ± 10nm) and NIR (780 ± 10nm) wavelength regions of the electromagnetic spectrum were collected by the active light sensor of the GreenSeeker. The red and NIR measurements collected by the GreenSeeker were used to compute the NDVI algorithm (equation 3.1) and measure the canopy reflectance of the rice canopy for each variety-site-year trial. Canopy reflectance data was collected manually by consistently holding the GreenSeeker sensor head in a nadir position at about 1 m above the rice canopy. The GreenSeeker was walked at a constant pace through each of the rice plots when collecting NDVI readings from each variety-site-year trial for this study.

The UAS used to collect sensor data for this study was a Phantom 4 Pro unmanned aerial vehicle (UAV) mounted with a RedEdge-M multispectral camera by MicaSense. Multispectral images were collected with five narrowband electromagnetic wavelength regions: blue (475 nm center, 20 nm bandwidth), green (560 nm center, 20 nm bandwidth), red (668 nm center, 10 nm

bandwidth), red-edge (717 nm center, 10 nm bandwidth), and near-infrared (840 nm center, 40 nm bandwidth). NDVI was calculated by using the red (668 nm center, 20 nm bandwidth) and near-infrared (840 nm center, 40 nm bandwidth) wavelengths of the RedEdge-M multispectral camera as shown in equation 3.1. The UAS was flown autonomously at an altitude of 30 m and collected multispectral images at a rate of 10 m/s with a 75% side and frontal overlap.

Flight operations of the UAS were controlled through the DJI GO 4 application software. DJI GO 4 connects the Phantom 4 Pro to the UAS remote controller used to fly the UAS manually or autonomously. Main controller settings, visual navigation settings, remote controller settings, image transition settings, aircraft battery information, and gimbal settings were all controlled through DJI GO 4 software.

The RedEdge-M multispectral camera by MicaSense multispectral camera operations and flight route were controlled through the MicaSense Atlas application software. The MicaSense Atlas software was used for collecting and process the data and generate a reflectance map. The flight route can be uploaded into MicaSense Atlas in 2 ways: 1) manually drawn by the UAS remote pilot, which consists of a series of waypoints (x,y,z coordinates) or 2) UAS remote pilot can pre-choose the field or area of interest for the flight in the persons personal Atlas account and upload the field from the Atlas account to use as the flight boundaries. The speed, altitude, and overlap percentage is set to the desired settings for the collection of multispectral images after the flight route is established. For this particular study, the speed was set to 10 m/s, the altitude was set to 30 m, and the overlap percentage was set to 75%. The application software will automatically calculate the flight time and the number of images the multispectral camera will take during in the flight is dependent on the flight size and area.

The calibration of the RedEdge-M multispectral camera by MicaSense is done to help stabilize and decrease the chances of variability from the collected multispectral images. The calibration of the RedEdge-M was calibrated using a reflectance panel and the MicaSense Atlas software. The calibration reflectance panel was placed flat on the ground, away from any objects that could affect the light or present shadows over the panel. The UAS remote sensor was held over the reflectance panel with the person holding the UAS remote sensor back towards the sun. The RedEdge-M multispectral camera was held directly over the reflectance panel at chest level, avoiding any chance of shadows, and pointed so that the panel was centered in the field of view. The picture of the calibrated reflectance panel was saved on the memory card with the other multispectral images that were collected and was used to normalize the data in PIX4D.

A pre-flight checklist and mission summary were presented before the flight was set to launch. The mission summary provided the UAS remote pilot with the following information: camera updates, capture mode, internal storage availability, flight mode, picture distance, flight size coverage, and flight time. Once the MicaSense Atlas application software ensured all these settings were completed successfully, the UAS was then ready to be launched to conduct the assigned missions for each variety-site-year trial.

3.2.3. Multispectral Image Stitching and Data Manipulation/Collection

The multispectral images collected from the Phantom 4 Pro mounted with the RedEdge-M multispectral camera by MicaSense were stitched together and manipulated through the PIX4D software after the flight was conducted and finished. A new project was created for each site-year set of multispectral images in the PIX4D software. After a new project was selected in the software, PIX4D automatically goes through a series of steps to prepare the multispectral images for stitching. The multispectral images were then selected from the appropriate folder on

the computer desktop and added to the PIX4D software to begin the stitching process, PIX4D automatically set the image properties to the appropriate coordinate system (World Geodetic System 1984; Coordinate System: WDG 84 (egm96)), automatically set the geolation and orientation and accuracy, and the camera model was selected (Ag Multispectral). The output coordinate system selected was auto detected to WGS 84 / UTM zone 15N with the 'meters unit' selected. The processing options template selected was the 'ag multispectral' under the standard set of options. Then 'finished' was pressed and the next step before processing the images was the radiometric process and calibration to accurately develop a reflectance map.

Before the multispectral image processing could occur, the radiometric processing and calibration settings had to be set. The radiometric processing and calibrations tabs were found on the left-hand side, bottom set of tab options under the 'processing' tab. The index calculator was then selected under the DSM, ortho-mosaic, and index tab. The appropriate images of the calibrated reflectance panel and numbers provided on the calibrated reflectance panel were added to each of the appropriate sections (blue, green, red, NIR, and red-edge). The resolution was set to automatic and the GeoTIFF and merge tiles were both checked for the reflectance map. For this particular study, NDVI, was the vegetative indices evaluated and selected. The export grid size for index values as point shapefiles and index values and rates as polygon shapefiles were changed to 5 cm/grid. The processing of stitching the multispectral images together could begin after those settings were applied. The processing of the multispectral images goes through 3 steps: 1) initial processing, 2) point cloud and mesh, and 3) DSM, orth-mosaic, and index.

The NDVI reflectance map was then generated once PIX4D completed the multispectral images stitching process. After the processing of the multispectral images was completed, the 'Index Calculator' tab on the left-hand side bar was selected to input the appropriate index

calculator equation. In the index calculator tab, there are three steps. The first is the reflectance map step, which shows the wavelength band measurements used to develop the reflectance map. The second step shows the regions of the map. For this study, the whole map was selected for the regions of the reflectance map. The third step was for developing the actual reflectance map by inputting the appropriate NDVI equation. The NDVI equation was the formula input for this study. The number of classes chosen were twenty, set at equal areas, with a minimum value of 0 and a maximum value of 1. The reflectance map was then exported as index values and rates as polygon shapefiles (SHP) with grid size [cm/grid], colored index map (GeoTIFF), and GeoJPG (JPG).

Once the NDVI reflectance map was developed and exported from PIX4D, the NDVI values could then be collected from the NDVI reflectance map. The SHP file developed in PIX4D of the NDVI reflectance map was then imported into Farm Works Trimble Ag software. The Farm Works Trimble Ag Software allowed for the manual collection of the NDVI values from each reflectance map for each individual variety-site-year trial.

3.2.4. Data Analysis

Statistical analyses were performed on all data collected for each variety-site-year using R-Studio 1.1.456 (RStudio, Inc., 2009-2018). Linear regression statistical analysis was conducted in RStudio to determine the relationship between GreenSeeker and UAS remote sensor derived NDVI measurements for each site-year. The coefficients of determination (R^2) of the linear regression analysis were used to determine if a significant relationship was present between GreenSeeker and UAS derived NDVI measurements. A sensitivity analysis was also performed to remove outliers from each of the site-year data sets.

3.3. Results and Discussion

3.3.1. Evaluation of the linear regression relationship between GreenSeeker and UAV derived normalized difference vegetation index (NDVI)

Table 3.3 provides the slopes and coefficients of determination (R^2) of the linear regression analysis obtained from the linear relationship between the GreenSeeker and UAS remote sensor derived NDVI measurements for each site-year trial. The estimated linear relationship between the GreenSeeker and UAS remote sensor derived NDVI were based on NDVI measurements collected at either the panicle initiation or panicle differentiation growth stage, depending on the location and time of remote sensing for the data collected at each location. The R^2 values range were found to be between 0.57 to 0.89 for 2017 and 2018 at the five separate locations (Table 3.3). All linear regression analysis between the GreenSeeker and UAS remote sensor derived NDVI were found to be statistically significant ($P<0.001$). The linear relationships formed were inconsistent between each of the locations. The differences of these relationships between each location is potentially from the different climatic conditions during the growth and development of rice. Planting dates among the five locations for this study vary between early-March to early-May. The different planting dates can result in different growing conditions and, in return, can dramatically affect the growth and development of rice resulting in a change in the NDVI measurements between each location. Panicle differentiation was the growth stage for collecting NDVI measurements for five out of the seven locations NDVI measurements were collected with each of the remote sensing tools. Panicle initiation was the growth stage for collecting NDVI measurements for the other two locations. Lower linear relationships between GreenSeeker and UAS remote sensor derived NDVI were found at the two locations where sensor data was collected at panicle initiation.

Table 3.3. Linear regression relationship of GreenSeeker and UAS remote sensor derived NDVI in 2017 and 2018 at all 5 locations.

		GreenSeeker vs. UAS derived NDVI Model	
Location	Year	R^2	Linear Regression Equation
Crowley, LA	2017	0.632***	Y = 0.7598x + 0.1995
Palmetto, LA	2017	0.641***	Y = 0.3905x + 0.5955
Crowley, LA	2018	0.899***	Y = 0.7988x + 0.1354
Palmetto, LA	2018	0.792***	Y = 0.4249x + 0.5207
Iowa, LA	2018	0.319***	Y = 0.283x + 0.593
Monroe, LA	2018	0.682***	Y = 0.3196x + 0.590
Saint Joseph, LA	2018	0.575***	Y = 0.354x + 0.5576

*** P-value<0.001

Besides a difference in NDVI measurements between each of the locations, there were also differences found between the two different years of the data collection for this study. Figure 3.1 shows the relationship between GreenSeeker and UAS derived NDVI in 2017 at Crowley, LA. Figure 3.2 shows the relationship between GreenSeeker and UAS derived NDVI in 2018 at Crowley, LA. A stronger linear relationship at the Rice Research Station in Crowley, LA was produced in 2018, compared to the linear relationship produced in 2017. The linear relationship between GreenSeeker and UAS remote sensor derived NDVI at the Rice Research Station in 2017 estimated an R^2 value of 0.63 and the R^2 value rose to 0.89 in 2018. In 2017, the 'Diamond' rice variety is distinctly separated from the other rice varieties. The 'Diamond' variety didn't result in that separation in 2018 which could've caused the higher estimated relationship between the NDVI of the two remote sensors.

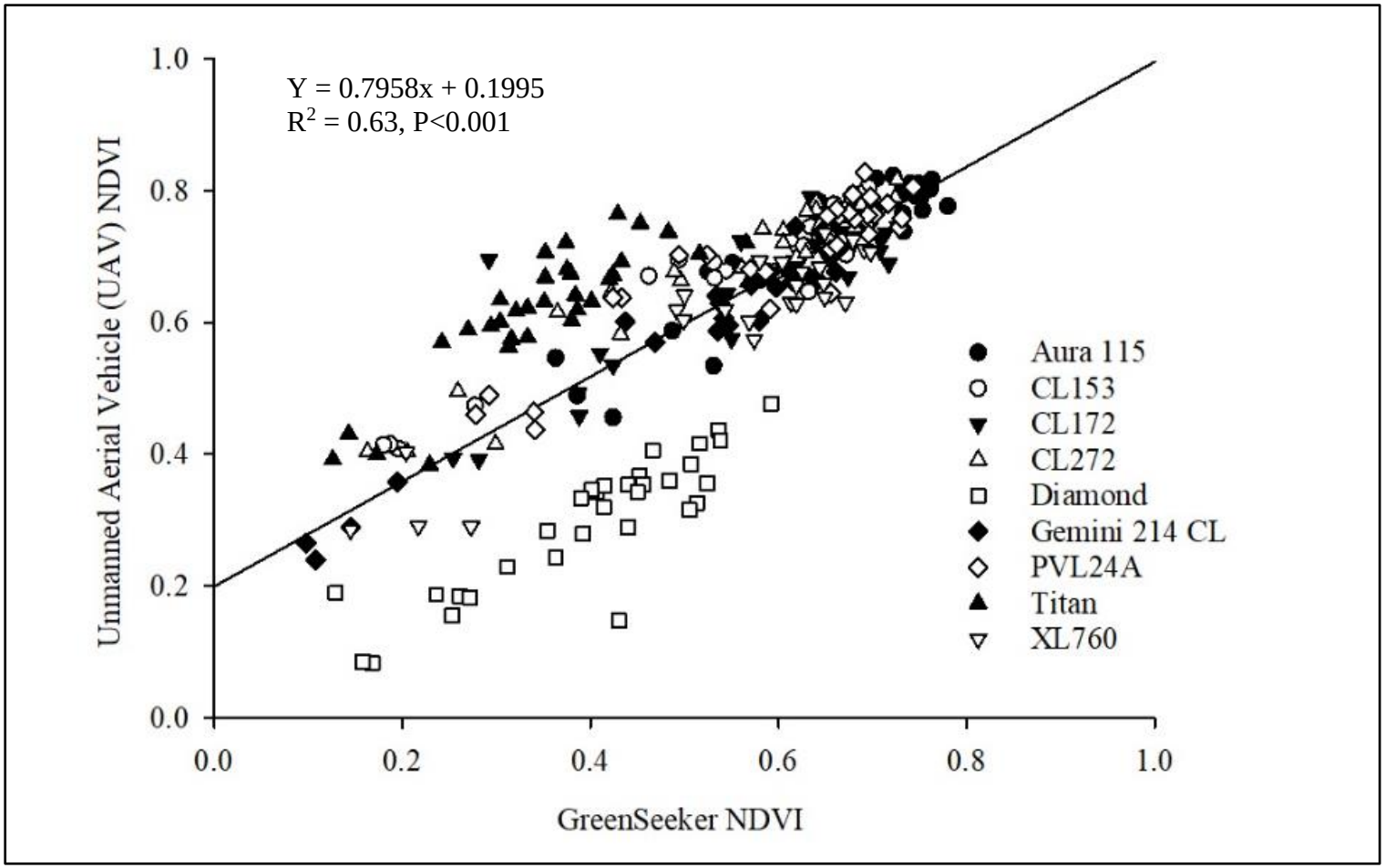

Figure 3.1. Relationship between GreenSeeker and Unmanned Aerial Vehicle (UAV) derived NDVI at the Rice Research Station in Crowley, LA in 2017.

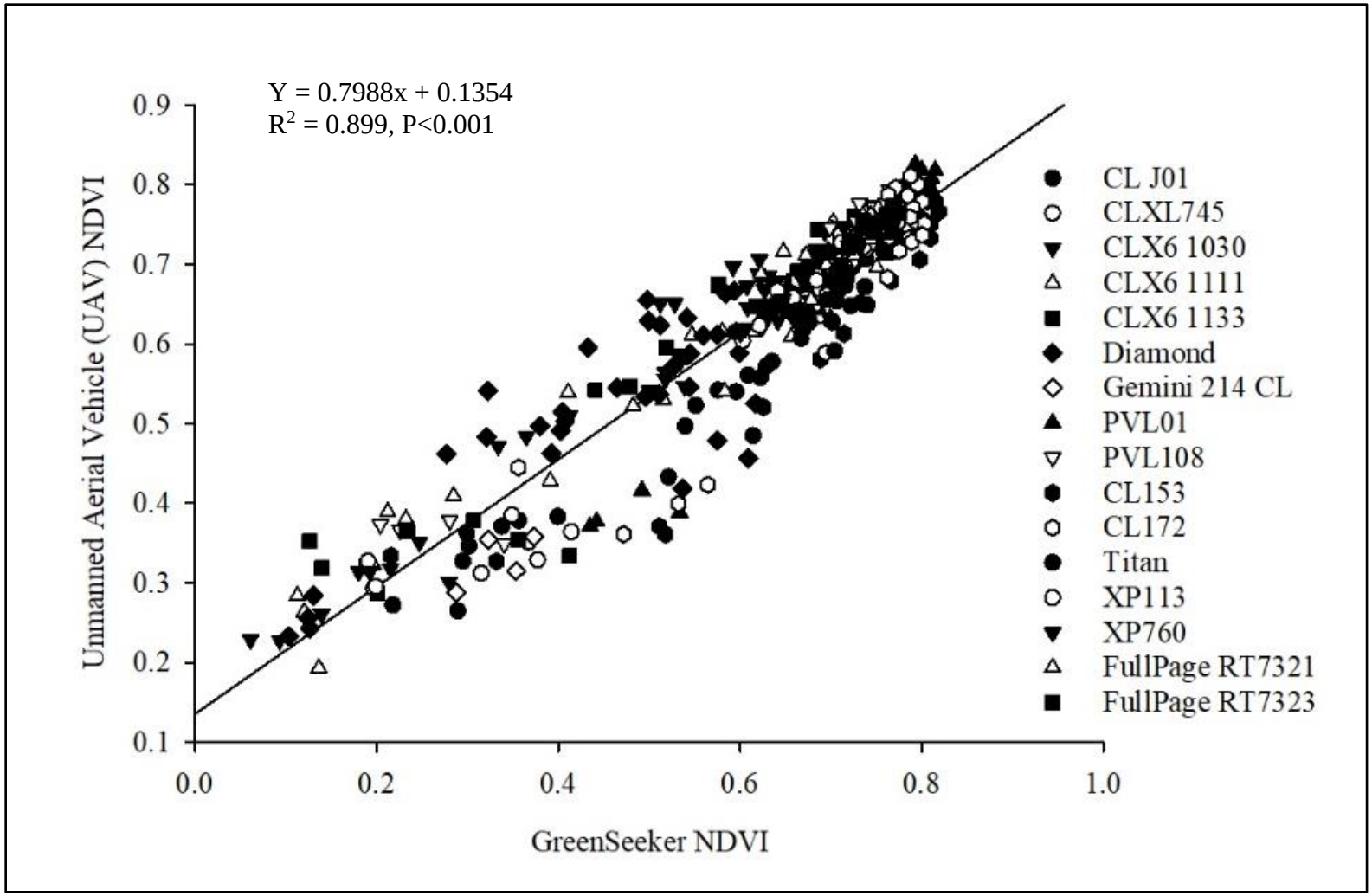

Figure 3.2. Relationship between GreenSeeker and Unmanned Aerial Vehicle (UAV) derived NDVI at the Rice Research Station in Crowley, LA in 2018.

Figure 3.3 shows the relationship between GreenSeeker and UAS derived NDVI in 2017 at the St. Landry Parish location. Figure 3.4 shows the relationship between the GreenSeeker and UAS derived NDVI in 2018 at St. Landry Parish. The R^2 value in 2017 was 0.641, which is a relatively high R^2 value. However, the linear relationship in 2018 at St. Landry Parish showed an increase in the linear relationship. The linear relationship at St. Landry Parish increased to an R^2 value of 0.79 in 2018 (Figure 3.4). Variation occurs between the different years of crop production systems due to the environmental changes, soil nutrient variations, and different rice varieties grown from year to year. Figure 3.3 and Figure 3.4 show the GreenSeeker remote sensor tool resulting in greater separation of NDVI values on the NDVI scale. The UAS remote sensor derived NDVI values show greater saturation on the higher end of the NDVI scale. This could mean the GreenSeeker derived NDVI could be a greater and more accurate predictor of NDVI than the UAS remote sensor derived NDVI. Rasmussen et al. (2015) argues that the most challenging aspect of UAS multispectral image data collection is the multispectral image analysis and interpretation. The advancement of technology for the UAS remote sensors is steadily increasing as is the software used for the analysis and interpretation of the multispectral images. Therefore, with more practice and experience with using the UAS and the UAS software applications will help analyze more accurate, closely related NDVI measurements when compared to the GreenSeeker derived NDVI.

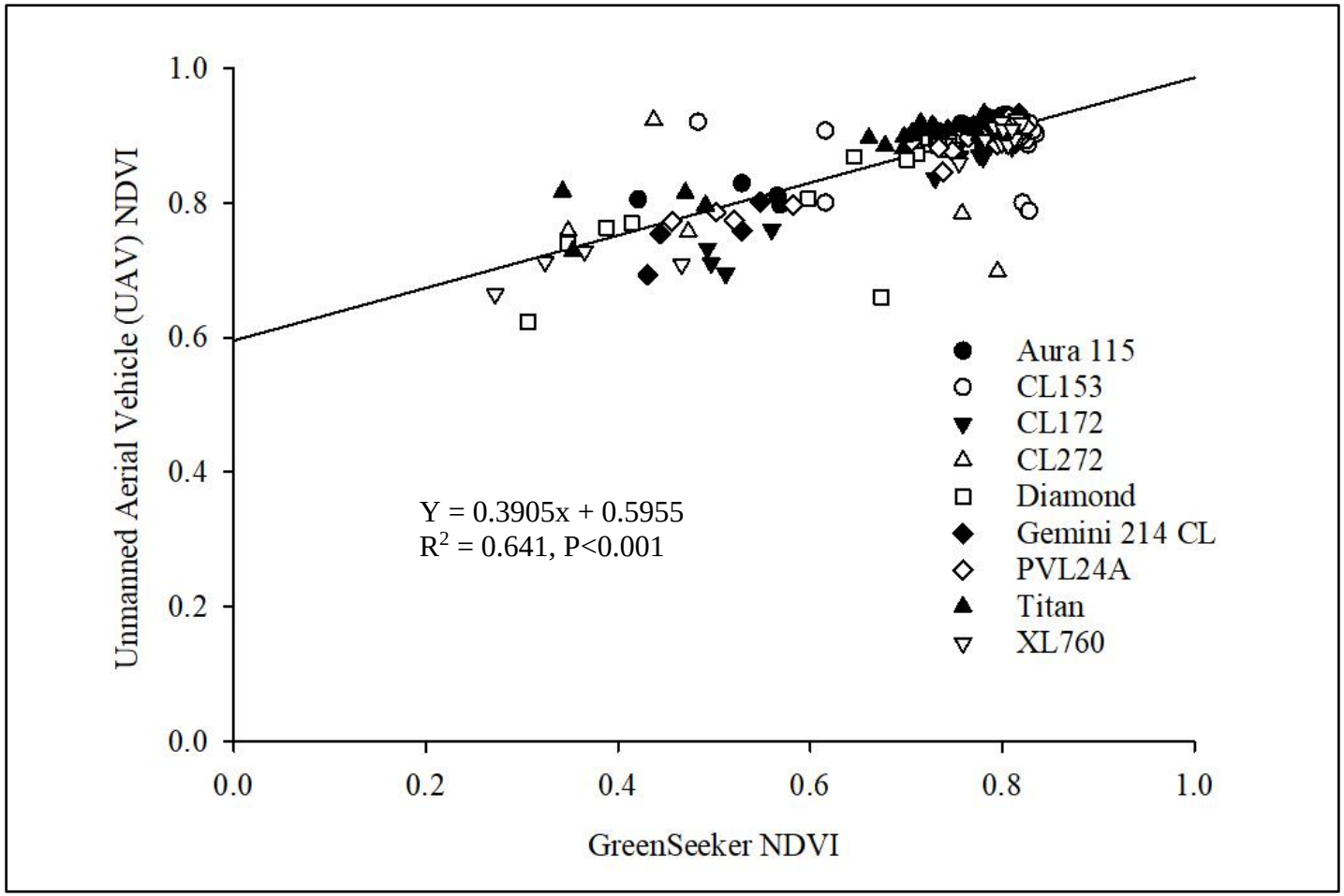

Figure 3.3. Relationship between GreenSeeker and Unmanned Aerial Vehicle (UAV) derived NDVI at St. Landry Parish in Palmetto, LA in 2017.

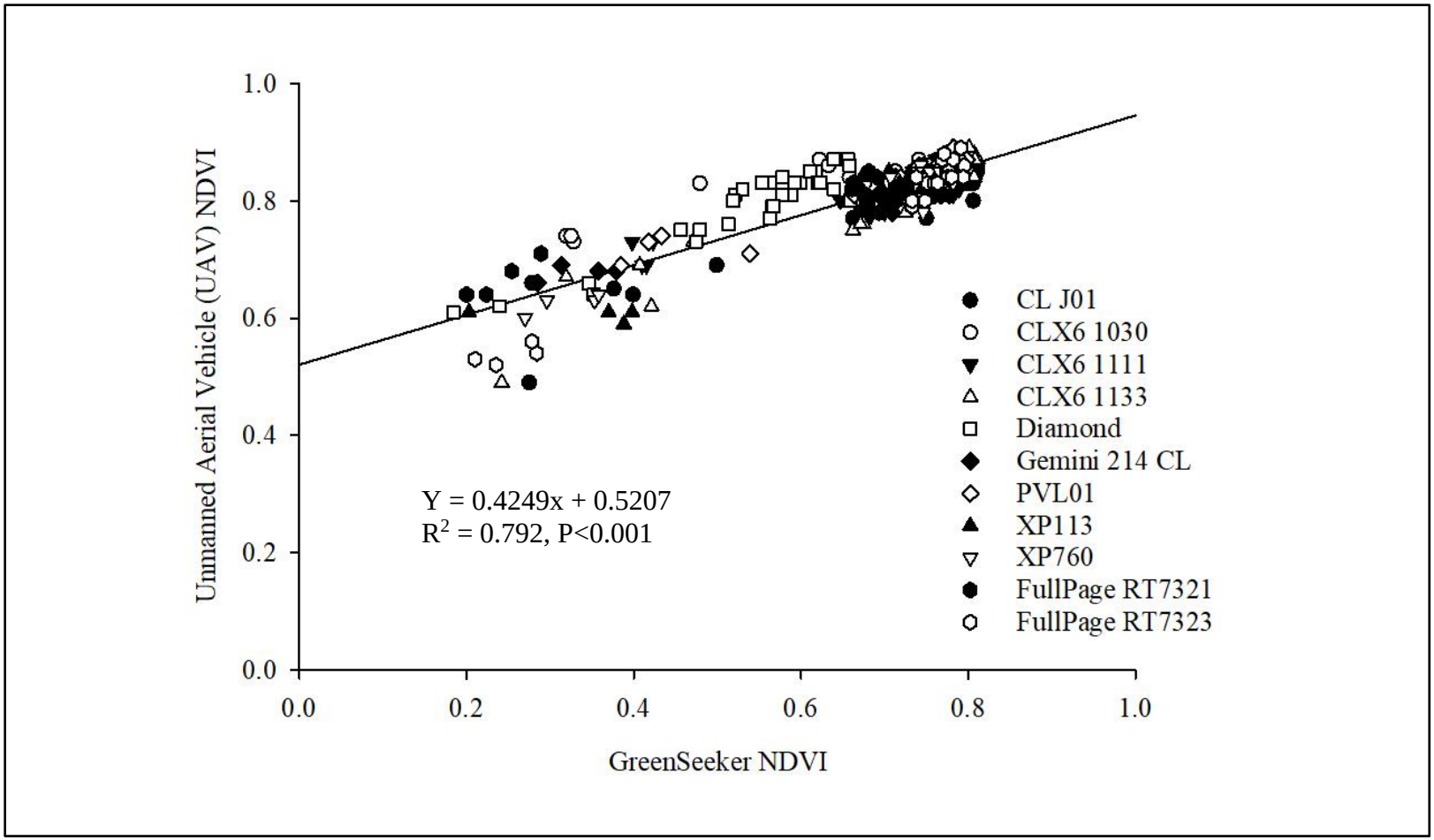

Figure 3.4. Relationship between GreenSeeker and Unmanned Aerial Vehicle (UAV) derived NDVI at St. Landry Parish in Palmetto, LA in 2018.

The relationship between GreenSeeker and UAS derived NDVI in 2018 at Tensas Parish in Saint Joseph, LA is shown in Figure 3.5. The relationship between GreenSeeker and UAS derived NDVI in 2018 at Richland Parish near Monroe, LA is shown in Figure 3.6. A similar linear relationship and R^2 value was found between the GreenSeeker and UAS derived NDVI measurements at Tensas Parish in Saint Joseph, LA and Richland Parish near Monroe, LA. The R^2 value at Tensas Parish in Saint Joseph, LA was 0.575 and the R^2 value at Richland Parish near Monroe, LA was 0.682. The two linear relationships between GreenSeeker derived NDVI and UAS remote sensor derived NDVI at the two locations were both relatively high relationships. The two locations are both located near each other in the Northern region of Louisiana and the NDVI measurements for the two locations were taken within one day of each other. The closely related climatic conditions and growth stages of the rice plots at the time of sensing for these two locations could be why similar NDVI measurements were produced from these two locations with each of the remote sensing tools. These two locations also show higher saturation of NDVI measurements on the higher end of the NDVI scale with most of the NDVI measurements sitting around the 0.6 value. A potential reasoning for this could be for the UAS remote sensor collecting data at higher spatial resolutions having a harder time differentiating between the NDVI values of the rice crop and other features present in the rice field during the time of remote sensing. The higher saturation of the UAS remote sensor could also be from the passive light sensor equipped onto the UAS which can easily be affected by climatic conditions at the time of remote sensing.

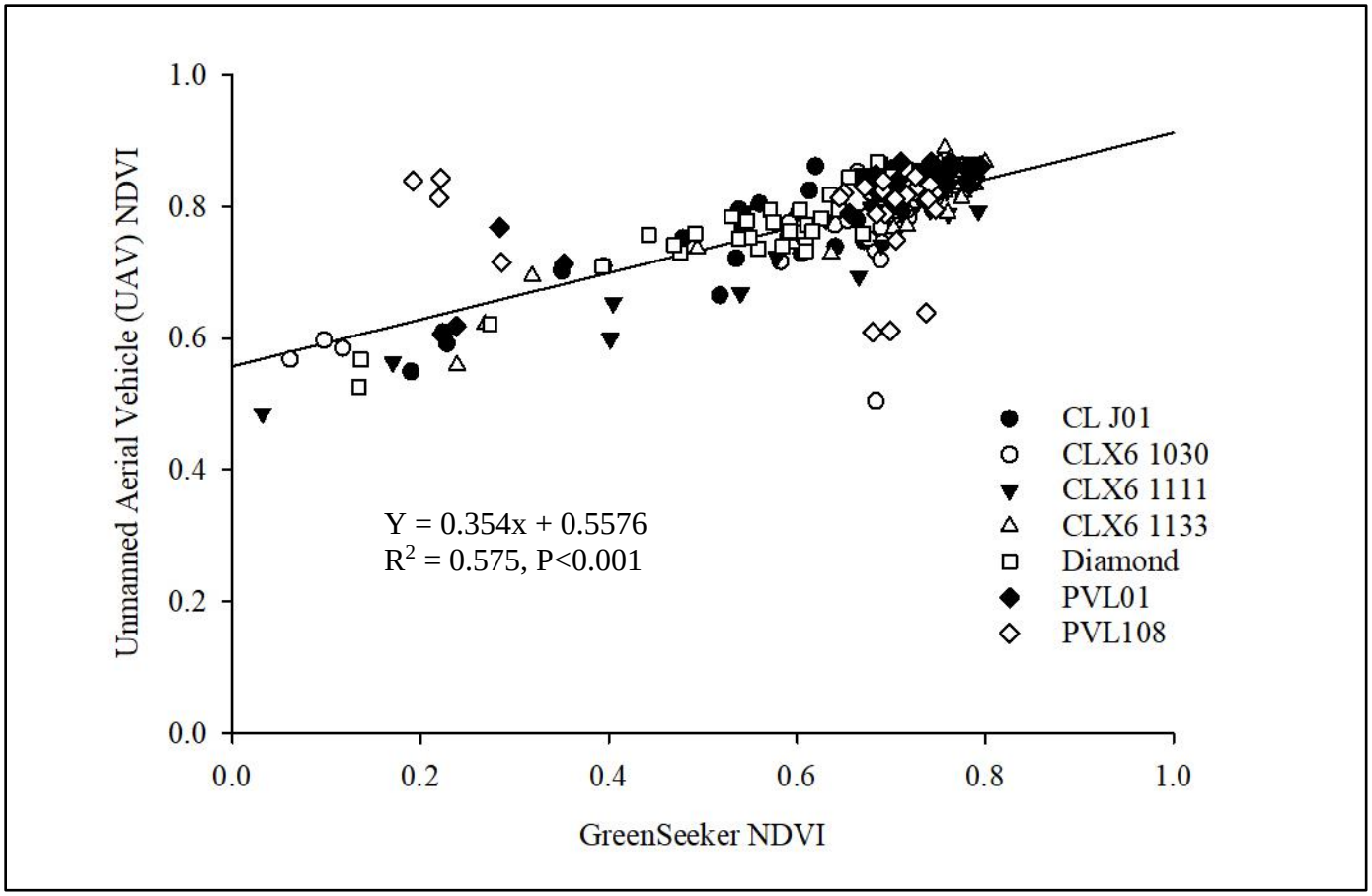

Figure 3.5. Relationship between GreenSeeker and Unmanned Aerial Vehicle (UAV) derived NDVI at Saint Joseph, LA in Tensas Parish in 2018.

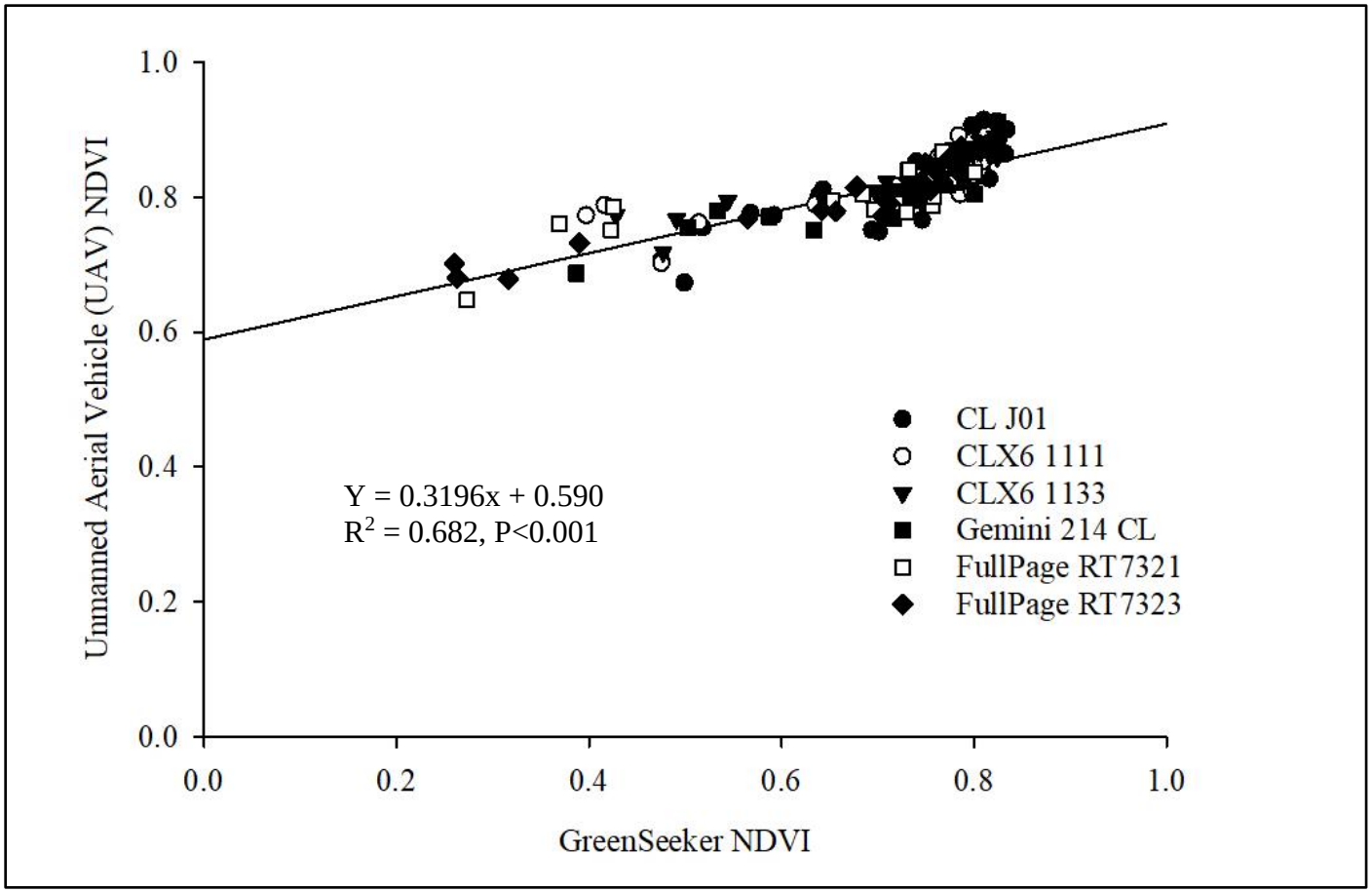

Figure 3.6. Relationship between GreenSeeker and Unmanned Aerial Vehicle (UAV) derived NDVI in Richland Parish near Monroe, LA in 2018.

The lowest linear relationship between GreenSeeker and UAS derived NDVI was produced at Calcasieu Parish in Iowa, LA in 2018 shown in Figure 3.7. Approximately only 32% of the variation in GreenSeeker derived NDVI could be explained by UAS derived NDVI. Calcasieu Parish was situated on a Crowley-Vidrine complex soil type. Bacterial panicle blight and rice sheath blight were recorded at high levels in almost all rice plots for this location. A successful rice production system is strongly restricted if rice diseases, such as rice sheath blight, are present in the field during rice growth and development. Most of the NDVI measurements collected with the GreenSeeker and UAS remote sensor are situated between 0.6 to 0.8 meaning the crop at mid-season was relatively healthy. However, sheath blight begins in the lower crop canopy and may not be detectable using remote sensors until after the infection reaches the top of the canopy. Unmanned aerial systems have been shown to be able to detect diseases such as sheath blight. Zhang et al. (2017) found a strong correlation between UAS-extracted NDVIs and disease severity with an accuracy of disease detection 63% of the time. However, any change in growing conditions post-sensing could lead to vegetative indices, such as NDVI, inaccurately determine the growth and development of rice (Forestieri, 2017). The UAS remote sensor NDVI values were heavily saturated between 0.7 and 0.9 NDVI values. The GreenSeeker showed more separation of NDVI values between 0.3 and 0.8. This indicates the GreenSeeker could be a better predictor in collecting more accurate and representative NDVI values of the rice plots.

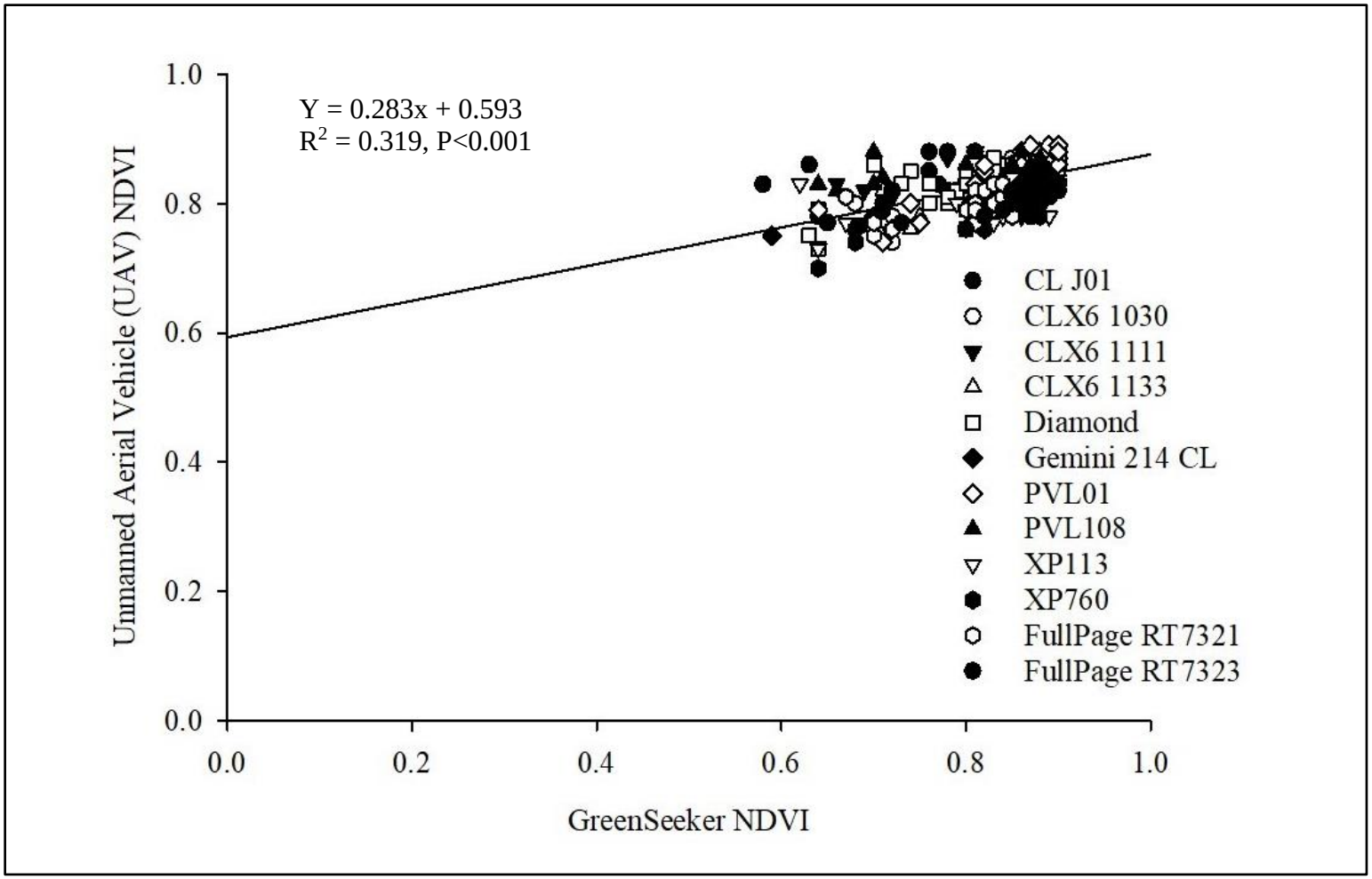

Figure 3.7. Relationship between GreenSeeker and Unmanned Aerial Vehicle (UAV) derived NDVI in Calcasieu Parish in Iowa, LA in 2018.

The linear relationships between the GreenSeeker and UAS remote sensor derived NDVI values at each of the five locations in either year were not on a 1:1 basis. The reasoning for the data not sitting on a 1:1 basis could have been caused from residuals and outliers present in the dataset. Table 3.4. shows the R^2 values for each site-year trial consisting of outliers and the R^2 values for each site-year trial with the outliers removed. A sensitivity analysis was performed to remove a certain percentage of outliers. In this case, 5% of the outliers were removed for each site-year trial. The data that is sitting more closely on a 1:1 basis with the linear regression line formed is the data that is kept when removing the outliers from the data set that are not as close to the linear regression line. There was an increase in the R^2 value for each site-year trial when 5% of the outliers were removed from each of the data sets. The relationship between GreenSeeker and UAS remote sensor derived NDVI at Crowley, LA in 2017 had a distinct set of outliers that weren't sitting on a 1:1 basis with the rest of the NDVI measurements (Figure 3.1). The relationship in 2017 with outliers had an R^2 value of 0.632, but when those outliers were removed the R^2 value increased to 0.718. The outliers in each of the data sets could've came from any of the factors that can cause skewed data when using remote sensing tools; human error, cloud cover at the time of sensing with the UAS remote sensor, or different growth stages of the rice varieties at the time of sensing.

Table 3.4. The R2 values of the linear relationship between GreenSeeker and UAS derived NDVI with outliers and without outliers for each site-year trial.

		Outliers		No Outliers	
Variety	Year	R^2	Linear Regression Equation	R^2	Linear Regression Equation
Crowley, LA	2017	0.632	Y = 0.7598x + 0.1995	0.718	Y = 0.828x + 0.026
Palmetto, LA	2017	0.641	Y = 0.3905x + 0.5955	0.861	Y = 1.85x - 0.896

(Table 3.4 Cont'd.)

		Outliers		No Outliers	
Variety	Year	R^2	Linear Regression Equation	R^2	Linear Regression Equation
Crowley, LA	2018	0.899	Y = 0.7988x + 0.1354	0.942	Y = 1.158x - 0.112
Palmetto, LA	2018	0.792	Y = 0.4249x + 0.5207	0.848	Y = 1.882x -0.837
Iowa, LA	2018	0.319	Y = 0.283x + 0.593	0.339	Y = 1.126x -0.172
Monroe, LA	2018	0.682	Y = 0.3196x + 0.590	0.725	Y = 1.865x -0.802
Saint Joseph, LA	2018	0.575	Y = 0.354x + 0.5576	0.807	Y = 1.875x - 0.8297

The linear relationships between the GreenSeeker and UAS remote sensor derived NDVI for each site-year trial were based on the whole location with all of the rice varieties combined. However, each location had a different number of rice varieties that were evaluated. The different rice varieties have different characteristics with some being hybrid rice varieties and some being conventional rice varieties. The different rice varieties could have different growth rates, yielding potential, and be affected differently by certain environmental conditions or diseases present in the field. The linear relationships between the two remote sensors were relatively low when all the rice varieties are taken into consideration. The low linear relationship could be from evaluating the rice varieties together. The data shows that each variety develops a separate linear regression line (Figure 3.8.). This shows that each variety has a separate relationship with GreenSeeker and UAS remote sensor derived NDVI measurements. For future work, the linear regression of each rice variety could be taken into consideration to increase the relationship between GreenSeeker and UAS remote sensor derived NDVI and predict more accurate linear relationships between the two remote sensors.

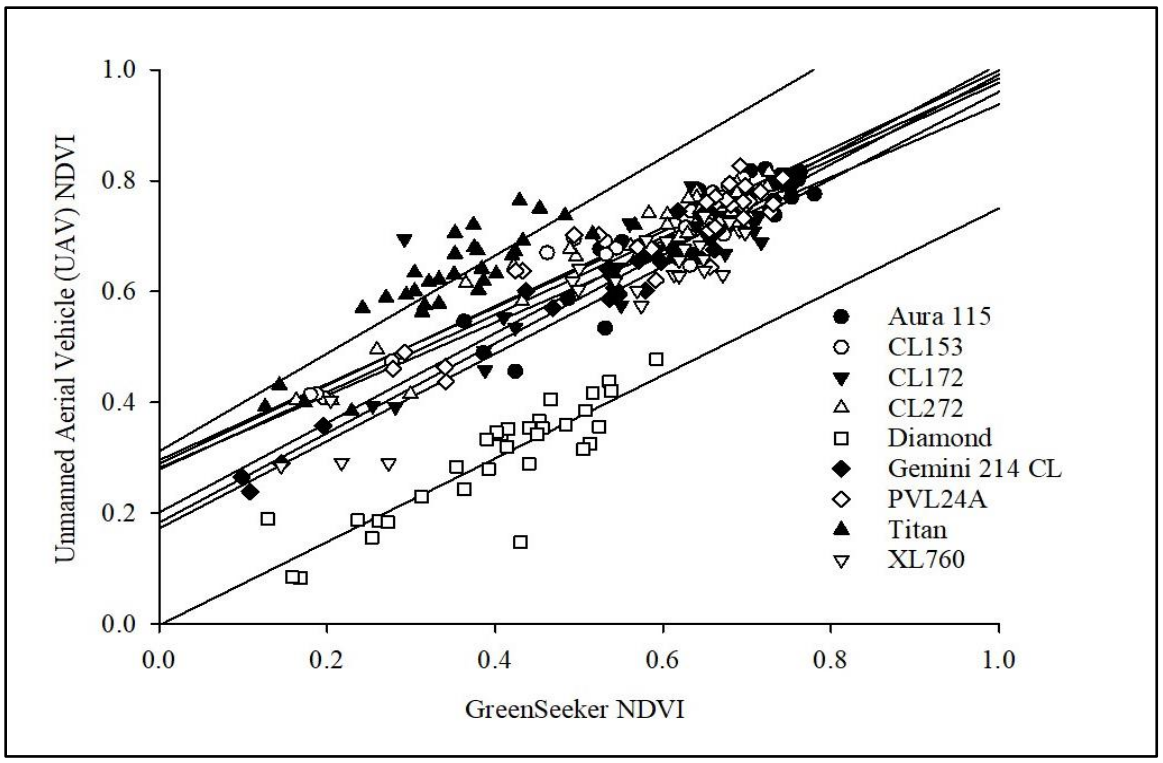

Figure 3.8. The linear relationship between GreenSeeker and UAV remote sensor derived NDVI with the linear regression of each variety in Crowley, LA in 2017.

We can conclude from the data of this study that the GreenSeeker derived NDVI will be different as compared to the UAS derived NDVI measurements. The UAS values were more heavily saturated on the higher end of the measurement scale compared to the GreenSeeker derived NDVI. The cause of this could be from the higher spatial resolution used with the collection of the UAS multispectral image collection. The high spatial resolution and high flight altitude of the UAS could make it more difficult for the multispectral remote sensor to separate certain physical attributes of the rice crop canopy and collect skewed NDVI data. The higher spatial resolution means possibility of lower-resolution multispectral images, which may not be appropriate for small-scale studies and be more prone to collect inaccurate data (Wojtowicz et al., 2016). Flexibility of the UAS to maneuver through a field and the ability to change the flight altitude is an advantage of the remote sensing tool. Collecting data from a range of different

altitudes to help improve the spatial and multispectral image resolution could still allow the UAS to be stable and collect more accurate measurements (Ni et al., 2017). Adjusting the height of the UAS during the flight can also help avoid the cause of light fluctuations and shadows present during the time of flight. Rasmussen et al. (2016) recommends the UAS flight and collection of multispectral images be done in cloudy conditions or the angle of view be kept constant in relation to the angel of illumination. Despite the differences in NDVI values collected with the GreenSeeker and UAS remote sensors, there is accommodations which can be made to help produce more accurate, similar NDVI readings derived from the UAS and GreenSeeker.

It is important to note that the GreenSeeker and UAS each use a different light source when collecting data to evaluate a rice field. The GreenSeeker is equipped with an active light source. Less potential from environmental occurrences is found with the use of the GreenSeeker derived vegetative indices since the light source is built onto the remote sensing tool. Climatic conditions are more effective with the UAS derived vegetative indices because of the passive light source. Variability among readings is more prone to happen with UAS data collections because of the intensity of sunlight, time of day data is collected, and opportunity of shadows to exist in the multispectral images. If climatic conditions are not adequate for flying an UAS persisted on the day of data collection, it could cause a lower relationship between GreenSeeker and UAS derived NDVI measurements. Overall, the R^2 derived from the comparison of GreenSeeker and UAS derived NDVI at each site-year trial were found to be similar, but the data points didn't sit on a 1:1 basis.

3.4. Conclusion

This study showed that overall both 2017 and 2018 linear relationships between GreenSeeker and UAS remote sensor derived NDVI were relatively significant and similar. The

relationships between GreenSeeker and UAS remote sensor derived NDVI did change between each of the years and each of the five locations. Sensor-based readings can have the potential to change if growth changes occur between the two years of remote-sensing. Rice response and rice growth stages vary at each of the locations because of agronomic and environmental differences present at each of the locations. The different soil properties at each location provided different soil pH levels, extractable nutrient amounts, and organic matter, which could cause a change in the growth and development for the site-year-location trials. Soil fertility differences will cause rice varieties to develop at different rates which could cause the different NDVI values produced and the different NDVI relationships derived from the GreenSeeker and UAS remote sensors. The remote sensing time for two of the locations was done at panicle differentiation compared to the other locations when remote sensing was done at panicle initiation. Previous research has shown NDVI values collected at panicle initiation and panicle differentiation will differ. The data for this study showed that the vegetative indices for data taken at panicle differentiation was lower than data collected at panicle initiation. Sensor timing is a critical component in collecting reliable and useful quantitative data for agronomic measurements of a rice crop.

Rice fertilization needs can be met if the rice needs can be determined in a timely manner. GreenSeeker derived NDVI has been used successfully in determining rice N requirements. The UAS remote sensor derived NDVI has potential to do the same, however the data from this trial indicates that the NDVI from the two remote sensors are different. Some of this difference could be due to the higher spatial resolution, different wavelength regions of the electromagnetic spectrum used for each tool, and different effects on the remote sensing tools from the climatic conditions present on the days of sensing.

Despite the differences in NDVI values derived from the GreenSeeker and UAS remote sensor, the linear relationship between the two sensors were relatively strong. Passive light sensors are known to skew data due to change in environmental conditions at the time of sensing. This variability can be reduced by flying the UAS in the appropriate environmental conditions, georeferencing the data points, setting the appropriate altitude and overlap percentage settings of the UAS multispectral image collection, and stitching the multispectral images together through an advanced software. The relationship between the vegetative indices not sitting on the 1:1 basis potentially occurred because of the different light sources (passive and active) on the remote sensors. Even though some of the variability can be accommodated for with the UAS remote sensor, some variability in the data will persist which will cause the two remote sensors to derive different NDVI results. The NDVI data for this study was heavily saturated between 0.65 and 0.9 at each site-year. The high altitude of the UAS remote sensor when the multispectral images were taken may account for some of the increased saturation of the UAS remote sensor images as compared to the GreenSeeker. Further research should be done to evaluate the effect of altitude level on UAS remote sensor data. Other vegetative indices that utilize other wavelengths may provide increased resolution and may be a better predictor than NDVI for UAS remote sensors.

Overall, our data indicated a strong relationship between the GreenSeeker and UAS remote sensor derived NDVI data. Therefore, the UAS remote sensor has the potential to be another tool which could be used to determine mid-season N rates in rice. However, more research will need to be conducted and an algorithm will need to be developed before the UAS remote sensor can be used in commercial rice production.

Chapter 4. Evaluation of the Linear Relationship Between GreenSeeker and UAV Derived Normalized Difference Vegetation Index (NDVI) to Rice Grain Yield

4.1. Introduction

Rice (*Oryza sativa*) serves as one of the most important cereal crops producing approximately 162 million hectares of rice worldwide (USDA, 2019). In the United States, rice is grown on about 1 million hectares in the states of California, Arkansas, Mississippi, Missouri, Louisiana, and Texas (USDA, 2019). Louisiana is the third leading state in rice production for the United States. Rice is an edible starchy grain and of high importance of human consumption. Rice is highly valuable to our world, therefore new techniques and rice production management strategies should continuously be developed to allow for rice to produce maximum yields with a more profitable, sustainable approach.

A rice producers' goal is to create an economically efficient management strategy to produce rice with maximum grain yields. The nutrients available and provided to rice during the season are critical to maximize the yield potential of the crop. Nitrogen (N), phosphorus (P), and potassium (K) are three of the main macronutrients needed to develop a healthy, nutritious crop. The most impactful and abundantly applied nutrient of the three is nitrogen (Leghari, 2016). Nitrogen can be supplied to rice through fertilizer applications to accommodate for the N needs of rice. Nitrogen deficiency symptoms will occur in rice if N is needed or inadequately supplied. Symptoms of N deficiency are presented in the rice field as chlorosis of the older leaves, decrease in plant heights, and reduced tillering. An over-application of N fertilizer can also negatively affect rice. Excessive N application symptoms will be presented as excessive vegetative growth, delayed maturity, lodging, and increased disease. Developing a management strategy to determine the right N fertilizer source, correct N fertilizer rate, most efficient N

fertilizer application time, and appropriate N fertilizer placement will help eliminate the potential of N deficiency and inaccurate N fertilizer applications to rice.

Nitrogen is the most expensive fertilizer input of rice but can also help develop rice to give the greatest economical return. The application timing, method, and rate of N fertilizer should be accurately determined so growers can apply N to rice in an economically efficient strategy while minimizing N losses and maximizing rice grain yield. The behavior of N within the soil and plant is very dynamic. Nitrogen exist in organic and inorganic-N forms. The N form most abundantly found and used in rice is inorganic-N (Fageria, 2001). There are two inorganic-N forms available for uptake by rice: nitrate (NO_3^-) and ammonium (NH_4^+). Ammonium-N fertilizer sources are preferred over NO_3^- fertilizer sources because NH_4^+ remains stable under the anaerobic field conditions used for growing rice. Nitrate-N sources become unstable and can be lost quickly in anaerobic field conditions via denitrification. Leaching is another major loss pathway for NO_3^- because of the solubility and mobility characteristics of NO_3^- (Havlin et al., 2014). Ammonium-N fertilizer sources remain stable in anaerobic, flooded soil conditions, but NH_4^+ can be quickly lost by nitrification when oxygen is present. Nitrification occurs when the flood is not established on the rice field in a timely manner after the pre-flood N fertilizer application or the flood is not maintained throughout the growing season. The N-loss pathways, for both NH_4^+ and NO_3^- fertilizer sources, are impacted by environmental conditions, management practices, N fertilizer application rates, and irrigation techniques.

Nitrogen fertilizer losses can be lessened if the appropriate application method is used to apply N fertilizer to rice. The preferred application method of N fertilizer is done in a two-way split application. The two-way split application method is beneficial to rice when the flood establishment and maintenance is difficult, increasing the potential of N fertilizer losses to occur

(Snyder and Slaton, 2002). The first N fertilizer application is broadcast at pre-flood, at the 4- to 5- leaf growth stage. The pre-flood N rate is determined by N response trials conducted by research scientists, across multiple locations, evaluating multiple rice varieties. The response trials conducted provide rice growers with a N rate range for every currently available rice variety. In Louisiana, two-thirds of the recommended N rate provided by LSU AgCenter is applied at pre-flood. The range of N fertilizer application rates in Louisiana is between 135 – 230 kg ha^{-1} (Rice Management Tips, 2018). Adjustments of the recommended pre-flood N fertilizer rate should be made by the individual growers based on the rice variety being grown, cultural management, soil texture, and environmental conditions at the time of N fertilizer application. The N fertilizer is incorporated and taken up by rice once a flood is established onto the dry-soil bed within one to three days after the N fertilizer application. The incorporation of the N fertilizer into the soil will decrease the chances of N losses through volatilization and nitrification/denitrification (Snyder and Slaton, 2002).

The second N fertilizer application time is at mid-season between panicle initiation (green ring or beginning internode elongation [BIE]) and panicle differentiation (1/2-inche IE). Mid-season N fertilizer applications have a significant effect on rice grain yield and grain quality (Nguyen and Lee, 2006). Nitrogen fertilizer rates for mid-season applications are determined by visual observation done by the grower or consultant. Nitrogen fertilizer rates can be inaccurately determined at mid-season because not all in-season characteristics of rice can be accurately determined through visual observations. The inaccuracy of N fertilizer applications at mid-season can lead to under or over-application of N fertilizer, decrease in rice grain yield, economic losses, and N-losses that are hazardous to the environment. It is crucial to develop a

management strategy that can accurately determine mid-season N fertilizer rates for rice because mid-season N fertilizer plays a large role in rice quality and yield potential.

The development of tools to help accurately predict mid-season N needs will be an asset for farmers to optimize N fertilizer applications that efficiently stimulate the growth and development of rice. Crop yield goals are often used to help predict N fertilization requirements. Crop yield goal are based on crop yield history, soil characteristics, management practices, and the crop variety being planted. However, a crop yield goal does not justify for the spatial and temporal variation that occurs within a rice field. Crop yield can be greatly affected by soil properties, history of field management, and weather conditions that vary from year-to-year (Krienke et al., 2017). Rice growers today are growing rice on an increased amount of acreage, making it harder to account for the variation caused by spatial and temporal variability. The advancement of tools to predict N fertilizer needs would greatly benefit rice producers that are growing rice across multiple, large fields. Precision agricultural tools like the GreenSeeker, have been used to improve the determination of mid-season N fertilizer rates and improve management strategies in rice. Rice growers have been able to make more efficient strategical, tactical, and operational decisions based on data collected with precision agricultural tools. Nitrogen fertilizer rates can be determined for site-specific regions in a rice field creating variable N fertilizer recommendations with precision agriculture tools. Precision agricultural tools collect a large amount of data that can be used to optimize N fertilizer recommendations, improve the profitability of rice, and decrease N losses.

Active crop canopy remote sensors are a precision farming tool used for predicting in-season, site-specific, quantitative measurements of the health status of plants. Active crop canopy remote sensing can account for the spatial and temporal variation found in rice and can

play a part in determining more accurate N fertilizer recommendations in rice. Remote sensing assessments in rice have advanced greatly and are able to deliver data (Elarab, 2016). Active crop canopy remote sensing tools are used in many crops to help detect the health and N status of a crop (Xue et al., 2004; Lee et al., 2008). Foster et al. (2017) demonstrated how active crop canopy sensors can be efficiently used in rice with the potential of lowering the amount of N applied to rice, while still optimizing rice grain yield. The predominant active crop canopy remote sensing tool used to aid in predicting a rice crop's health during major growth and developmental phases is the GreenSeeker handheld sensor. Growers have become more sustainable farmers and made more suitable in-season fertilizer applications using GreenSeeker based technology (Yao et al., 2012). The GreenSeeker tool is unaffected by environmental conditions because it is equipped with a pre-calibrated, active, optical light sensor. Specific regions in the red (670 ± 10 nm) and near-infrared (780 ± 10 nm) wavelength bands of the electromagnetic spectrum are used to measure the canopy reflectance derived with the GreenSeeker remote sensing tool. Canopy reflectance measurements can determine the chlorophyll level of the rice crop to conclude the amount of N present. GreenSeeker evaluates the reflectance value of the crop canopy by calculating the normalized difference vegetation index (NDVI) using the red and near-infrared wavelengths in the following equation:

$$NDVI = \frac{(NIR + R)}{(NIR - R)} \quad [4.1]$$

where:

NIR = Reflectance at the near-infrared region of the electromagnetic spectrum

R = Reflectance at the red region of the electromagnetic spectrum

GreenSeeker derived NDVI can evaluate the rice response to pre-flood N fertilizer applications and can be used to help determine future N requirements of rice at critical growth stages (Xue and Yang, 2008). GreenSeeker derived NDVI can currently be used with a N rate calculator developed by the LSU AgCenter to determine mid-season N fertilizer requirements (Harrell et al., 2011). The algorithm is composed from 3 factors:1) response index, 2) rice grain yield potential, and 3) N response to fertilization (Harrell et al., 2011). The on-site, sensor-based N rate calculator can predict in-season N needs of rice in a timely manner because of the GreenSeekers ability to collect NDVI data. LSU AgCenter's developed algorithm using GreenSeeker derived NDVI can be a beneficial tool that can potentially save rice growers money and maximize rice grain yield.

Response index is used for computing the on-site, sensor-based N rate algorithm. Response index is a quantitative measurement used to evaluate the crops response to N fertilization. Calculating the response index is only feasible when a grower has a controlled, non-fertilized N strip within a highly representative portion of characteristics throughout the rice field. The non-fertilized N strip is used to determine the growth conditions of rice without any fertilizer additions. Check plots have shown variation of N available in the soil between years of crop growth seasons. Response index gives feedback of N available to determine mid-season N requirements, even after temporal variation forces have occurred. Response index can be calculated by dividing the average NDVI of the non-fertilized N strip by the average NDVI from the area where the N rate applied was determined by the farmers practice (Raun et al., 2001). If the response index calculated is greater than one, then a rice response to N fertilization is expected. If the response index is less than one, then a response to N fertilization is not expected.

The response index of N fertilizer recommendations, determined with the sensor-based approach, has shown to have a positive correlation with rice grain yield (Raun et al., 2002).

Crop yield potential is also used in the algorithm developed to predict mid-season N fertilizer recommendations for rice. Yield potential can be affected by certain soil and weather conditions that change from year-to-year. The definition of yield potential is the maximum grain yield with ideal management, soil, and weather conditions (Raun et al., 2001). The GreenSeeker derived NDVI has shown to be a suitable indicator of crop yield potential and final grain yield measurements (Teal et al., 2006; Tubaña et al., 2008; Raun et al., 2010; Harrell et al., 2011). Crop yield potential of rice is known to be the yield potential achieved with no N fertilizer additions (Raun et al., 2011). The crop yield potential for areas with N fertilizer additions is calculated by multiplying the response index by the yield potential of the non-additional N fertilized areas (Raun et al., 2002). Raun et al. (2010) found that both the yield and crop response to N fertilization influences the N fertilizer recommendations. Crop yield potential and crop response to N fertilization each act independently and must both be used when determining accurate in-season N fertilizer rates (Raun et al., 2010).

The GreenSeeker derived NDVI has shown to be successful in computing the algorithm developed by the LSU AgCenter to predict mid-season N fertilizer recommendations. However, the on-site, sensor-based N rate algorithm developed by LSU AgCenter has not been extensively adopted by growers or consultants. This is because the GreenSeeker lacks the ability to account for variation across a whole field. The GreenSeeker collects NDVI values on a point-to-point basis in site-specific regions across a rice field. Advancements in technology have shown that unmanned aerial systems (UAS), an air-borne remote sensor, have the potential to be used to evaluate a crops health status and determine N fertilizer recommendations. Data is collected on a

whole field basis with a UAS mounted remote sensor which accounts for variation across the field as compared to the single point-to-point basis of the GreenSeeker data collection. The UAS remote sensor can produce an increase in the field scale average data collection when evaluating rice across the whole field. The UAS has shown a similar ability to evaluate different crop responses compared to other remote sensing tools (Rasmussen et al., 2015). The UAS remote sensor collects NDVI values at a higher spatial resolution compared to the low spatial resolution of the GreenSeeker. Primicero et al. (2012) found there to be a strong correlation between air-borne and ground-sensor derived NDVI measurements even though both tools use different spatial resolutions for obtaining data. Kienke et al. (2017) also found no difference between the ground-season and air-borne sensors ability to detect different N rate effects on corn. These results increase the possibility of the UAS remote sensor being used like the GreenSeeker has been used in the past.

The GreenSeeker must be manually walked through a rice field to collect NDVI values, which can be less beneficial for farmers who have several fields to obtain data from. The flexibility to maneuver the GreenSeeker is not easily done within the field boundaries. This is especially true in a flooded production system like rice. A UAS mounted remote sensor has a more feasible transportation method within a field and can be flown autonomously. Pre-programmed flight operations for the UAS are prepared before a flight takes place in order to collect data in a faster, easier method. The flexible maneuverability advantages the UAS imposes are due to the vertical take-off and landing and the ability to fly forwards, backwards, and laterally to collect data across the whole entire field (Huang et al., 2013). Farmers can spend less time on field assessments and make timelier, more efficient crop decisions from the rapid data collection and easier transportation that comes with the UAS (Zhu et al., 2009).

The GreenSeeker and UAS remote sensors are equipped with two different types of light sensors. The GreenSeeker is equipped with an active, optical light sensor (has its own light source), so the GreenSeeker derived NDVI values are not affected by the surrounding environmental conditions. The UAS is equipped with a passive light sensor (uses sunlight as its light source). Variation among the NDVI data collected with the UAS remote sensor can occur because the UAS remote sensors light source relies on the sun and is easily affected by environmental conditions. Three of the factors that cause variability in the UAS remote sensor derived NDVI data are intensity of the sunlight, bidirectional reflectance, and environmental conditions. These conditions can be overcome when using the right techniques and strategies recommended for the operation of the UAS. Geographical and geometric data points are georeferenced to help stabilize and eliminate the causes of variability caused by deformations in the multispectral image collected from the UAV (Lelong et al., 2008). Operating the UAS in the appropriate flight conditions will also help diminish the possibility of the environmental factors affecting the multispectral images collected with the UAS passive light sensor. Advanced software applications have been developed to stitch the multispectral images collected by the UAS together accounting for possible variation occurrences and decreasing the chances of the UAS producing invalid data.

Vegetative indices collected with a UAS remote sensor have shown stable relationships with other rice health status measurements, such as leaf area index, N uptake, and rice grain yield (Duan et al., year; Lelong et al., 2008). Many studies have been conducted using the UAS technology evaluating chlorophyll and N content in cereals (Li et al., 2015; Zheng et al., 2016), weed mapping (Stropiana et al., 2018), and disease damage (Yang et al., 2017). The GreenSeeker and UAS, used together or separately, provide producers with valuable information to determine

different crop needs. Data collected from the GreenSeeker and UAS remote sensors can lower N fertilizer inputs, determine disease infestations, increase the profitability, and produce maximum rice grain yield potential.

Rice producers are always looking for more feasible ways to manage the growth and development of rice and determine N fertilizer needs. Developing more efficient techniques to evaluate the growth and development of rice have become increasingly important to producers that have large amounts of acres to cover in a short amount of time. The UAS can allow for producers to obtain information on their rice crop in a faster, less destructive method and make crop decisions in a timelier manner. The GreenSeeker and UAV remote sensor derived NDVI result in a strong correlation meaning the tools could have similar ability to predict mid-season N fertilizer recommendations. It is unknown if a UAS remote sensor can be used as a replacement in the LSU AgCenter algorithm that has already been successfully used with the GreenSeeker, to determine on-site, mid-season N fertilizer requirements. The objective of this study was to determine the linear relationship between GreenSeeker and UAS derived NDVI to rice grain yield potential.

4.2. Materials and Methods

4.2.1. Site Description, Planting Method, Treatment Structure, and Trail Establishment

The data for this study was collected from two locations in 2017 and five locations in 2018. The two sites in 2017 were: 1) Rice Research Station in Crowley, LA and 2) St. Landry Parish in Palmetto, LA. Those same sites were used in 2018 plus an additional three sites: 1) Calcasieu Parish in Iowa, LA, 2) Tensas Parish in Saint Joseph, LA, and 3) Richland Parish near Monroe, LA (Table 4.1.).

The Rice Research Station in Crowley, LA is situated on a Crowley silt loam (fine, smectitic, thermic Typic Albaqualfs). In 2017, ten rice varieties were evaluated, and fifteen cultivars were evaluated in 2018. The second location was in St. Landry Parish in Palmetto, LA on a dundee silty clay loam (fine-silty, mixed, active, thermic Typic Endoaqualfs). There were ten rice cultivars evaluated in 2017 and twelve rice cultivars in 2018. Calcasieu Parish in Iowa, LA, was the third site in 2018 on a Crowley-Vidrine complex (fine, smectitic, thermic Typic Albaqualfs and Aquic Glossudalfs). There were twelve rice cultivars evaluated at this location. Saint Joseph, LA, in Tensas Parish, was the fourth location on a commerce silt loam (fine-silty, mixed, superactive, nonacid, thermic Fluvaquentic Endoaquepts). There were seven rice cultivars evaluated at this location. Richland Parish, near Monroe, LA, was the fifth location on a Herbert silty clay (fine-silty, mixed, active, thermic Aeric Eqiaqualfs). There was six rice cultivars evaluated at this location.

Table 4.1. The soil series, taxonomy, and taxonomic classification for each individual location-year.

Location	GPS Location	Year	Series	Taxonomy	Taxonomic Classification
Crowley, LA	30°14’50.8”N 92°20’56.8”W	2017-2018	Crowley	Silt loam	Fine, smectitic, thermic Typic Albaqualf
Palmetto, LA	30°47’41.9”N 91°53’29.9”W	2017-2018	Dundee	Silty clay loam	Fine-silty, mixed, active, thermic, Typic Endoalqualf
Iowa, LA	30°13’08,9”N 93°03’52.7”W	2018	Crowley	Vidrine-complex	Fine, smectitic, thermic Typic Albaqualf & Aquic Glossudalf
Monroe, LA	32°23’23.8”N 91°58’47.2”W	2018	Herbert	Silty clay	Fine-silty, mixed, active, thermic, Aeric Eqiaqualf
Saint Joseph, LA	31°56’41.3”N 91°13’54.0”W	2018	Commerce	Silt loam	Fine-silty, mixed, superactive, nonacid, thermic Fluvaquentic Endoaquepts

Important agronomic dates including planting date, pre-flood N application date, flood establishment date, sensor readings date and growth stages for each site-year trial is shown in Table 4.2. The rice seeds were drill-seeded into a dry soil bed to a depth of 1.27 cm at a seeding rate of 366 seeds per m^2 for rice varieties and 111 seeds per m^2 for the hybrids. The rice plots size were 4.88 m in length consisting of 7 rows with 20 cm spacing. The seed treatment for the rice varieties consisted of mancozeb (Dithane - fungicide), gibberellic acid (Release), zinc plus (10% Zn & 4.9% combined S), and anthraquinone (AV-1011 - bird repellent), and chlorantraniliprole (Dermacor – insecticide). Hybrid seed was treated with clothianidin (Nipsit Inside), fludioxonil (Spirato 480FS), fludioxonil (Maxim 4FS), gibberellic acid, zinc, and anthraquinone (AV-1011 - bird repellent). There were eight pre-flood N rates for the rice varieties (0, 34, 67, 101, 134, 168, 202, and 235 kg ha^{-1}) and there were six pre-flood N rates for the hybrid varieties (0, 67, 101, 135, 168, and 202 kg ha^{-1}). The pre-flood N rates were broadcast applied at the 4- to 5-leaf growth stage. The fertilizer was incorporated into the root zone of the rice by the flood establishment one to three days after the pre-flood N fertilizer application. A small plot combine equipped with a HarvestMaster H2 high capacity graingage (Logan, Utah) was used to determine the weight and moisture of the harvested rice plots.

Table 4.2. Important agronomic dates including planting date, pre-flood N application timing, flood establishment, and sensor reading dates for each location-year.

Location	Year	Planting Date	Pre-Flood N Application	Flood Establishment	Sensor Readings	Growth Stage at Sensor Readings
Crowley, LA	2017	13-Mar	2-May	3-May	26-May	PD
Palmetto, LA	2017	21-Mar	11-May	12-May	8-Jun	PD
Crowley, LA	2018	14-Mar	1-May	3-May	28-May	PD

(Table 4.2 Cont'd.)

Location	Year	Planting Date	Pre-Flood N Application	Flood Establishment	Sensor Readings	Growth Stage at Sensor Readings
Palmetto, LA	2018	27-Mar	17-May	18-May	7-Jun	PD
Iowa, LA	2018	20-Mar	2-May	3-May	25-May	PI
Monroe, LA	2018	1-May	23-May	25-May	20-Jun	PD
Saint Joseph, LA	2018	3-May	22-May	23-May	19-Jun	PI

4.2.2. Image Acquisition

Sensor data was collected for each site-year-variety test between panicle initiation and panicle differentiation using two remote sensing tools. A GreenSeeker handheld optical active sensor and an unmanned aerial system (UAS) remote sensor were used to collect sensor data for this study. The GreenSeeker handheld optical active sensor is a pre-calibrated, active remote sensor. Two specific wavelength regions of the electromagnetic spectrum were used to collect reflectance measurements of the rice crops canopy. Red (670 ± 10 nm) and NIR (780 ± 10 nm) wavelength regions were used to compute the NDVI measurements. The GreenSeeker was held manually approximately 1 m above the rice crop canopy with the sensor in a nadir position. Crop canopy reflectance readings were obtained by manually walking the GreenSeeker at a constant pace throughout the rice plots at each of the five locations.

The Phantom 4 Pro was the UAS used to collect data for this study. The Phantom 4 Pro was mounted with a RedEdge-M multispectral camera by MicaSense. The RedEdge-M multispectral camera collected crop canopy reflectance measurements with five narrowband electromagnetic wavelength regions: blue (475 nm center, 20 nm bandwidth), green (560 nm center, 20 nm bandwidth), red (668 nm center, 10 nm bandwidth), red-edge (717 nm center, 10 nm bandwidth), and near-infrared (840 nm center, 40 nm bandwidth). The red (668 nm) and the

near-infrared (840 nm) were collected by the UAS remote sensor to calculate NDVI. For this study, the UAS remote sensor was flown autonomously at an altitude of 30 m and collected multispectral images at a rate of 10 m/s with a 75% side and frontal overlap.

Flight operations of the UAS, remote controller connection, and wi-fi settings were set through the DJI GO 4 application software. Main controller settings, visual navigation settings, remote controller settings, image transition settings, aircraft battery information, and gimbal settings are set and controlled through this software application. The remote controller of the Phantom 4 Pro that is used to manually control the aircraft is connected to the UAS through the DJI GO 4 software.

MicaSense Atlas software is the software used to control the multispectral camera operations of the RedEdge-M multispectral camera and the flight route of the Phantom 4 Pro. The flight route was set with MicaSense Atlas and could be uploaded in 2 ways: 1) manually drawn right before the flight by the UAS remote pilot, which consists of waypoints or 2) a UAS remote pilot can pre-choose the field or area of interest in the persons personal MicaSense Atlas account and upload the field from the MicaSense Atlas account to use as the flight boundaries. The speed, altitude, and overlap percentage is set to the desired settings for the collection of the multispectral images once the area of interest for the flight is uploaded properly. For our study, the settings were set to collect multispectral images at an altitude of 30 m and at a rate of 10 m/s with a 75% side and frontal overlap. The application software will automatically calculate the flight time and number of multispectral images the multispectral camera will collect based on the speed, altitude, and overlap percentage.

The multispectral images collected were stabilized to decrease variability among the reflectance values from the multispectral images by calibrating the calibration reflectance panel

in the MicaSense Atlas software application. The calibrated reflectance panel was provided at the time of purchase of the RedEdge-M multispectral camera by MicaSenseand provides set numbers for each of the five narrowband wavelengths for the calibration. The calibrated reflectance panel was placed on the ground in a location away from any potential light fluctuations or shadows affecting the calibration. With our backs towards the sun, the UAS and RedEdge-M multispectral camera was held over the reflectance panel making sure no shadows were caused by the UAS over the reflectance panel. The UAS then took multiple pictures of the calibrated reflectance panel and the pictures were saved with the multispectral images collected. This process was repeated before and after the flight.

After the flight route was set, the multispectral image collection settings were set, and the calibration of the reflectance panel was done, then a pre-flight checklist and mission summary was presented before the flight was set to launch. The mission summary provides the remote pilot with the following information: camera updates, capture mode, internal storage availability, flight mode, picture distance, flight size coverage, and flight time. The UAS remote sensor mission was launched once all the settings were completed successfully.

4.2.3. Multispectral Image Processing

An important factor of the multispectral image data collection and creating valuable data is the stitching process and stitching software used to create a reflectance map from the multispectral images collected. The software used for this study to stitch the images together was the PIX4D software application.

A new project was created for each of the year-sites used for this study with the PIX4D software. Once the new project was selected and created, PIX4D went through multiple steps and settings to prepare the multispectral images to be stitched together. Each location had a separate

folder on the computer desktop with the multispectral images from each of the locations. The multispectral images were uploaded into the PIX4D software separately, by location. PIX4D automatically set the image properties to the appropriate coordinate system (World Geodetic System 1984; Coordinate System: WGS 84 (egm96)). Geolocation and orientation and accuracy were also automatically set, along with the camera model that was automatically selected. The output coordinate system was set to WGS 84 / UTM zone 15N with the 'meters' output unit chosen. Ag multispectral was the processing options template that was selected under the standard set options. Once these steps were completed, then 'Finish' could be selected, and the multispectral images were uploaded into the PIX4D software (Appendix).

Before the process of stitching the images together could begin, the calibration images of the calibrated reflectance panel and the numbers provided on the panel were uploaded through the 'processing' tab button under the 'DSM, ortho-mosaic, and index' section. Each of the numbers provided on the calibrated reflectance panel for the blue, green, red, NIR, and red-edge wavelengths were entered to the appropriate sections. The resolution was set to automatic, GeoTIFF, and merge tiles were both checked for the reflectance map. For our study, the NDVI indices was checked to make sure the reflectance map would be generated with the NDVI algorithm. The export grid size for index values as point shapefiles and index values and rates as polygon shapefiles was changed to five cm/grid. The lower cm/grid value, a better resolution was obtained from the exported SHP files. After the calibrated reflectance information was added, then the process of stitching the multispectral images together could begin. Three steps are involved in the multispectral image stitching process: 1) initial processing, 2) point cloud and mesh, and 3) DSM, otho-mosaic, and index.

After the multispectral images were stitched together, the NDVI equation was entered into the 'Index Calculator' portion of the PIX4D software. A reflectance map consisting of NDVI values was created during this step. In the index calculator, three steps occur. The first step is the wavelength band measurements used to develop the reflectance map. The second step is selecting which regions of the map should be created with the NDVI index calculator. For our study, the whole map was selected. The third step was selecting the number of classes, area, minimum NDVI value, and maximum NDVI value. For our study, twenty classes were chosen at equal area with a minimum value of zero and a maximum value of one. The reflectance map was then generated and then exported as index values and rates as polygon shapefiles (SHP) with the grid size [cm/grid], colored index map (GeoTIFF), and GeoJPG (JPG) (Appendix).

The NDVI reflectance map developed in PIX4D could then be used for the collection of NDVI values for each of the rice plots and each of the five locations. The SHP filed produced through PIX4D of the NDVI reflectance map was uploaded into Farm Works Trimble Ag software. All the NDVI values for each of the plots were then collected manually through the Farm Works software.

4.2.4. Data Analysis

Linear regression analysis was conducted to evaluate the relationship between GreenSeeker derived NDVI and rice grain yield and UAS derived NDVI and rice grain yield and R-Studio RStudio, Inc., 2009-2018). The significance and closeness of the two relationships were demonstrated with the coefficients of determination (R^2) from the linear regression analysis.

4.3. Results and Discussion

4.3.1. Evaluation of the linear regression relationship between GreenSeeker and UAV derived normalized difference vegetation index (NDVI) and rice grain yield.

The linear relationship between GreenSeeker derived NDVI and UAS derived NDVI to rice grain yield at Crowley, LA in 2017 is presented in Figure 4.1. Approximately 53% of the variation in rice grain yield could be explained by GreenSeeker derived NDVI in 2017 and approximately 32% of the variation in rice grain yield could be explained by the UAS derived NDVI in 2017 (Figure 4.1.). The linear relationship between GreenSeeker derived NDVI and rice grain yield was higher than the UAS derived NDVI to rice grain yield relationship. The UAS remote sensor data was saturated on the high end of the NDVI range. In addition, the data from the Diamond variety seemed to separate compared to the other varieties which, in turn, could explain some of the reduced R^2 from the UAS derived NDVI relationship to rice grain yield. The linear relationship between GreenSeeker derived NDVI and UAS derived NDVI to rice grain yield at Crowley, LA in 2018 is presented in Figure 4.2. Approximately 44% of the variation in rice grain yield could be explained by GreenSeeker derived NDVI, while approximately 52% of the variation in rice grain yield could be explained by UAS derived NDVI. The R^2 value between UAS derived NDVI and rice grain yield was improved from 2017 to 2018, while the GreenSeeker derived NDVI and rice grain yield from 2017 to 2018 was reduced. The relationship between the UAS derived NDVI was greater than the GreenSeeker derived NDVI in 2018. In addition, the separation of the Diamond variety in the 2017 UAS NDVI relationship was not observed in 2018, which could have caused the increase relationship of UAS derived NDIV and rice grain yield.

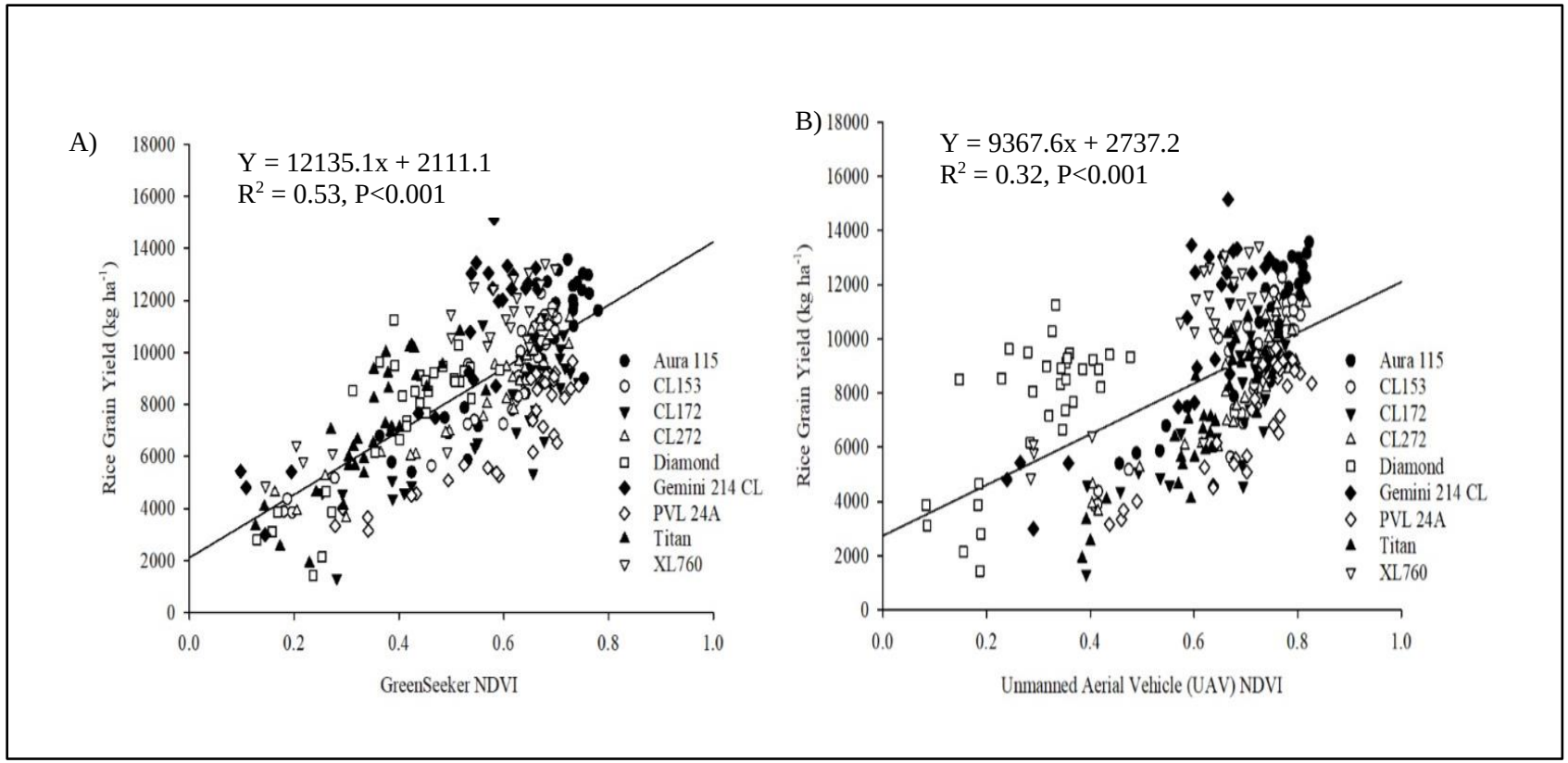

Figure 4.1. Linear regression analysis between A) GreenSeeker derived normalized difference vegetation index (NDVI) and rice grain yield (kg ha-1) at Crowley, LA in 2017; and B) Unmanned aerial system (UAS) derived NDVI at and rice grain yield (kg ha-1) at Crowley, LA in 2017.

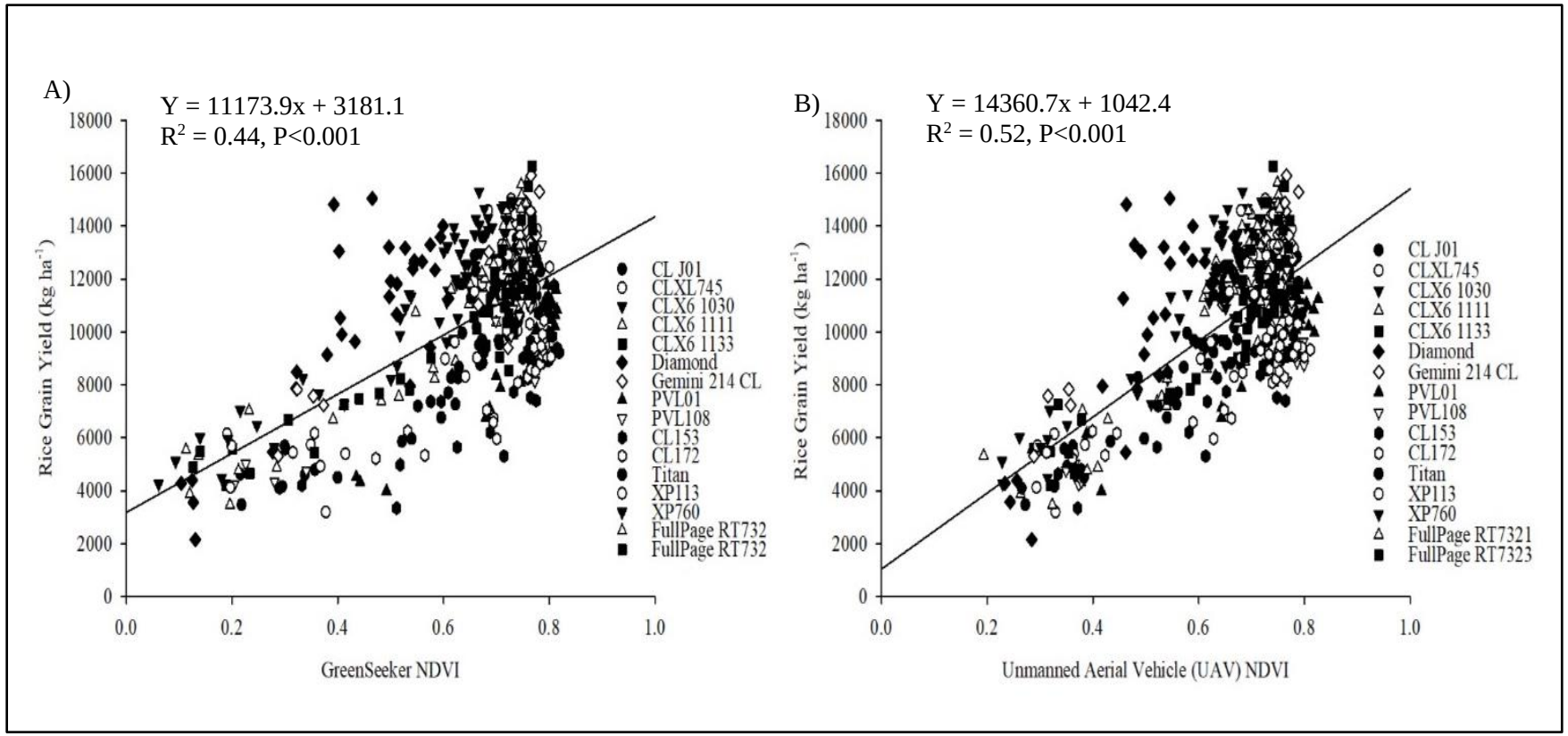

Figure 4.2. Linear regression analysis between A) GreenSeeker derived normalized difference vegetation index (NDVI) and rice grain yield (kg ha^{-1}) at Crowley, LA in 2018 and, B) Unmanned aerial system (UAS) derived NDVI and rice grain yield (kg ha^{-1}) at Crowley, LA in 2018.

The linear relationship between GreenSeeker derived NDVI and UAS derived NDVI to rice grain yield at Iowa, LA, in 2018 is presented in Figure 4.3. Approximately 5% of the variation in rice grain yield could be explained by GreenSeeker derived NDVI. Approximately 15% of the variation in rice grain yield could be explained by UAS derived NDVI. The Iowa location had heavy sheath blight and bacterial panicle blight disease pressure. The disease occurrence may have been a factor in the poor relationship between GreenSeeker and UAS derived NDVI to rice grain yield. The vegetative indices collected with the GreenSeeker and UAS remote sensing tools showed approximately 80% of the measurements between 0.7 and 0.9, a relatively high NDVI value. The high NDVI values were recorded between panicle initiation and panicle differentiation. Any change in growing conditions post-sensing could lead to vegetative indices, such as NDVI, inaccurately determining the growth and development of rice (Forestieri, 2017). Sheath blight first forms in the lower crop canopy, therefore the disease may have not been detectable by the remote sensors when NDVI measurements were recorded. The rice grain yields were low for the rice varieties, which may have caused the low relationship to the GreenSeeker and UAS derived NDVI. Ability for rice to recover from a disease is more difficult when the disease occurs during the latter growth and developmental stages. A higher relationship between UAS derived NDVI and rice grain yield as compared to the Greenseeker NDVI at this location. Zhang et al. (2017) found a strong relationship between UAS derived NDVIs and disease severity with an accurate disease detection 63% of the time. Therefore, the NDVI values from both the GreenSeeker and the UAS may be more representative of the sheath blight disease pressure at the time of sensing although the relationship with yield was very poor.

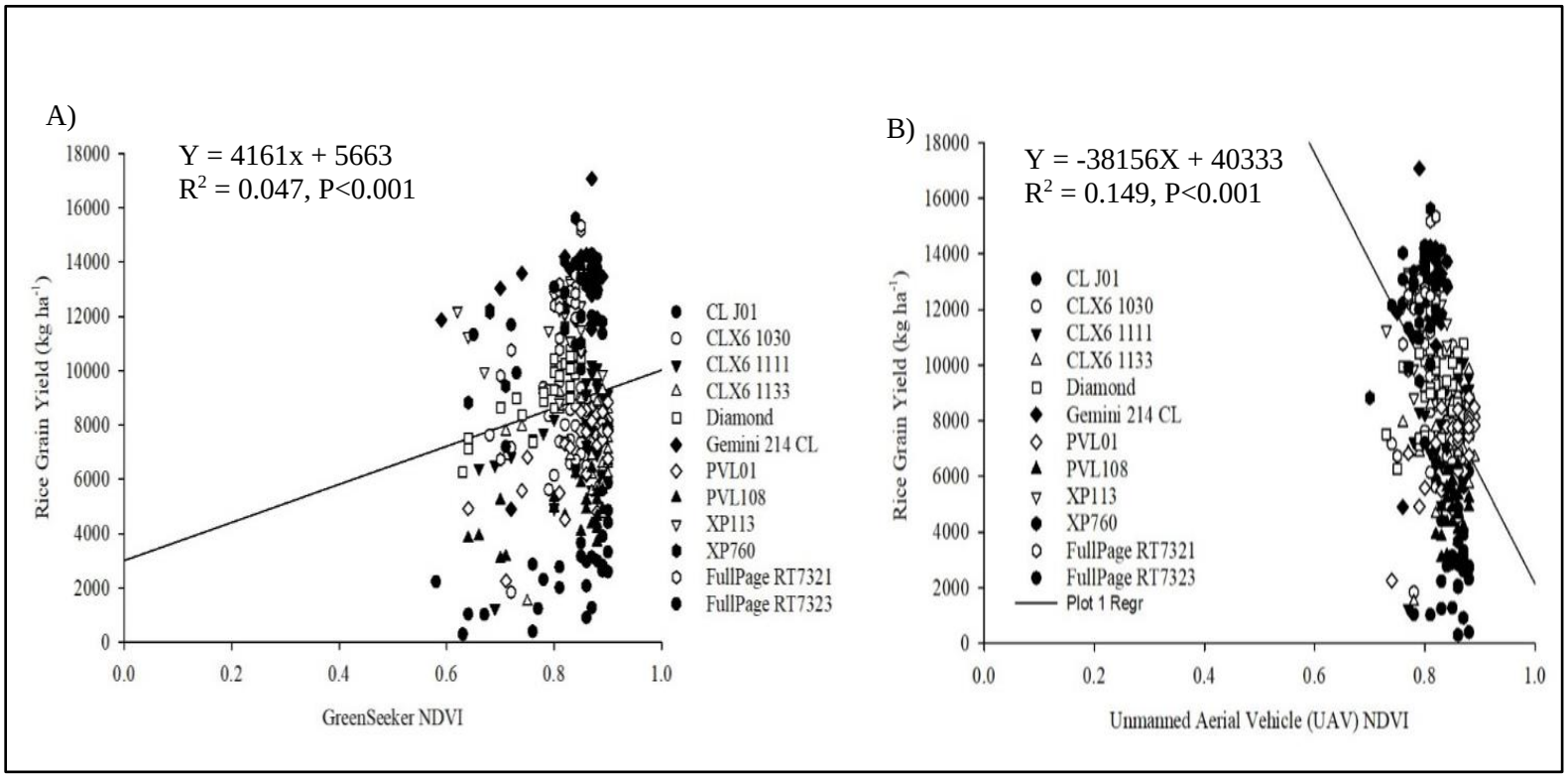

Figure 4.3. Linear regression analysis between A) GreenSeeker normalized difference vegetation index (NDVI) and rice grain yield (kg ha^{-1}) at Iowa, LA in 2018 and B) Unmanned aerial system (UAS) derived NDVI and rice grain yield (kg ha^{-1}) at Iowa, LA in 2018.

The linear relationship between GreenSeeker derived NDVI and UAS remote sensor derived NDVI to rice grain yield at Palmetto, LA in St. Landry Parish in 2017 is presented in Figure 4.4. The linear relationship between GreenSeeker derived NDVI and UAS remote sensor derived NDVI to rice grain yield at Palmetto in 2018 is presented in Figure 4.5. In 2017, approximately 9% of the variation in rice grain yield could be explained by GreenSeeker derived NDIV, while 16% of the variation in rice grain yield could be explained by UAS remote sensor derived NDVI. In 2018, approximately 16% of the variation in rice grain yield could be explained by GreenSeeker derived NDVI and 17% of the variation in rice grain yield could be explained by UAS remote sensor derived NDVI. The Palmetto location had a high incidence of sheath blight in both 2017 and 2018. Sheath blight occurrence may have been partially responsible for the poor relationship. Also, the NDVI readings for this location were collected at the panicle differentiation growth stage instead of panicle initiation. Harrell et al. (2011) demonstrated that vegetative indices data collected near panicle differentiation have less predictive ability of rice grain yield as compared to data collected at panicle initiation. Our data showed a high rate of saturation in all relationships for both years. This could be caused from the NDVI measurements taken closer to panicle differentiation when the rice has a more dense vegetation stand. The decreased ability for the two remote sensing tools to estimate rice grain yield at this location could have occurred because of the canopy reflectance changes between the panicle initiation and panicle differentiation sensing times (Duan et al., 2019).

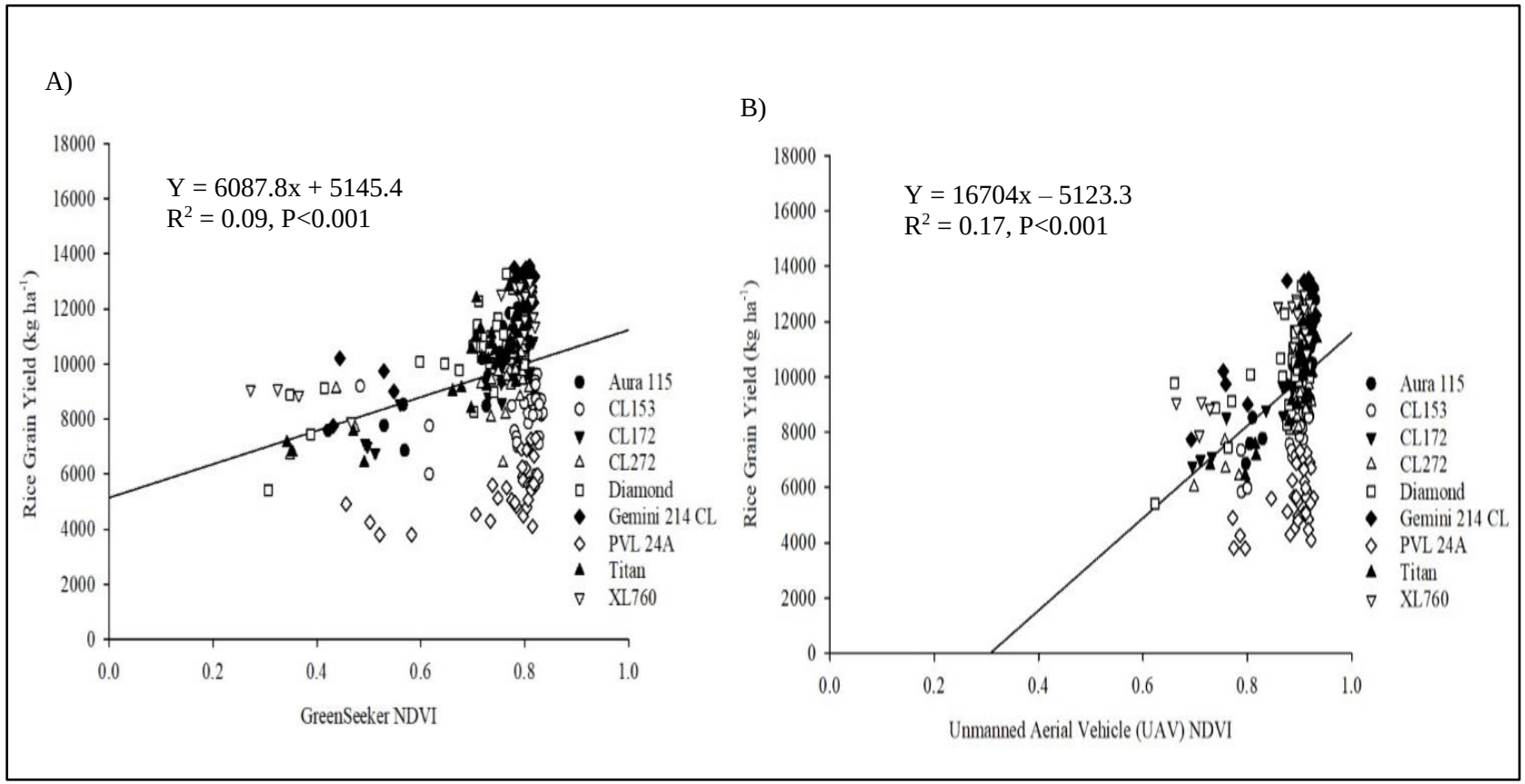

Figure 4.4. Linear regression analysis between A) GreenSeeker normalized difference vegetation index (NDVI) and rice grain yield (kg ha^{-1}) at Palmetto, LA in 2017 and B) Unmanned aerial system (UAS) derived NDVI and rice grain yield (kg ha^{-1}) at Palmetto, LA in 2017.

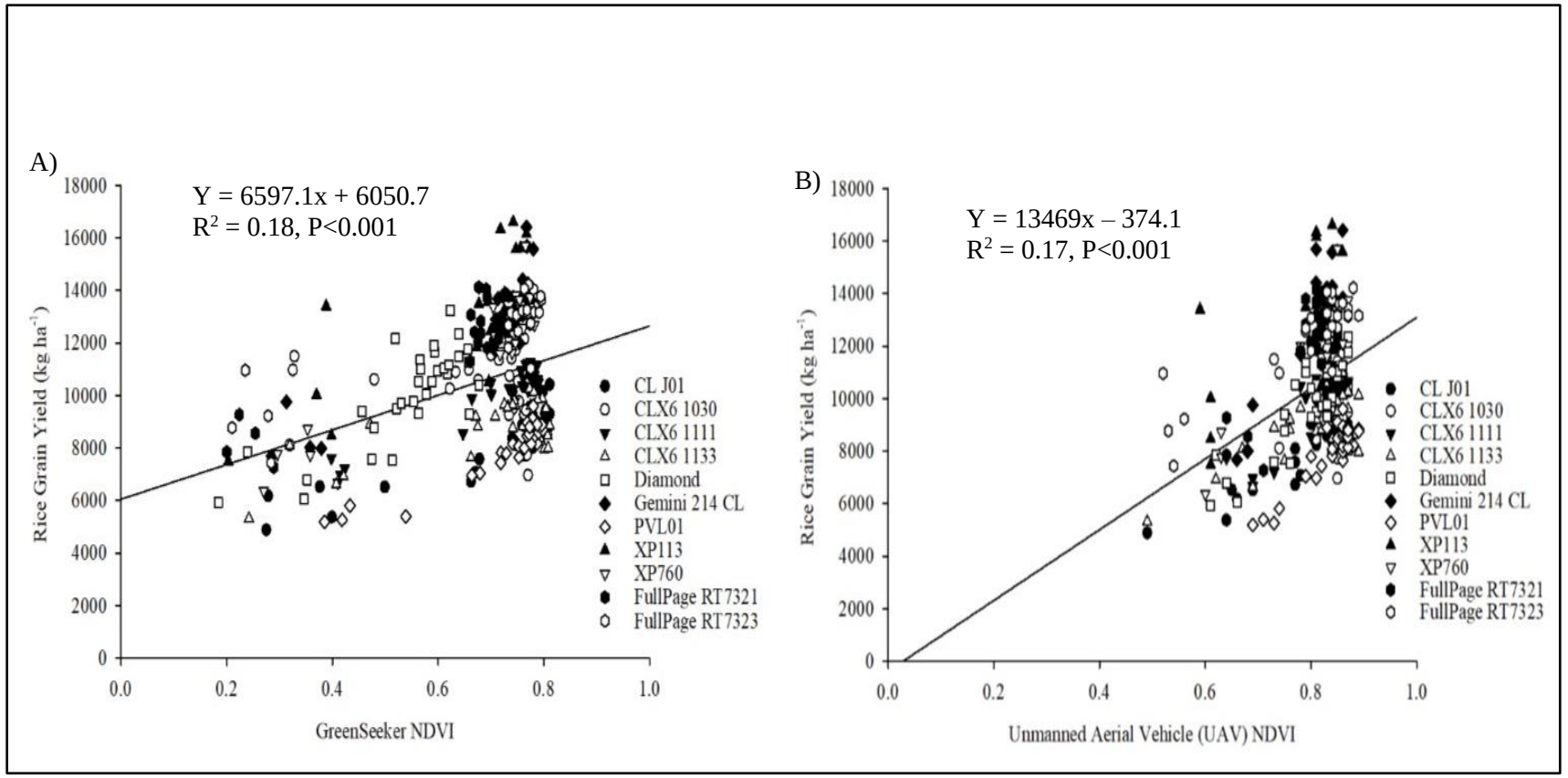

Figure 4.5. Linear regression analysis between A) GreenSeeker normalized difference vegetation index (NDVI) and rice grain yield (kg ha^{-1}) at Palmetto, LA in 2018 and B) Unmanned aerial system (UAS) and rice grain yield (kg ha^{-1}) at Palmetto, LA in 2018.

The linear relationship between GreenSeeker derived NDVI and UAS derived NDVI at Richland Parish near Monroe, LA in 2018 is presented in Figure 4.6. Approximately 35% of the variation in rice grain yield could be explained by the GreenSeeker derived NDVI. Approximately 24% of the variation in rice grain yield could be explained by the UAS derived NDVI. The NDVI measurements at Richland Parish were taken at panicle differentiation, but the relationship was estimated to be higher compared to the relationship at St. Landry Parish when the NDVI readings were also taken at panicle differentiation. The linear relationship between GreenSeeker derived NDVI and UAS remote sensor derived NDVI to rice grain yield at Saint Joseph, LA in Tensas Parish in 2018 is presented in Figure 4.7. Approximately 27% of the variation in rice grain yield could be explained by GreenSeeker remote sensing derived NDVI and approximately 27% of the variation in rice grain yield could be explained by UAS remote sensor derived NDVI. The relationship between GreenSeeker and UAS derived NDVI to rice grain yield at Saint Joseph, LA estimated a similar relationship to the relationship predicted at Richland Parish. The two locations were remote sensed on back to back days with the same persisting environmental conditions. The similar environmental conditions and days of sensing may have been a reasoning for the similar linear relationship predicted. The UAS derived NDVI was heavily saturated at the two locations. This could have been caused from the UAS having a difficult time being able to differentiate between the characteristics of the rice and NDVI values of the rice plots. This can result in the UAS remote sensor not being an accurate predictor of yield potential.

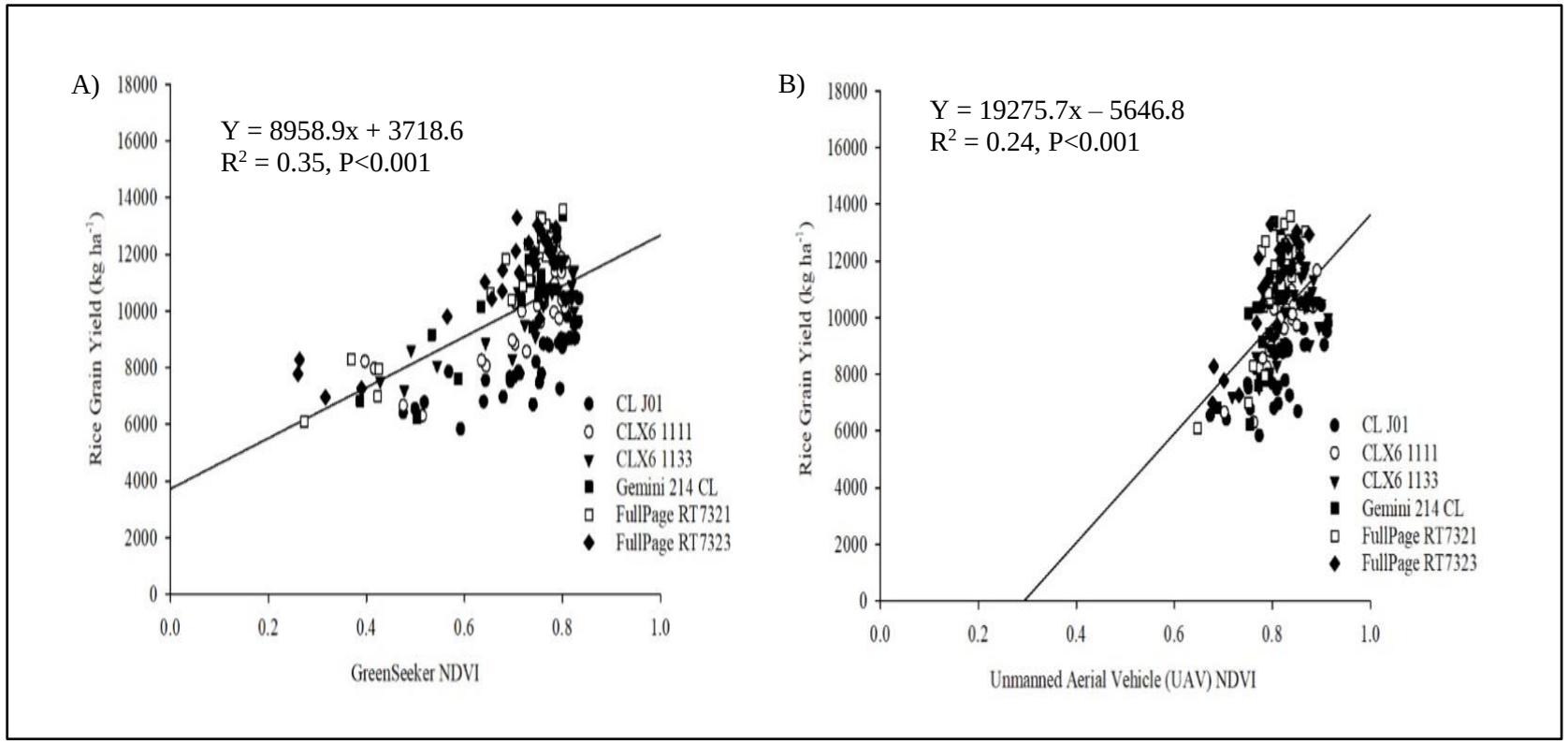

Figure 4.6. Linear regression analysis between A) GreenSeeker derived normalized difference vegetation index (NDVI) and rice grain yield (kg ha-1) at Monroe, LA in 2018 and B) Unmanned aerial system (UAS) and rice grain yield (kg ha-1) at Monroe, LA in 2018.

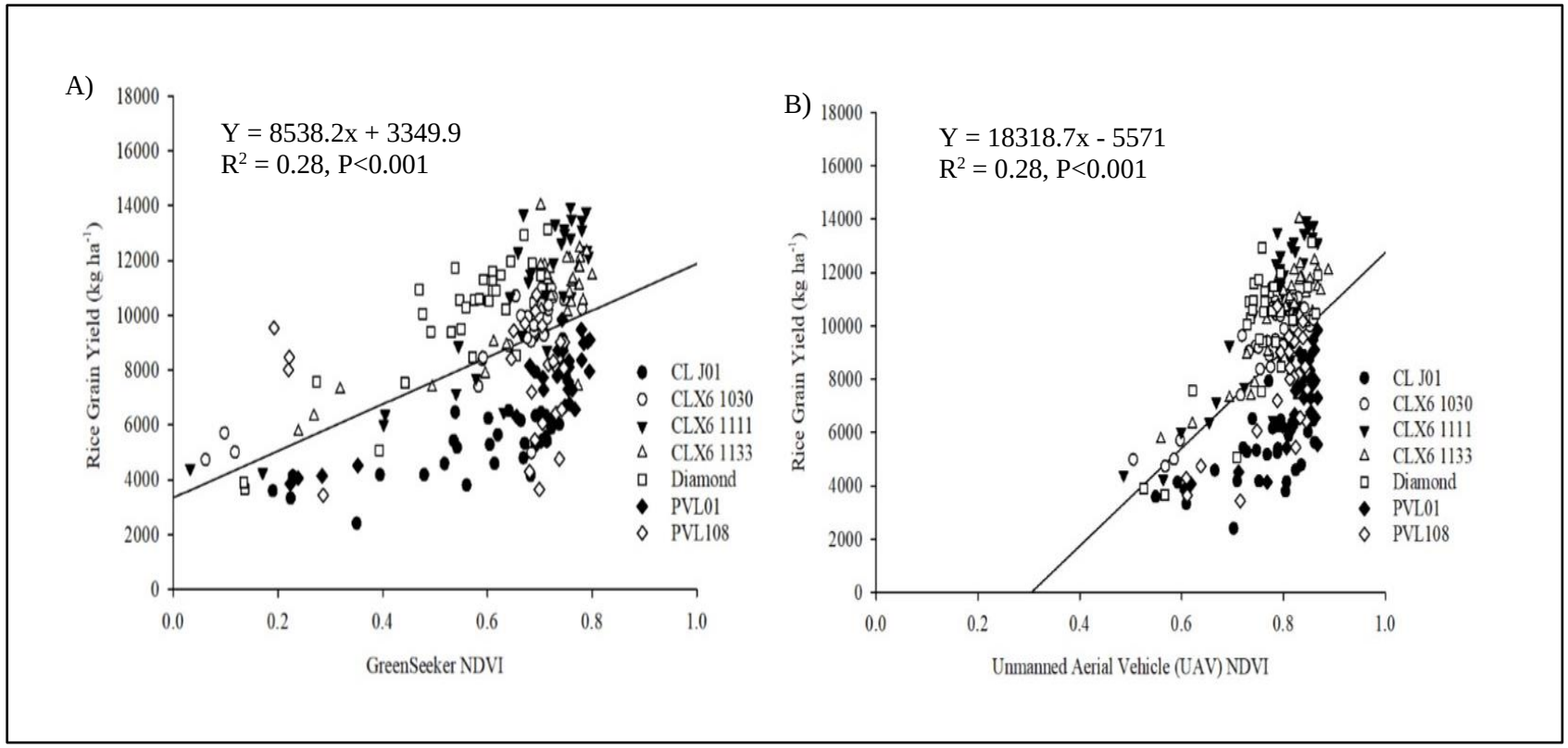

Figure 4.7. Linear regression analysis between A) GreenSeeker derived normalized difference vegetation index (NDVI) and rice grain yield (kg ha-1) at Saint Joseph, LA in 2018 and B) Unmanned aerial system (UAS) derived NDVI and rice grain yield (kg ha-1) at Saint Joseph, LA in 2018.

The relationships of GreenSeeker and UAS remote sensor derived NDVI to rice grain yield both changed between each year and site the data was collected from. A change in both NDVI values and rice grain yield can occur between years because of the effect from different environmental conditions on the growth and development of rice. The drastic change in environmental conditions or inadequate environmental conditions for sensing can cause the ability of rice grain yield to be estimated from NDVI values to decrease. Rice grain yield is highly affected by temporal variation and possesses a major challenge in estimating mid-season N recommendations when crop yield is used because of the variation of conditions between each crop year (Krienke et al., 2017).

The strongest relationship developed between GreenSeeker and UAS remote sensor derived NDVI to rice grain yield was at the Rice Research Station in Crowley, LA. Even though the relationships are closely related, the NDVI values weren't found to be based on the same 1:1 basis in neither 2017 nor 2018. These results showed that the NDVI values of each of the two remote sensing tools compared to rice grain yield were not found to be exactly alike. An explanation for this could be the different wavelength band measurements of the red and near-infrared regions used by each of the remote sensing tools to collect the NDVI measurements. The UAS remote sensor also captures multispectral images at a higher spatial resolution compared to the GreenSeeker. We can conclude from this the UAS remote sensor could have a hard time depicting certain characteristics of the rice due to the high spatial resolutions. Geometric deformations can be caused by multispectral images collected with the UAS remote sensor from the lack of accurate geographical data (LeLong et al., 2008).

4.4. Conclusions

The data accumulated for this study in 2017 and 2018 showed how the UAS has potential to be another successful tool in collecting NDVI measurements. However, the UAS derived NDVI measurements are not exactly the same as the GreenSeeker derived NDVI measurements. The linear relationships between GreenSeeker derived NDVI to rice grain yield and UAS derived NDVI to rice grain yield changed between each of the locations and years. The linear relationship between GreenSeeker derived NDVI to rice grain yield was reduced from 2017 to 2018, while the linear relationship between UAS derived NDVI to rice grain yield was increased from 2017 to 2018. The different relationships formed between the two remote sensors and rice grain yield could lead to skewed data and different mid-season N rates calculated. The variability between the two remote sensors could be from the GreenSeeker obtaining an active light sensor and the UAS obtaining a passive light sensor. The passive light sensor mounted onto the UAS can easily be affected by conditions that cause change in the sunlight and climatic conditions. The high spatial resolution of the UAS data collection can also cause different NDVI measurements compared to the low spatial resolution of the GreenSeeker derived NDVI. This could potentially be a reason for the different relationships found between GreenSeeker and UAS derived NDVI to rice grain yield. The high spatial resolution could also account for some of the reasoning of the high saturation from the UAS derived NDVI data points. The UAS derived NDVI values were all highly saturated between 0.7 and 0.9 at most of the locations.

The LSU AgCenter has already successfully developed an algorithm used to calculate mid-season N fertilization requirements using the handheld GreenSeeker active remote sensor. The LSU AgCenter mid-season N rate calculator must obtain three numeric features in the algorithm to calculate the mid-season N requirement: 1) yield potential, 2) response index, and 3)

rice response to N fertilization. The GreenSeeker and UAS would currently present different numbers for each of these factors based on our data and the GreenSeeker and UAS derived NDVI forming different relationships with rice grain yield. This study demonstrates how the UAS derived NDVI and GreenSeeker derived NDVI are inconsistent of each other. Therefore, more research needs to be done for the UAS derived NDVI to be successfully used in the LSU AgCenter mid-season N rate calculator. This study showed how an algorithm to calculate mid-season N requirements based solely using data collected with the UAS remote sensor should be developed for the UAS remote sensor to be successfully used by people in the rice industry. In addition, additional research with other vegetative indices might be helpful and prove to be better predictors of rice grain yield.

Chapter 5. Conclusions

Nitrogen (N) fertilization is a key component in producing maximum rice grain yields because rice grain yield is directly affected by N fertilizer applications. An effective management strategy used to determine N fertilization requirements is essential in optimizing rice productivity. The potential of under-and-over N fertilizer applications can occur if the appropriate N fertilization rates aren't applied to the rice. Developing a profitable N fertilizer recommendation rate is important to rice producers. The first goal of this research was to determine the economical optimum N rate (EONR) of fertilization based on 3 response models: 1) linear-plateau, 2) quadratic-plateau, and 3) quadratic. The EONR of fertilization will be affected by any changes in input (N fertilizer) or output (rice grain yield) prices.

The EONR of fertilization was estimated by fitting the linear-plateau, quadratic-plateau, and quadratic response models to the response of rice grain yields to N fertilizer applications. The data resulted in high R^2 values for the linear-plateau, quadratic-plateau, and quadratic response models (0.77, 0.79, and 0.78). This is an indication that each of the response models fits the data equally well and should be able to predict useful EONR of fertilization for the individual variety-site-years. However, determining which of the three response models to use in predicting the EONR of fertilization should not be based solely of the R^2 data. The linear-plateau, quadratic-plateau, and quadratic models could each estimate different EONR of fertilization despite the relatively similar R^2 values. Therefore, other factors should be taken into consideration when choosing which of the three response models best fits the data set and should be used to estimate the EONR of fertilization for an individual variety. The profitability and economical return of rice could be increased by selecting the response model with the most appropriate EONR of fertilization.

The second goal of this study was to compare GreenSeeker and unmanned aerial system (UAS) remote sensor derived normalized difference vegetative index (NDVI). NDVI collected with remote sensors can be used to estimate mid-season N fertilization rate recommendations. The GreenSeeker has been the predominant remote sensor in collecting NDVI measurements of crops. Unmanned aerial system (UAS) remote sensors have shown the possibility of having the ability to collect NDVI measurements like the GreenSeeker. The data from this study in 2017 and 2018 predicted GreenSeeker and UAS remote sensor derived NDVI to have a strong linear relationship. However, the relationships estimated between the GreenSeeker and UAS remote sensor derived NDVI at each of the five locations and years were inconsistent of each other. The relationship difference between locations could be a result from the different soil properties at each location, different rice growth stages at the time of NDVI readings, and different climatic conditions on the day of remote sensing. Soil fertility differences will cause rice varieties to develop at different rates which, in turn, could skew the NDVI values produced and create different GreenSeeker and UAS remote sensor derived NDVI relationships. Time of remote sensing is an important consideration in collecting NDVI measurements. In addition, the UAS remote sensor is a passive sensor that relies on sunlight as its light source. A passive light sensor can create variability in NDVI measurements from the angle and intensity of the sunlight, bidirectional reflectance, and cloud cover at the time of readings. UAS remote sensor derived NDVI values were heavily saturated between the 0.65 and 0.9 NDVI values at each site-year compared to the GreenSeeker derived NDVI measurements. The high altitude and high spatial resolution of the UAS remote sensor may account for some of the increased saturation of the UAS remote sensor derived NDVI. Other vegetative indices could potentially reduce the heavy saturation from the UAS derived NDVI and should be evaluated.

The third goal of this research was to evaluate the linear relationship between GreenSeeker derived NDVI and UAS derived NDVI to rice grain yield for each location-year. GreenSeeker derived NDVI had a different linear relationship to rice grain yield at each location compared to the UAS derived NDVI. UAS derived NDVI showed an increased relationship (R^2 = 0.52) in 2018 compared to the relationship in 2017 (R^2 = 0.32). The GreenSeeker derived NDVI showed a decreased relationship (R^2 = 0.44) in 2018 compared to the relationship in 2017 (R^2 = 0.54). Calcasieu Parish and St. Landry Parish produced the lowest linear relationships between GreenSeeker and UAS derived NDVI to rice grain yield. Sheath blight occurred in the field at both Calcasieu and St. Landry Parish which, in turn, may have potentially been a reasoning for the poor linear relationships at these two locations. The linear relationship between GreenSeeker derived NDVI and rice grain yield (R^2 = 0.35) was higher compared to the UAS derived NDVI relationship to rice grain yield (R^2 = 0.24) at Richland Parish. Time of remote sensing was done at panicle differentiation. UAS remote sensors are flown at a higher spatial resolution compared to GreenSeekers, which may have caused the UAS to potentially have harder time differentiating NDVI values when the rice is at latter growth stages. The linear relationship between GreenSeeker derived NDVI to rice grain yield (R^2 = 0.27) was the same linear relationship between UAS derived NDVI to rice grain yield (R^2 = 0.27) at Saint Joseph, LA in 2018. However, the UAS remote sensor derived NDVI values were heavily saturated between 0.7 and 0.9 compared to the wider spread of GreenSeeker derived NDVI measurements. UAS remote sensors are flown at high altitudes with high spatial resolution which could potentially cause the heavy saturation.

Overall, the linear relationships between GreenSeeker derived NDVI to rice grain yield were not the same as the linear relationship between UAS derived NDVI to rice grain yield at six

of the seven locations. GreenSeeker and UAS remote sensors in the data from this study collect different NDVI measurements. Different NDVI measurements can cause the two remote sensors to predict different mid-season N requirements in an on-site sensor-based N rate calculator. Additional research using different vegetative indices collected from the two remote sensors should be evaluated to determine if other vegetative indices prove to have a stronger relationship with rice grain yield to predict accurate mid-season N rates. The algorithm already successfully used with the GreenSeeker derived NDVI could result in different mid-season N rate requirements from the UAS derived NDVI because of the different relationships shown with this data between the two remote sensors. Therefore, an algorithm should be developed for UAS remote sensor derived NDVI to have the ability to predict reliable mid-season N requirements.

List of References

Alivelu, K., S. Srivastava, A.S. Rao, K.N. Singh, G. Selvakumari, and N.S. Raju. 2003. Comparison of modified mitscherlich and response plateau models for calibrating soil test-based nitrogen recommendations for rice on typic ustropept. Communications in Soil Science and Plant Analysis 34: 2633–2643.

Bahmani, O., S.B. Nasab, M. Behzad, and A.A. Naseri. 2009. Assessment of nitrogen accumulation and movement in soil profile under different irrigation and fertilization regime. Asian J. Agr. Res. 3(29):38-46.

Bajwa, S.G., A.R. Mishra, and R.J. Norman. 2010. Canopy reflectance response to plant nitrogen accumulation in rice. Precision Agri. 11:488-506.

Be´langer, G., J.R. Walsh, J.E. Richards, P.H. Milburn, and N. Ziadi. 2000. Comparison of three statistical models describing potato yield response to nitrogen fertilizer. Agronomy Journal 92: 902-908.

Beaudoin, N., J.K. Saad, C.V. Laethem, J.M. Machet, J. Maucorps, B. Mary. 2005. Nitrate leaching in intensive agriculture in Northern France: Effect of farming practices, soils, and crop rotations. Agric. Ecosyst. Environ. 111:292-310.

Bronson K.F. 2008. Forms of inorganic nitrogen in the soil. In: J.S. Schepers and W.R. Raun (Eds.), Nitrogen in agricultural systems. Agron. Monogr. 49. ASA, CSSA, and SSSA, Madison, WI. pp. 31-56.

Candiago, S., F. Remondino, M.D. Giglio, M. Dubbini, and M. Gattelli. 2015. Evaluating Multispectral Images and Vegetation Indices for Precision Farming Applications from UAV Images. Remote Sensing 7: 4026–4047.

Cerrato, M.E., and A.M. Blackmer. 1990. Comparison of models for describing corn yield response to nitrogen fertilizer. Agronomy Journal 82: 138-143.

Chen, J., Y. Huang, and Y. Tang. 2011. Quantifying economically and ecologically optimum nitrogen rates for rice production in south-eastern China. Agriculture, Ecosystems & Environment 142:195–204.

Colaco, A.F., and R.G.V. Bramley. 2018. Do crop sensors promote improved nitrogen management in grain crops? Field Crops Research 218:126-140.

Corwin, D.L. Delineating site-specific crop management units: Precision agriculture application in GIS.

Duan B., S. Fang, R. Zhu, X. Wu, S. Wang, Y. Gong, and Y. Peng. 2019. Remote estimation of rice yield with unmanned aerial vehicle (UAV) data and spectral mixture analysis. Frontiers in Plant Science. 10.

Elarab, M. 2016. The application of unmanned aerial vehicle to precision agriculture: Chlorophyll, nitrogen, and evapotranspiration estimation. All Graduate Theses and Dissertations. 4891.

Engels, C., and H. Marschner. 1995. Plant uptake and utilization of nitrogen. In: P.E. Alexander, (Ed.), Nitrogen fertilization in the environment. Marcel Dekker, Inc. New York, NY. pp. 41-82.

Fageria, V.D. 2001. Nutrient Interactions in crop plants. J. Plant Nutr. 24:1269-1290.

Fontes, P.C.R., H. Braun, C. Busato, and P.R. Cecon. 2010. Economic optimum nitrogen fertilization rates and nitrogen fertilization rate effects on tuber characteristics of potato cultivars. Potato Research 53: 167–179.

Forestieri, D.E. 2017. Improving nitrogen use efficiency and yield in Louisiana sugarcane production systems. LSU Master's Theses. 4454.

Fox, R.H., and C.L. Watlhall. 2008. Crop monitoring technologies to assess nitrogen status. In: J.S. Schepers and W.R. Raun (Eds.), Nitrogen in agricultural systems. Agron. Monogr. 49. ASA, CSSA, and SSSA, Madison, WI. pp. 647-674.

Girma, K., K.L. Martin, R.H. Anderson, D.B. Arnall, K.D. Brixey, M.A. Casillas, B. Chung, B.C. Dobey, S.K. Kamenidou, S.K. Kariuki, E.E. Katsalirou, J.C. Morris, J.Q. Moss, C.T. Rohla, B.J. Sudbury, B.S. Tubaña, and W.R. Raun. 2006. Mid-season prediction of wheat-grain yield potential using plant, soil, and sensor measurements. J. Plant Nutr. 29:873-897.

Gnanamanickam, S.S. 2002. Biological control of crop diseases. M. Dekker, New York.

Gross, J.W., and B.W. Heumann. 2016. A statistical examination of image stitching software packages for use with unmanned aerial systems. Photogrammetric Engineering & Remote Sensing 82:419–425.

Guan, S., K. Fukami, H. Matsunaka, M. Okami, R. Tanaka, H. Nakano, T. Sakai, K. Nakano, H. Ohdan, and K. Takahashi. 2019. Assessing correlation of high-resolution NDVI with fertilizer application level and yield of rice and wheat crops using small UAVs. Remote Sensing 11:112.

Harrell, D.L., B.S. Tubaña, T.W. Walker, and B.S. Phillips. 2011. Estimating rice grain yield potential using normalized difference vegetation index. Agron. J. 103:1717-1723.

Harrell, D.L., T.W. Walker, M.E. Salassi, J.A. Bond, and P.D. Gerard. 2011. Modeling rice grain yield response to nitrogen fertilization for delayed-flood production. J. Plant Nutr. 34:2158–2171.

Havlin, J.L., J.D. Beaton, S.L. Tisdale, and W.L. Nelson. 2014. Soil fertility and fertilizers. 8th ed. Pearson. Upper Saddle River, NJ.

Hernandez, J.A., and D.J. Mulla. 2008. Estimating uncertainty of economically optimum fertilizer rates. Agronomy Journal 100: 1221-1229.

Hong, N., P.C. Scharf, J.G. Davis, N.R. Kitchen, and K.A. Sudduth. 2007. Economically optimal nitrogen nate reduces soil residual nitrate. Journal of Environment Quality 36: 354-362.

Huang, Y., S.J. Thomson, W.C. Hoffman, Y. Lan, and B.K. Fritz. 2013. Development and prospect of unmanned aerial vehicle technologies for agricultural production management. Int. J. Agric & Biol. Eng. 6:1-10.

Johnson, G.V., W.R. Raun. 2003. Nitrogen response index as a guide to fertilizer management. J. Plant. Nutr. 26:249-262.

Kanke, Y. 2013. Optimizing yield and crop nitrogen response characterization by integrating spectral reflectance and agronomic properties in sugarcane and rice. Dissertation. Louisiana State University. Electronic and thesis dissertation collection. Web. 21 Feb. 2019

Kanke, Y., B. Tubaña, M. Dalen, and D. Harrell. 2016. Evaluation of red and red-edge reflectance-based vegetation indices for rice biomass and grain yield prediction models in paddy fields. Precision Agri. 17:507-530.

Katsigiannis, P., L. Misopolinos, V. Liakopoulos, T.K. Alexandridis, and G. Zalidis. 2016. An autonomous multi-sensor UAV system for reduced-input precision agriculture applications. 2016 24th Mediterranean Conference on Control and Automation (MED).

Kissel, D.E., M.L. Cabrera, and S. Paramasivam. 2008. Ammonium, ammonia, and urea reactions in soil. In: J.S. Schepers and W.R. Raun (Eds.), Nitrogen in agricultural systems. Agron. Monogr. 49. ASA, CSSA, and SSSA, Madison, WI. pp. 101-156.

Krienke, B., R.B. Ferguson, M. Schlemmer, K. Holland, D. Marx, and K. Eskridge. 2017. Using an unmanned aerial vehicle to evaluate nitrogen variability and height effect with an active crop canopy sensor. Precision Agri. 18:900–915.

Lan, Y., C. Shengde, B. K. Fritz. 2017. Current status and future trends of precision agricultural aviation technologies. Int J Agric & Biol Eng. 10:1-17.

Lee, Y.-J., C.-M. Yang, K.-W. Chang, and Y. Shen. 2008. A simple spectral index using reflectance of 735 nm to assess nitrogen status of rice canopy. Agronomy Journal 100:205-212.

Leghari, S.J., N.A. Wahocho, G.M. Laghari, A.H. Laghari, G.M. Bhabhan, K.H. Talpur, T.A. Bhutto, S.A. Wahocho, A.A. Lashari. 2016. Role of nitrogen for plant growth and development: a review. Advances in Environmental Biology 10: 209-218.

Lelong, C., P. Burger, G. Jubelin, B. Roux, S. Labbé, and F. Baret. 2008. Assessment of unmanned aerial vehicles imagery for quantitative monitoring of wheat crop in small plots. Sensors 8:3557–3585.

Li, J., F. Zhang, X. Qian, Y. Zhu, and G. Shen. 2015. Quantification of rice canopy nitrogen balance index with digital imagery from unmanned aerial vehicle. Remote Sensing Letters 6: 183– 189.

LSU AgCenter. 2019. Rice varieties and management tips. LSU AgCenter 2270: 1-28.

Mae, T. 1997. Physiological nitrogen efficiency in rice: Nitrogen utilization, photosynthesis, and yield potential. Plant and Soil. 196:201-210.

Mamo, M., G.L. Malzer, D.J. Mulla, D.R. Huggins, and J. Strock. 2003. Spatial and temporal variation in economically optimum nitrogen rate for corn. Agronomy Journal 95: 958-964.

Moldenhauer, K., P. Counce, and J. Hardke. 2013. Rice growth and development. Arkansas Rice Production Handbook. pp. 9-20.

Mullen, R.W., K.W. Freeman, W.R. Raun, G.V. Johnson, M.L. Stone, and J.B. Solie. 2003. Identifying an in-season response index and the potential to increase wheat yield with nitrogen. Agron. J. 95:347-351.

Myrold, D.D, and P.J. Bottomely. 2008. Mineralization and immobilization of soil nitrogen. In: J.S. Schepers and W.R. Raun (Eds.), Nitrogen in agricultural systems. Agron. Monogr. 49. ASA, CSSA, SSSA, Madison, WI. pp. 157-172.

Neeteson, J.J., and W.P. Wadman. 1987. Assessment of economically optimum application rates of fertilizer N on the basis of response curves. Fertilizer Research 12: 37–52.

Nguyen, H.T., and B.-W. Lee. 2006. Assessment of rice leaf growth and nitrogen status by hyperspectral canopy reflectance and partial leaf square regression. Europ. J. Agron. 26:349-356.

Nguyen, H.T., J.H. Kim, A.T. Nguyen, L.T. Nguyen, J.C. Shin, and B.-W. Lee. 2006. Using canopy reflectance and partial least squares regression to calculate within-field statistical variation in crop growth and nitrogen status of rice. Precision Agric. 7:249–264.

Ni, J., L. Yao, J. Zhang, W. Cao, Y. Zhu, and X. Tai. 2017. Development of an Unmanned Aerial Vehicle-Borne Crop-Growth Monitoring System. Sensors 17(3): 502.

Norton, J. 2003. Mineralization in soil. In: J.S. Schepers and W.R. Raun (Eds.), Nitrogen in agricultural systems. Agron. Monogr. 49. ASA, CSSA, and SSSA, Madison, WI. pp. 173-199.

Pajares, G. 2015. Overview and Current Status of Remote Sensing Applications Based on Unmanned Aerial Vehicles (UAVs). Photogrammetric Engineering & Remote Sensing 81: 281–330.

Peng, S., R. Buresh, J. Huang, X. Zhong, Y. Zou, J. Yang, G. Wang, Y. Liu, R. Hu, Q. Tang, K. Cui, F. Zhang, and A. Dobermann. 2010. Improving nitrogen fertilization in rice by site-specific N management. A review. Agron. Sustain. Dev. 30:649-656.

Primicerio, J., S.F.D. Gennaro, E. Fiorillo, L. Genesio, E. Lugato, A. Matese, and F.P. Vaccari. 2012. A flexible unmanned aerial vehicle for precision agriculture. Precision Agric. 13: 517–523.

Puri, V., A. Nayyar, and L. Raja. 2017. Agriculture drones: A modern breakthrough in precision agriculture. Journal of Statistics and Management Systems 20: 507–518.

Quemada, M., J. Gabriel, and P. Zarco-Tejada. 2014. Airborne hyperspectral images and ground-level optical sensors as assessment tools for maize nitrogen fertilization. Remote Sensing 6: 2940–2962.

Rasmussen, J., G. Ntakos, J. Nielsen, J. Svensgaard, R.N. Poulsen, and S. Christensen. 2015. Are vegetative indices derived from consumer-grade cameras mounted on UAVs sufficiently reliable for assessing experimental plots? Agron. J. 74:75-92.

Rattey, A.R. and D.M. Hogarth. 2001. The effect of different nitrogen rates on CCS accumulation over time. Proc. Int. Soc. Sugar Cane Technol., 24:360-366.

Raun, W.R., J.B. Solie, G.V. Johnson, M.L. Stone, E.V. Lukina, W.E. Thomason, and J.S. Schepers. 2001. In-season prediction of potential rice grain yield in winter wheat using crop canopy reflectance. Agron. J. 93:131-138.

Raun, W.R., J.B. Solie, G.V. Johnson, M.L. Stone, R.W. Mullen, K.W. Freeman, W.E. Thomason, and E.V. Lukina. 2002. Improving nitrogen use efficiency in cereal grain production with optical sensing and variable rate application. Agron. J. 94:815-820.

Raun, W.R., J.B. Solie, and M.L. Stone. 2011. Independence of yield potential and crop nitrogen response. Precision Agric. 12:508-518.

Robertson, G.P., and P.M. Vitousek. 2009. Nitrogen in Agriculture: Balancing the cost of an essential resource. Annual Review of Environment and Resources 34: 97–125.

Saichuk, J. 2014. Louisiana Rice Production Handbook. Louisiana State University Agricultural Center, Baton Rouge, LA.

Salami, E., C. Barrado, and E. Pastor. 2014. UAV flight experiments applied to remote sensing of vegetated areas. Remote Sensing 6(11): 11051-11081.

Scharf, P. 2015. Managing nitrogen in crop production. ASA, CSSA, and SSSA, Madison, WI.

Shanahan, J.F., J.S. Schepers, D.D. Francis, G.E. Varvel, W.W. Wilhelm, J.M. Tringe, M.R. Schlemmer, and D.J. Major. 2001. Use of remote-sensing imagery to estimate corn grain yield. Agronomy Journal 93: 583.

Shanahan, J.F., N.R. Kitchen, W.R. Raun, and J.S. Schepers. 2008. Responsive in-season nitrogen management for cereals. Comp. Elect. Agri. 61:5-62.

Singh, B., and V.K. Singh. 2017. Fertilizer management in rice. In: B.S. Chauhan, K. Jabran, and G. Mahajan (Eds.), Rice Production Worldwide. Springer. pp. 217-253.

Slaton, N.A., R.D. Cartwright, J. Meng, E.E. Gbur, and R.J. Norman. 2003. Sheath blight severity and rice yield as affected by nitrogen fertilizer rate, application method, and fungicide. Agronomy Journal 95: 1489-1496.

Snyder, C.S., N.A. Slaton. 2002. Rice production in the United States – an overview. Better Crops International 16: 30-35.

Stafford, J.V. 2000. Implementing precision agriculture in the 21st century. J. Agric. Engng Res. 76:267–275.

Stewart, W.M., D.W. Dibb, A.E. Johnston, and T.J. Smyth. 2005. The Contribution of commercial fertilizer nutrients to food production. Agronomy Journal 97: 1-6.

Stroppiana, D., P. Villa, G. Sona, G. Ronchetti, G. Candiani, M. Pepe, L. Busetto, M. Migliazzi, and M. Boschetti. 2018. Early season weed mapping in rice crops using multi-spectral UAV data. International Journal of Remote Sensing 39: 5432–5452.

Sui, B., X. Feng, G. Tian, X. Hu, Q. Shen, and S. Guo. 2013. Optimizing nitrogen supply increases rice yield and nitrogen use efficiency by regulating yield formation factors. Field Crops Research 150: 99–107.

Swain, K.C., S.J. Thomson, and H.P.W. Jayasuriya. 2010. Adoption of an unmanned helicopter for low-altitude remote sensing to estimate yield and total biomass of a rice crop. Transactions of the ASABE 53(1): 21–27.

Teal, R.K., B. Tubaña, K. Girma, K.W. Freeman, D.B. Arnall, O. Walsh, and W.R. Raun. 2006. In-season prediction of corn grain yield potential using normalized difference vegetation index. Agron. J. 98:1488-1494.

Tubaña, B.S., D.B. Arnall, O. Walsh, B. Chung, J.B. Solie, K. Girma, and W.R. Raun. 2008. Adjusting midseason nitrogen rate using sensor-based optimization algorithm to increase efficiency in corn. J. Plant Nutr. 31:1393-1419.

Tubaña, B.S., D. Harrell, T. Walker, and S. Phillips. 2011. Midseason nitrogen fertilization rate decision tool for rice using remote sensing technology. Better Crops. 95:22-24.

Tumusiime, E., B.B. Wade, J. Mosali, J. Johnson, J. Locke, and J.T. Biermacher. 2011. Determining optimal levels of nitrogen fertilizer using random parameter models. Journal of Agricultural and Applied Economics 43: 541–552.

USDA (United States Department of Agriculture). 2019. Crop production 2018 summary.

USDA (United States Department of Agriculture). 2019. World Agricultural Production.

Watts, A.S., V.G. Ambrosia, E.A. Hinkley. 2012. Unmanned aircraft systems in remote sensing and scientific research: classification and considerations of use. Remote Sens. 4:1671-1692.

Xia, Y., and X. Yan. 2011. Comparison of statistical models for predicting cost effective nitrogen rate at rice–wheat cropping systems. Soil Science and Plant Nutri. 57: 320–330.

Xue, L., W. Cao, W. Luo, T. Dai, and Y. Zhu. 2003. Monitoring leaf nitrogen status in rice with canopy spectral reflectance. Agron. J. 96:135-142.

Xue, L., and L. Yang. 2008. Recommendations for nitrogen fertilizer topdressing rates in rice using canopy reflectance spectra. Biosystems Engineering 100:524–534.

Xue, Y., H. Duan, L. Liu, Z. Wang, J. Yang, and J. Zhang. 2013. An improved crop management increases grain yield and nitrogen and water use efficiency in rice. Crop Sci. 53:271-284.

Yang, M. D., K. S. Huang, Y. H. Kuo, H. P. Tsai, and L. M. Lin. 2017. Spatial and spectral hybrid image classification for rice lodging assessment through UAV imagery. Remote Sensing 9:583.

Yoshida, S. 1981. Fundamentals of rice crop science. International Rice Research Institute, Los Baños, Laguna, Philippines.

Zhang, N., M. Wang, and N. Wang. 2002. Precision agriculture—A worldwide overview. Computers and Electronics in Agriculture 36: 113–132.

Zhang, C., and J.M. Kovacs. 2012. The application of small unmanned aerial systems for precision agriculture: a review. Precision Agri 13:693-712.

Zhang, D., Z. Xingen, J. Zhang, Y. Lan, C. Xu, D. Liang. 2018. Detection of rice sheath blight using an unmanned aerial system with high-resolution color and multispectral imaging. Plos One 13(5).

Zheng, H., T. Cheng, D. Li, X. Zhou, X. Yao, Y. Tian, W. Cao, and Y. Zhu. 2018. Evaluation of RGB, Color-Infrared and Multispectral Images Acquired from Unmanned Aerial Systems for the Estimation of Nitrogen Accumulation in Rice. Remote Sensing 10(6): 824.

Zhu, J., K. Wang, J. Deng, and T. Harmon. 2009. Quantifying nitrogen status of rice using low altitude UAV-mounted system and object-oriented segmentation methodology. Volume 3: ASME/IEEE 2009 International Conference on Mechatronic and Embedded Systems and Applications; 20th Reliability, Stress Analysis, and Failure Prevention Conference.

Vita

Anna E. Coker was born in Stuttgart, Arkansas in July of 1995. She attended the University of Arkansas in Fayetteville, AR and received a Bachelor of Science in Crop, Environmental, and Soil Sciences in May of 2017. After graduating, she came to Louisiana State University and started the Master program in the School of Plant, Environmental, and Soil Science under the guidance of Dr. Dustin Harrell in June of 2017. Her research is comparing the relationship between GreenSeeker derived normalized difference vegetative index (NDVI) and unmanned aerial system (UAS) derived NDVI. Her research also involves evaluating the relationship between GreenSeeker derived NDVI to rice grain yield and UAS derived NDVI to rice grain yield. Coker plans to graduate with a Master of Science from Louisiana State University in December of 2019.